SYNTHESIS AND CHARACTERISATION OF PALLADIUM, PLATINUM AND GOLD COMPLEXES AND THEIR BIOLOGICAL ACTIVITY AGAINST OESOPHAGEAL CANCER CELL LINES

Haleden Chiririwa

UNIVERSITY OF CAPE TOWN

2010

Synthesis and Characterisation of Palladium, Platinum and Gold complexes and their Biological activity against Oesophageal cancer cell lines

Thesis presented by:

Haleden Chiririwa

In fulfilment of the requirements for the degree of

Doctor of Philosophy

Supervisor: Prof J.R Moss

Co-supervisor: A/Prof D.T Hendricks

ABSTRACT

New iminophosphine ligands were synthesised in good yields from the condensation of *N*-(2-(diphenylphosphino)benzaldehyde with the appropriate amine. All the ligands were fully characterised using spectroscopic and analytical techniques, including melting point, ^{1}H, ^{13}C, ^{31}P NMR, MS, IR spectroscopy and elemental analysis. A series of new metal complexes (Pd, Pt and Au) were obtained by coordination of the iminophosphine ligands in good yields. The complexes were characterised using the spectroscopic and analytical techniques mentioned above, with the exception of the palladium dichloride complexes that are highly insoluble in organic solvents. The structures of palladium complexes **74**, **79**, **80**; platinum complexes **84**, **86**, **88** and gold complexes **91**, **93** and **94** were unambiguously determined using X-ray crystallography. The structures of novel tetradentate ligands **65**, **66** and **68** were also determined using X-ray crystallography but attempts to complex them with palladium or platinum were unsuccessful.

The metal complexes were evaluated for their cytotoxicity against the oesophageal cancer cell lines WHCO1 and KYSE450. Platinum and gold complexes block the proliferation of WHCO1 and KYSE450 cells with an IC_{50} range of 2.16 - 9.44μM. The platinum and gold complexes exhibited better activity than cisplatin, while the chloromethyl palladium complexes were moderately active and exhibited IC_{50} values in the range 10.99 – 68.54μM for both cell lines. Our results show that these metal complexes have little effect on normal fibroblast cells (DMB) exhibiting IC_{50} values > 100μM which shows that these novel complexes are selective towards oesophageal cancer cells.

DECLARATION

I declare that the thesis "*Synthesis and Characterisation of Palladium, Platinum and Gold complexes and their Biological activity against Oesophageal cancer cell lines* " is my own work, that it has not been submitted before for any degree or examination in any other university, and that all the sources I have used or quoted have been indicated and acknowledged as complete references.

……..

Haleden Chiririwa

ACKNOWLEDGEMENTS

I am extremely grateful to my supervisors Professor J. R. Moss and Associate Professor D. T. Hendricks for their guidance and assistance throughout the course of this work. Their guidance and support kept me going. Thank you for all the encouragement and pushing me further than I ever thought possible.

Mintek and Project AuTEK for funding this project.

The technical staff in the Chemistry Department particular Mr A. Josephs, Mr P. Benincasa, Mr N. Hendricks, Mr P. Roberts, Mr G. Hesselink and Mr K. Achleitner and not forgetting Hajira and Robert from the Department of Medical Biochemistry .

Dr Hong Su and Dyanne Cruickshank for solving X-ray crystal structures.

My colleagues, both in the Organometallic Research Group and Cancer Research Group provided a wonderful working environment in which to work, and I'd like to acknowledge them for all their assistance on a range of topics, particularly Luke Esau for help in running the Western blotting assays.

Professor Ray Haines and Dr Gregory Smith for proof reading parts of this thesis and valuable comments passed.

Finally, my family for their continuous encouragement, support and guidance throughout my studies without which I wouldn't have achieved what I have today. This thesis is dedicated to you – you don't have to read this one.

TABLE OF CONTENTS

LIST OF FIGURES

Chapter 1

Chapter 2

Chapter 3

LIST OF SCHEMES

Chapter 1

Chapter 2

LIST OF TABLES

Chapter 2

Chapter 3

Chapter 4

ABBREVIATIONS

°	degrees
Å	Angstrom
Ar	aromatic
atm	atmosphere
br	broad
BSA	bovine serum albumin
ca	approximately
calcd.	calculated
CH_2Cl_2	dichloromethane
cisplatin	*cis*-diamminedichloroplatinum(II)
COD	1,5-cyclooctadiene
δ	chemical shift
DMEM	dulbecco's modified eagle's medium
dmso-d_6	deuterated dimethyl sulfoxide
DNA	deoxyribonucleic acid
d	doublet
dd	doublet of doublets
(DSB)	DNA double-strand breaks
EDTA	ethylenediaminetetraacetic acid
EI-MS	electron ionization mass spectrometry
Equiv	equivalent(s)
Et_2O	diethyl ether
FACS	fluorescence activated cell sorter
FT-IR	fourier transform infrared spectroscopy
g	gram(s)
h	hour(s)
Hz	hertz
IC_{50}	concentration of compound needed to inhibit cell growth by 50% against a single cell line
^{i}Pr	isopropyl
IR	infrared

J	coupling constant
m	multiplet
mp	melting point
m/z	mass to charge ratio
MHz	megahertz
Me	methyl
µl	microlitre
min	minute(s)
ml	millilitres
mmol	millimoles
MTT	(3-[4,5-dimethylthiazol-2yl])-2,5 diphenyltetrazolium bromide
NMR	nuclear magnetic resonance
PBS	phosphate buffered saline
PGM	platinum group metal
Ph	phenyl
ppm	parts per million
RIPA	radio immunoprecipitation assay
s	singlet
SARs	structure activity relationships
sh	shoulder
t	triplet
^{t}Bu	tertiary-butyl
TBS	tris buffered saline
THF	tetrahydrofuran
tht	tetrahydrothiophene

CHAPTER 1

LITERATURE REVIEW: APPLICATION OF METAL COMPLEXES AS ANTICANCER AGENTS

CONTENT

1.1 Introduction

According to the International Agency for Research on Cancer (IARC), in the year 2005, oesophageal cancer was reported as the ninth most common cancer in the world, and the sixth leading cause of cancer-related deaths worldwide [1]. A unique epidemiological feature of oesophageal cancer is its very uneven geographic distribution, with high incidence found within sharply demarcated geographic confines [2]. These geographic 'hot spots' include areas in Northern Iran, Kazakhstan, South Africa, and Northern China [3]. On the African continent, a number of reports have documented a very high incidence of oesophageal cancer in South Africa, particularly in the Transkei districts [4]. Considering the high incidence of this disease in South Africa, oesophageal cancer will be the focus in this thesis.

Cancer is fundamentally a disease, in which the cells proliferate indefinitely, due to dysregulated control pathways. Consequently, cancer cells continue to grow and divide yielding an ever increasing mass referred to as a tumour [5]. The tumour grows invasively, destroying surrounding body tissues. Cancer cells from this primary tumour may then spread, or metastasize, to other parts of the body, where new tumours may begin to grow. Eventually the tumour load will cause death, often by physically blocking or compressing blood vessels or organs such as the brain, or disrupting critical processes.

Cancer makes a contribution to morbidity and mortality worldwide, with the International Agency for Research on Cancer (IARC) estimating that for 2008, there were 12.4 million new cases of cancer, 7.6 million deaths from cancer and 28 million people alive with cancer within five years from initial diagnosis. They do report that

about half of the cases and about 60% of the mortalities were from medium and low income countries [6].

Transition metal-based anticancer drugs such as cisplatin have found widespread use, since they form highly reactive, charged, platinum complexes that bind to nucleophilic groups such as GC-rich sites in DNA, inducing DNA cross-links that result in apoptosis and cell growth inhibition. In SA, like in other countries worldwide, cisplatin is the drug prescribed when treating oesophageal cancer with chemotherapeutic agents. However, due to the severe adverse effects of cisplatin, that include nephrotoxicity, neurotoxicity, ototoxicity, nausea and vommitting, a second-generation of platinum compounds was developed, like carboplatin, nedaplatin, satraplatin and other closely related platinum anticancer agents, some of which are still used for the treatment of certain types of tumors.

1.2 Non-metal containing anticancer drugs

Not all chemotherapeutic agents that are used to treat cancer are metal based compounds. Infact, a wide repertoire of agents are used to treat cancers and at present, natural products, their derivatives and analogues are used as remedies and represents over 50% of all drugs in clinical use, with higher plant-derived natural products representing approximately 25% of the total [7]. Natural products have played an important role in the development of contemporary cancer chemotherapy.

Between 1960 and 1982 the National Cancer Institute (NCI) screened around 114,000 extracts from an estimated 35,000 plant samples for anticancer activity [8]. These include transition based compounds, natural products, natural product analogues,

antibodies and other small molecules. *In vitro* studies done on these compounds have resulted in a number of clinically useful drugs that are now available. Among these clinically useful drugs are paclitaxel (Taxol), vincristine (Oncovin) [9], podophyllotoxin (a natural product precursor) [10] and camptothecin [9, 10]. Besides natural products that have found direct application as drug entities, e.g. Taxol (Figure 1.1), there are many others that have served as chemical models or templates for the design, synthesis, and semi-synthesis of novel substances for treating diseases some of them include (1-pyrenylmethyl)amino alcohol derivatives, 2-amino-1,3-propanediol [11] and camptothecin (Figure 1.1).

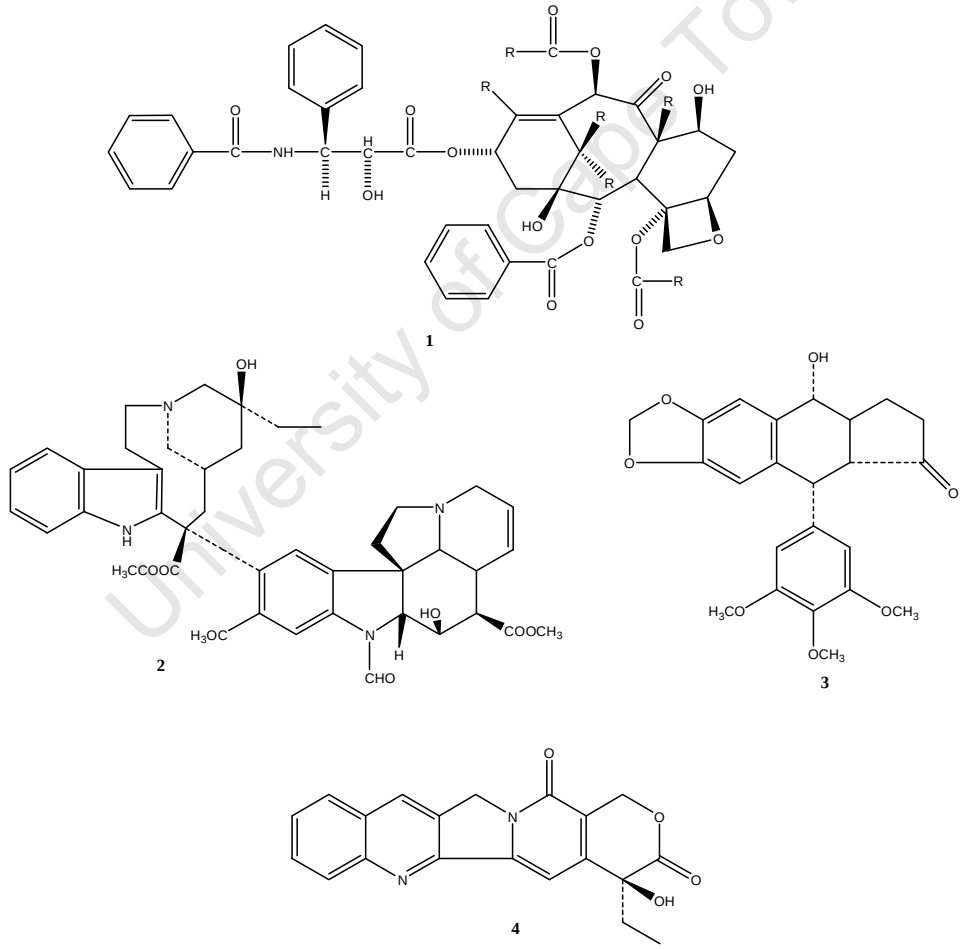

Figure 1.1. Structures of compounds among the clinically useful drugs. **1.** Taxol, **2**. Vincristine, **3**. Podophyllotoxin, **4**. Camptothecin.

Although significant progress has been made in cancer chemotherapy, some of the available drugs are less effective against many common cancers (colon, rectum, lung, prostate) [12] and are often very toxic. Paclitaxel (Figure 1.1) and tamoxifen (Figure 1.2) are the exceptions as they are effective drugs.

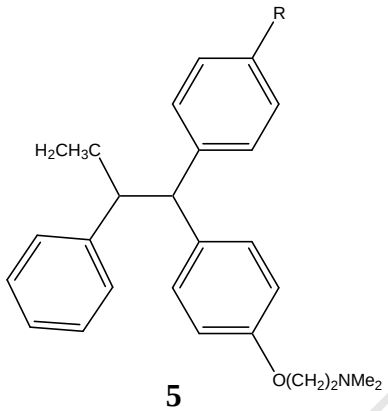

5

Figure 1.2 The structure of Tamoxifen (R= H) and its derivative Hydrotamoxifen (R= OH).

Despite wide repertoire of drugs other than cisplatin, there is still a place for metal containing drugs, inorganic compounds are relatively easy to synthesise whereas, the natural product compounds are found in smaller quantities in nature and their synthesis in the laboratory is very challenging, (considering it took 12 years to fully synthesise taxol). Even though these drugs, e.g. taxol and tamoxifen, have been shown to be more useful for certain types of cancer, e.g tamoxifen for breast cancer, further research on more effective drugs can be achieved by synthesis of other new metal containing compounds.

1.3 History of platinum based drugs

The first platinum-containing coordination complex to be used in cancer treatment was cisplatin (*cis*-dichlorodiammineplatinum(II)) (**6**) which was first synthesised 165 years ago by Peyrone [13] after whom it was named Peyrone's chloride. Its structure

was subsequently deduced by Alfred Werner [14]. In 1965, Rosenberg and colleagues reported its inhibitory activity on Escherichi coli division [15]. Cisplatin subsequently started being applied for clinical trials in the early 1970's and was approved for use by the US Food and Drug Administration (FDA) in 1978 [19].

In response to the chemotherapeutic effects of cisplatin, thousands of derivatives of cisplatin have since been synthesised and tested against cancer cells, but at most only about 30 reached clinical trials and more than half of these have already been rejected due to poor successes. Four other derivatives are available today and used clinically: cisplatin (**6**), available since 1978, and carboplatin (**7**), both being used world-wide, also oxaliplatin (**8**) which is available in a few countries, including France, and nedaplatin (**9**) which is available only in Japan and laboplatin (**10**). These compounds are not more active than cisplatin, but they are less toxic, thus they are prefered over cisplatin and their structures are in Figure 1.3.

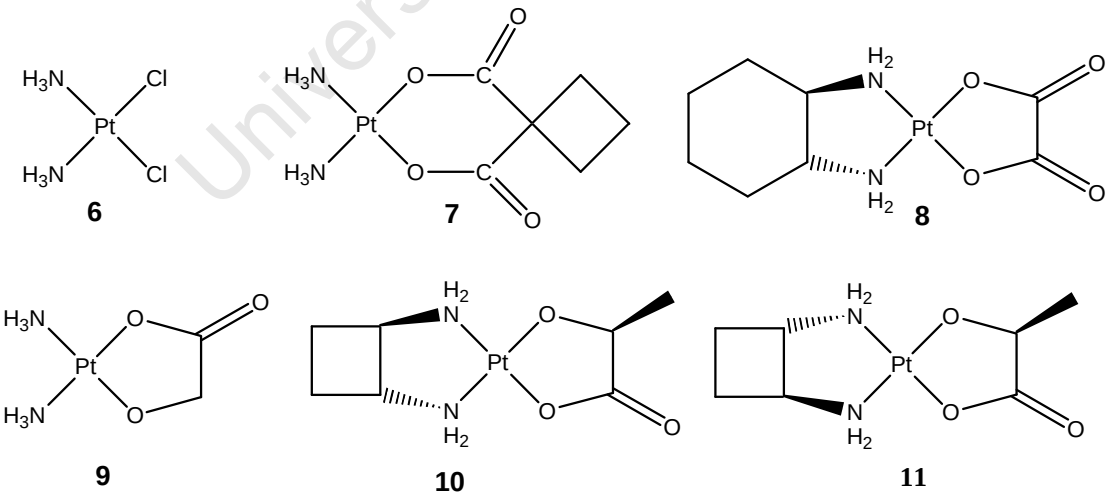

Figure 1.3 Structure of the platinum derivatives [16]. **6**. Cisplatin, **7**. Carboplatin, **8**. Oxaliplatin, **9**. Nedaplatin, **10**. **11**. Laboplatin

Further developments are shown schematically in Figure 1.4. Clinical use of cisplatin started in 1979, of carboplatin in 1989, and of oxaliplatin in 2004 [17]. The other compounds are not yet in routine clinical use. The ideas for new compounds arose from mechanistic findings on previous generations of drugs.

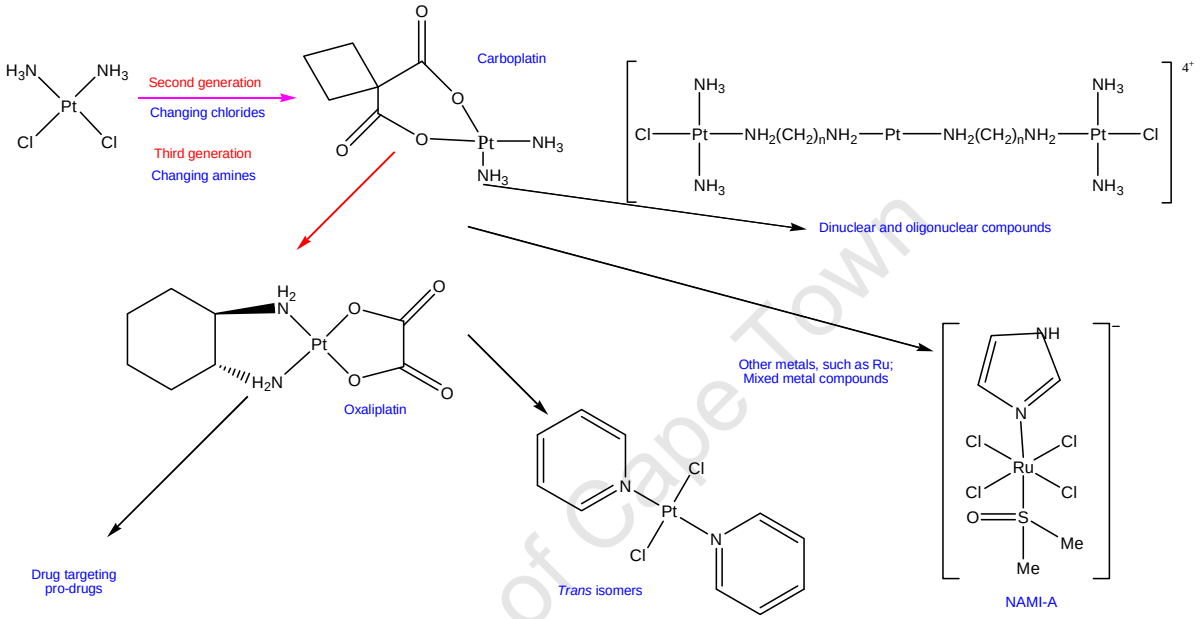

Figure 1.4 Schematic history of the development of platinum drugs. Substituting different amine and anionic ligands produced variations of cisplatin. Oxaliplatin has at least one H-donor function available on one of the amine groups. The steric and ligand exchange characteristics are different, especially for Pt(IV) compounds, as they react very slowly. The NH group assists by hydrogen bonding to a DNA backbone phosphate and makes the drug less prone to reversion by binding to the S-donor ligands in the cell.

Although compounds like cisplatin can effectively kill cancer cells, they have drawbacks, including intrinsic or acquired resistance, toxicity, and side effects such as gastrointestinal and haematological toxicity. These shortcomings of cisplatin provided a forceful impetus to the research on novel platinum complexes [18]. The initial driver for further platinum-drug development was the discovery of severe toxicity problems associated with cisplatin (**6**), especially nephrotoxicity.

Carboplatin (**7**) was selected for clinical use mainly because of its lower non-haematological toxicity compared with cisplatin (**6**) resulting in a more acceptable side-effect profile. The decreased toxicity is achieved by the substitution of the chloride leaving groups with a bidentate carboxylate, which renders the molecule less reactive. Unfortunately, it exhibits cross-resistance with its parent compound. The antitumour activity of carboplatin is not superior to that of cisplatin, but it has lower toxicity. Together, cisplatin and carboplatin now constitute the most important metal-based anti-cancer pharmaceuticals in general use.

Oxaliplatin (**8**) has a higher efficacy and a lower toxicity than cisplatin, and has no cross-resistance. It was designed to circumvent resistance, and thereby broaden the clinical utility of this class of compounds [19]. Oxaliplatin (**8**) is a more water-soluble variant of carboplatin (**7**), which retains activity against cancer cells with acquired resistance to cisplatin (**6**). Moreover, it has a broader spectrum of activity than cisplatin and carboplatin, proving valuable against colon cancers in combination therapy [20]. Oxaliplatin possesses a dicarboxylate leaving group, a bulky and hydrophobic chelating 1,2-diaminocyclohexane-carrier ligand, which increases the lipophilicity, which subsequently helps the drug to penetrate through cell membranes. The DNA adducts of oxaliplatin are more effective than those of cisplatin in inhibiting DNA chain elongation. Better cellular uptake and different conformation of DNA adducts are believed to help oxaliplatin in circumventing cisplatin resistance mechanisms [21, 22]. The hydrophobic chelating ligand is also believed to assist in inhibiting DNA transcription [23, 24, 25].

Nedaplatin (**9**) was developed because it produced better results than cisplatin in preclinical studies. Unfortunately, it shows cross-resistance with cisplatin. Other developments include the platinum(IV) drug satraplatin (**13**) (Figure 1.5), which is designed to be an orally available drug with a similar pharmacokinetic profile to carboplatin (**7**), and shows promise in this regard in terms of treatment regime, since it can be administered without hospitalisation. It shows low nephrotoxicity [26, 27, 28], possibly because Pt(IV) complexes are much more inert to ligand substitution reactions than their Pt(II) counterparts. It is also known that Pt(IV) complexes are reduced to Pt(II) complexes by extracellular and intercellular agents prior to reaction with DNA, and thus Pt(IV) complexes act as prodrugs [29, 30].

In solution, the large methylpyridine ligand of picoplatin (**12**) (Figure 1.5), is tilted 102° in relation to the platinum plane and this is designed to provide steric hindrance around the metal centre, thereby preventing the thiol coupling reactions that represent one of the main routes of cisplatin resistance. This hindrance reduces the reactivity of the drug towards water while maintaining reactivity with DNA [31]. Indeed, this compound has shown promising activity against both cisplatin sensitive and resistant cancers *in vivo* [32].

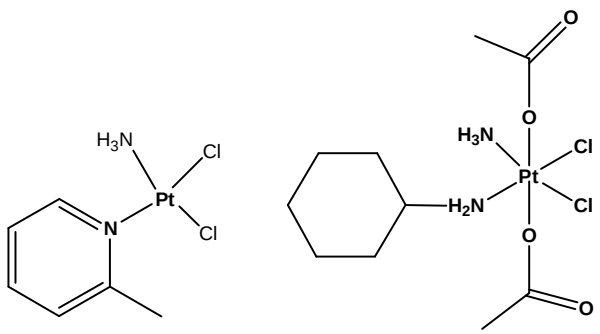

Picoplatin **Satraplatin**

12 **13**

Figure 1.5 Derivatives of cisplatin

Transplatin compounds follow different patterns of cell killing in comparison to cisplatin, thus giving a reason for optimism in their development as a new class of platinum-based anticancer drugs [33]. The initial report of anticancer properties of a dinuclear platinum complex in 1988 started a new paradigm in platinum-based chemotherapy. Several multinuclear platinum complexes have entered clinical trials in recent years, with varying results [34, 35].

1.3.1 Multinuclear platinum(II) complexes

Multinuclear platinum complexes comprise a novel class of compounds that have shown great potential for cancer chemotherapy [36]. These complexes contain two, three or four platinum centers with both *cis* and/or *trans* configurations and bind to DNA in a manner different from that of cisplatin. They react with DNA more rapidly than cisplatin and produce characteristic long-range inter- and intrastrand cross-linked DNA adducts [37]. The interstrand crosslinks are insensitive to repair by cellular extracts, which could enhance the cytotoxicity of multinuclear complexes [38].

One of the most popular examples of multinuclear Pt(II) anticancer complexes is BBR3464 (Figure 1.6), which exhibits antitumour activity against pancreatic, lung and melanoma cancers and is currently in phase II clinical evaluation [39]. The high positive charge and amine groups in BBR3464 facilitate the specific recognition of target sites on DNA through electrostatic and hydrogen-bonding interactions [40].

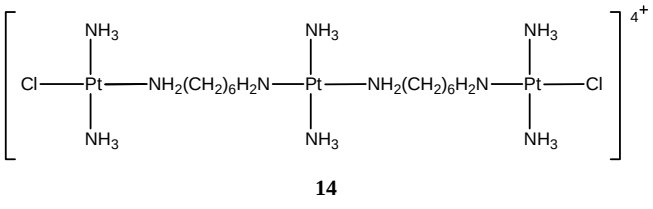

14

Figure 1.6 Structure of a multinuclear platinum drug BBR3464

Multi-nuclear platinum complexes are able to overcome both intrinsic and acquired resistance to cisplatin by a number of factors, including increased drug accumulation as well as forming more drug-DNA adducts [41, 42]. The additional positive charges assure a high affinity for polyanion DNA [43]. Therefore, DNA binding is usually much faster for cationic complexes as compared to neutral complexes such as cisplatin.

1.3.2 Structure/activity relationships of platinum complexes [44,45]

In general, for a platinum complex to have above average anticancer activity the compound needs to:

a) have a zero net charge;

b) have two leaving groups, or one bidentate leaving group;

c) have chloride leaving groups, or other similar ligands ;

d) have leaving groups in the *cis*-configuration;

e) not contain hydroxy or hydroxo ligands, as these make the complex highly toxic; and

f) have other non-leaving ligands which are inert, preferably amine ligands.

1.3.3 Biochemical mechanism of action of cisplatin

It is widely accepted that the main biochemical mechanism of action of cisplatin involves the binding of the drug to DNA in the cell nucleus and subsequent interference with transcription and/or DNA replication mechanisms [48]. Interestingly, the isomer of cisplatin, *trans*-diamminedichloroplatinum(II) or transplatin did not

show antitumor activity [46, 47]. A mechanistic explanation of transplatin inactivity has been based on the different type of DNA adducts formed by this isomer relative to cisplatin [48]. Cisplatin rapidly diffuses into tissues and is strongly bound to plasma proteins. Binding to plasma proteins is mainly due to the strong reactivity of platinum against sulphur of thiol groups of amino acids such as cysteine. Binding of cisplatin to cysteine-rich proteins in the kidney seems to be responsible for the dose-limiting nephrotoxic effects of the drug [49]. When cisplatin reaches a cell there are multiple potential reactions that could take place, including binding DNA as shown in Figure 1.7 below.

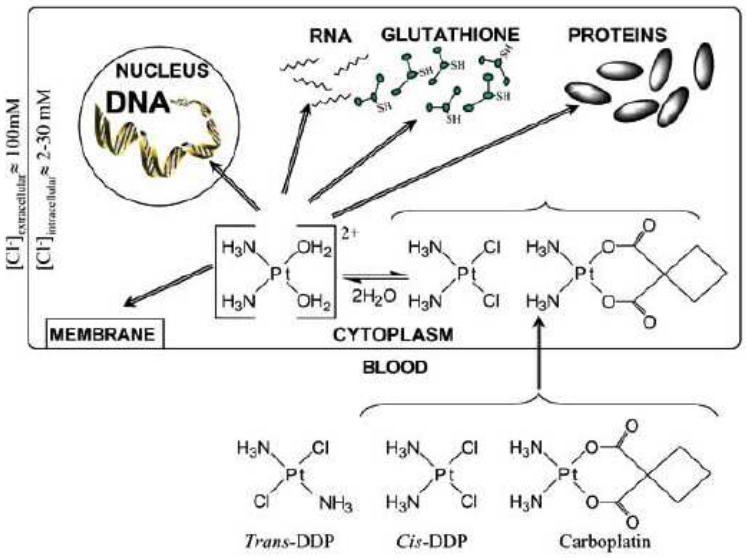

Figure 1.7 A schematic representation of the reactivity of *cis*-DDP inside cells. (Figure adapted from Fuertes *et al* [49]).

Available evidence suggests that cisplatin forms covalent adducts to purine bases on DNA, primarily guanine. In aqueous solution, the rate-limiting step in cisplatin complexation to DNA is 'activation' via the hydrolysis of labile Pt-Cl bonds (Figure 1.7). The kinetics of hydration are strongly dependent on the concentration of chloride ions in solution. Thus, in plasma ($[Cl^-] \geq 100$ mM), cisplatin is relatively stable,

whereas in the cytosol ($[Cl^-] \geq 20$ mM) the half-life for hydrolytic scission of a given bond is approximately 2 hours [50].

The hydrolysis of platinum drugs is of fundamental importance for the mechanism of action of these agents. Hydrolysis of cisplatin is believed to be the key activation step before the drug reaches intracellular DNA. Typical hydrolysis reactions of cisplatin and its diethylenetriamine (dien) analogue with the solvent effect have been studied by computational methods:

$$cis\text{-}[PtCl_2(NH_3)_2] + H_2O \rightarrow cis\text{-}[PtCl(OH_2)(NH_3)_2]^+ + Cl^- \quad \textbf{eqn 1}$$

$$cis\text{-}[PtCl(OH_2)(NH_3)_2]^+ + H_2O \rightarrow cis\text{-}[Pt(OH_2)_2(NH_3)_2]^{2+} + Cl^- \quad \textbf{eqn 2}$$

The positively charged mono and diaquo species of cisplatin {$[Pt(H_2O)Cl(NH_3)_2]^+$ and $[Pt(H_2O)_2(NH_3)_2]^{2+}$} are very reactive towards nucleophilic centres of biomolecules because H_2O is a much better leaving group than chloride [51]. Although the reactive species of both cisplatin and carboplatin are identical, Pt-O bonds are not as labile as Pt-Cl bonds which means that carboplatin is hydrolysed far more slowly and possesses a different pharmacologic profile [52].

The reaction of cisplatin with DNA may lead to the formation of various structurally different adducts. Initially, monofunctional DNA adducts are formed, but most of these react further to produce inter- or intrastrand cross-links [53, 54, 55]. It has been found that 60-65% of the adducts formed by cisplatin are 1,2-GpG intrastrand cross-links and 20-25% ApG intrastrand crosslinks. Minor adducts, include 1,3 intrastrand cross-links (≈ 2%) and interstrand cross-links (< 1%) as shown in Figure 1.8 below.

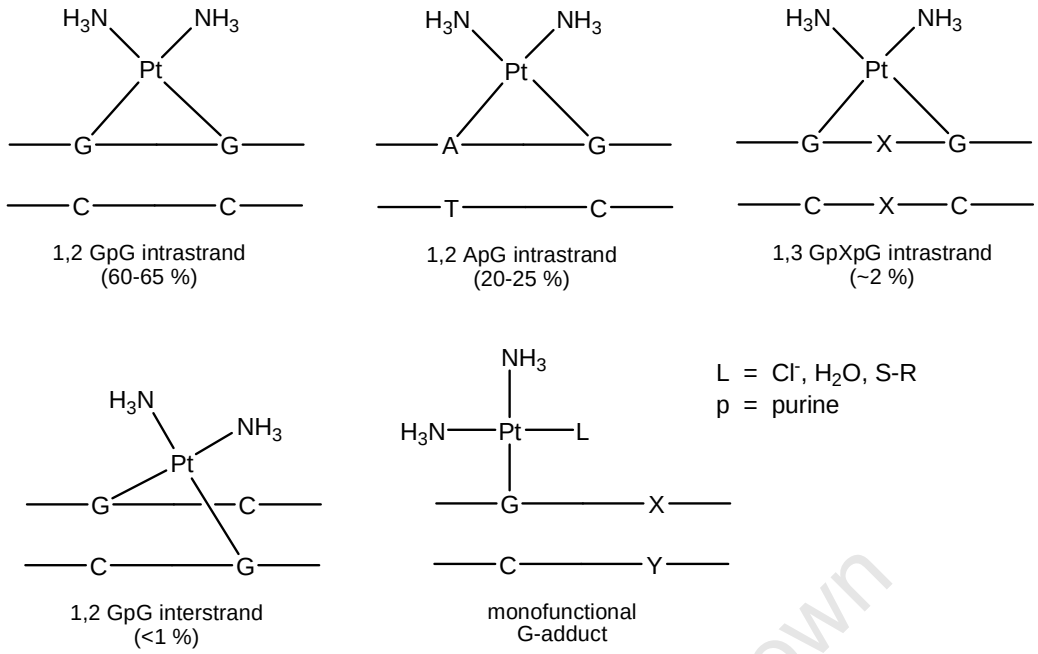

Figure 1.8 Types of cisplatin-DNA adducts and their frequency of formation [56].

DNA-protein crosslinks have also been reported [57, 58]. 1,2-intrastrand cross-links between two adjacent purine bases are the main adducts formed in the reaction of cisplatin with DNA. Therefore, the 1,2-intrastrand adducts are commonly held responsible for the anticancer activity of cisplatin, although this is not a proven fact. The binding of cisplatin to DNA induces structural distortions in the double helix, and attempts to repair cisplatin-DNA adducts may finally end up in the triggering of apoptosis (programmed cell death) [59, 60]. However, most cisplatin molecules bind to proteins rather than DNA, and there is experimental evidence that the former type of damage also plays a role in triggering the apoptotic pathways [60, 61]. Moreover, necrosis or cell death due to general cell machinery failure is also reported as a cell killing mechanism for cisplatin [60, 62].

The most important scavenger of cisplatin is the tripeptide glutathione (GSH) which is present in cells at concentrations of 0.5-10 mM. Glutathione and other thiols bind

rapidly and irreversibly to cisplatin [63]. The deactivated platinum-GSH adducts are excreted from the cell by the glutathione S-conjugate pump [64]. The non-specific toxic effects induced by binding to non-DNA targets may contribute to the mechanism of cytotoxicity of cisplatin in cancer cells. It is known, for instance, that the reaction with cisplatin blocks the enzymatic functions of several proteins [65, 66].

Cisplatin, and its early successes in the treatment of a variety of tumours, the topics of metal-DNA binding and platinum antitumour chemistry have attracted considerable interest from chemists, pharmacologists, biochemists, biologists and medical researchers. This interest has stimulated much interdisciplinary scientific activity, which has already yielded quite detailed understanding of the mechanism of action of cisplatin and related drugs. This knowledge has clearly resulted in much improved clinical administration protocols, as well as motivated research on other, related drugs containing transition metals, and their applications.

The unresolved disadvantages with cisplatin and its derivatives has stimulated research on novel non-platinum metal-containing antitumour therapeutics and considerable progress has been made in the development of such drugs. Complexes that have been tested in clinical phase I and phase II studies include those of ruthenium, titanium and gallium. Preclinical research has recently involved metal complexes containing metals such as iron, cobalt and gold.

This review describes some of the important and recent examples of new non-platinum based metal anticancer drugs which have shown promise.

1.4 Palladium(II) compounds

In the last 3 decades, the interest toward platinum(II) and palladium(II) complexes containing *N*- and *S* donor ligands has increased, resulting in the development of metal-based drugs exhibiting high anticancer activity together with reduced toxicity, compared to cisplatin and analogous compounds [67].

The development of palladium anticancer drugs has not been promising probably because their design has been based on structure-activity considerations generated from platinum antitumor drugs. Bearing in mind that Pd(II) complexes are about 105 times more reactive than their Pt(II) analogs, the low antitumoral activity of Pd compounds has been attributed to very rapid hydrolysis of the leaving groups that dissociate readily in solution [68] leading to reactive species far from their pharmacological targets. Palladium is a suitable candidate for metallodrugs because it displays structural properties similar to those of platinum and also exhibits promising cytotoxicity. Interestingly, the *trans*-$[PdL_2Cl_2]$-type complexes have been found to exhibit higher cytotoxicity than their *cis*-platinum analogues, *cis*-PtL_2Cl_2, for the same ligand system (L) dimethyl 5-(2-hydroxyphenyl)-1,3-dimethyl-1*H*-pyrazol-4-ylphosphonate and methyl 5-(2-hydroxyphenyl)-1,3-dimethyl-1*H*-pyrazole-4-carboxylate) [69, 70].

Several Pd(II) complexes have been reported to display favourable cytotoxicity at pH 6.8, a condition common in tumor cells, whereas the pH of normal cells is 7.4 [71]. Moreover, hydrolytic and DNA-binding studies on the Pd(II) and Pt(II) complexes with anticancer activities showed that the palladium complexes are kinetically labile,

produce new charged species to interact with DNA, and also bind to DNA at a faster rate than the platinum complexes [72].

The biomedical applications of metal complexes based on N-heterocyclic carbine ligand (NHC) [73, 74, 75] are just beginning to unfold, despite such complexes being very successful in homogeneous catalysis [76]. The group of Panda *et al* report the synthesis, structure, and biomedical applications of a series of transition metal-NHC complexes. They report two Pd complexes, [Pd(NHC)(pyridine)Cl_2] (**15**) and [Pd$(NHC)_2Cl_2$] (**16**), that display strong cytotoxicity against three different types of human tumor cell lines in culture shown in Figure 1.9.

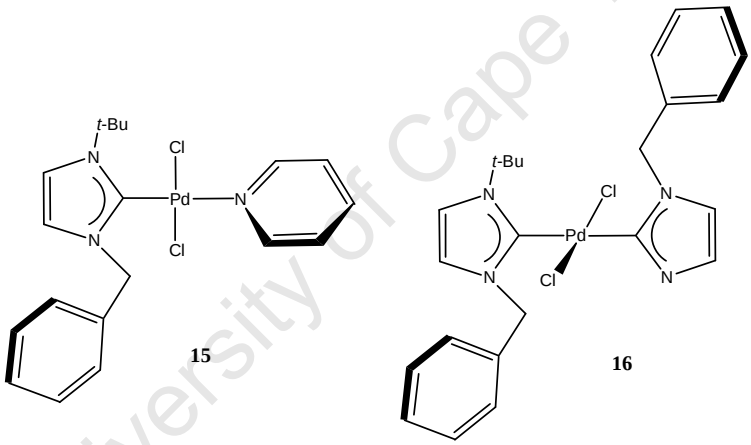

Figure 1.9 Structures of Palladium(II) compounds displaying strong cytotoxicity against cervical cancer, breast cancer and colon adenocarcinoma [77]

The Pd-NHC complexes **15** and **16** exhibit remarkable anticancer properties against cervical cancer (HeLa), breast cancer (MCF-7), and colon adenocarcinoma (HCT 116). **16** had a stronger inhibition effect on the proliferation of HeLa, MCF-7, and HCT 116 cells than cisplatin and a slightly lower inhibition of HeLa cell proliferation (3% at 10 μM) was observed in the case of **15**. **16** was found to be a more potent cytotoxic agent than the prevalent benchmark metallodrug, cisplatin. The observation of higher cytotoxicity in the *trans*-[Pd$(NHC)_2Cl_2$] complex **16**, containing two NHC

ligands with strong electron-donating abilities, as compared to the [Pd(NHC)-(pyridine)Cl_2] complex **15**, containing one NHC ligand, may be correlated to the relatively more electron-rich metal center in the former. The mode of action of **16** involves arresting the cells at the G2 phase, thereby preventing the mitotic entry of the cells. The blocked cells underwent cell death by a p53-dependent pathway [77].

Although a number of interesting Pd(II) targets have been investigated [78], the biological utility of such agents continues to be questioned, primarily due to the poor solubility of common Pd(II) complexes under physiological conditions. Recently Mostafa and Badria [79] have reported a new water-soluble mixed ligand complex [Pd(bpy)(dahmp)]Cl as shown in Figure 1.10.

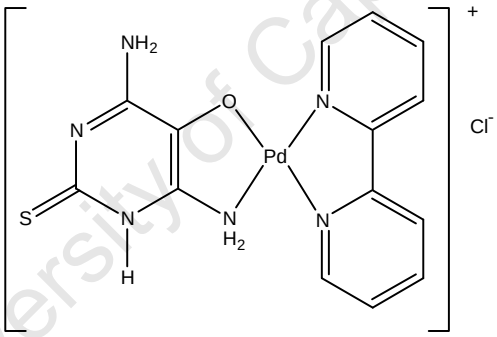

17

Figure 1.10 Structure of a water soluble [Pd(bpy)(dahmp)]Cl complex [79]

[Pd(bpy)(dahmp)]Cl is more effective than the free Hdahmp ligand itself, as the presence of both bpy and dahmp in the complexes possess a multi-ring planar structure with nitrogen bases and hence higher hydrophobicity, which would lead the intercalation more deeply into DNA. The reported complex displays significant anticancer activity against Ehrlich ascites tumor cells (EACs). The higher activity of the complex corresponds to its complete ionization in aqueous solution.

In order to investigate the action of Pd(II) complexes in the tumor DNA, the intercalated complexes affecting the structure of the DNA prevent polymerase and other DNA binding proteins from functioning properly. As the complexes covalently bind to DNA with preferential binding to the N-7 position of guanine and adenine, they are able to bind two different sites on DNA, producing cross-links that cause increase in the viscosity in comparison to the normal unbound DNA. This results in the prevention of DNA synthesis, inhibition of transcription, and induction of mutations [80].

Recently Keter *et al* [81] reported the study of the pro-apoptotic activity of palladium and platinum compounds in Chinese hamster ovary (CHO) cells, human cervical epitheloid carcinoma cells (HeLa and CaSki), and human T-cell leukaemia cells (Jurkat). The aim of their study was to evaluate the use of these complexes as possible anticancer agents in terms of their ability to induce apoptosis. Two palladium compounds (complexes **18** and **19**) and two platinum compounds (complexes **20** and **21**) were evaluated in this study. The platinum complexes were more cytotoxic than the palladium complexes. Platinum compounds (complexes **20**, **21** and cisplatin) displayed higher pro-apoptotic activity than the palladium compounds (complexes **18** and **19**). In addition, the pro-apoptotic activity of complexes **20** and **21** were also higher than for cisplatin.

Despite palladium and platinum being metals of the same group, their respective pyrazole complexes exhibit different activities. The authors attribute this to an associative substitution mechanism similar to that reported by Rauterkus *et al* [82] in which the kinetic behaviour of the two metal complexes differ. Platinum compounds

have been reported to be more stable in solution than palladium compounds [83] and thus would be less susceptible to translabilization, especially in the biological milieu, as opposed to palladium compounds.

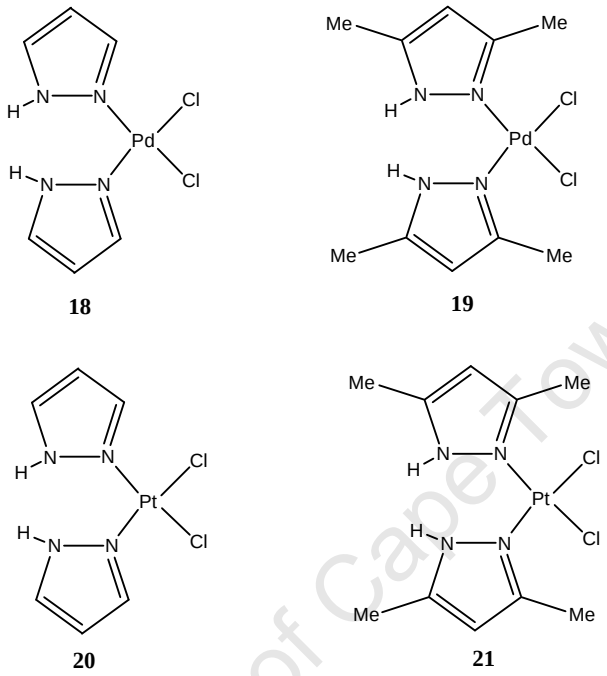

18 **19**

20 **21**

Figure 1.11 Palladium and platinum complexes tested for anticancer activity dichlorobis(pyrazole)palladium(II) (**18**), dichloro-bis(3,5-dimethylpyrazole)palladium(II) (**19**), dichloro-bis(pyrazole)platinum(II) (**20**), and dichloro-bis(3,5-dimethylpyrazole)platinum(II) (**21**) [81]

The authors chose palladium(II) and platinum(II) pyrazole complexes for this study for two reasons. Firstly, they all resemble cisplatin structurally and are expected to bind biological molecules in a similar manner. Secondly, the electronic properties of pyrazole ligands offer metal centres for late transition metals that are quite electrophilic to allow coordination to biological molecules. The bulkiness of the pyrazole ligands also appears to affect activity. For example the activity of complex **20** was significantly higher than that of cisplatin. There is a probability that such bulky ligands prevent translabilization and undesired displacement of the non-leaving ligand by other nitrogen donors [84] and complex **20** could be acting through a similar

mechanism that induces the formation of DNA-adducts, promoting the activation of apoptosis.

1.5 Gold(I) compounds

Auranofin (**25**), an orally absorbed gold(I) phosphine complex, had been used for the treatment of rheumatoid arthritis [32], and early reports also suggested that this compound and other gold phosphine complexes were also active against the growth of cultured tumour cells [85, 86, 87, 88]. Auranofin itself has proved cytotoxic against HeLa cells *in vitro* and P388 leukaemia cells *in vivo* [89, 90].

Gold(I) thiolates employed clinically in the treatment of rheumatoid arthritis display some potency against various tumours but a greater potential is found in their analogues [91]. In particular, analogues featuring a linear P-Au-S arrangement in which the thiolate ligand is derived from a biologically active thiol display high potency.

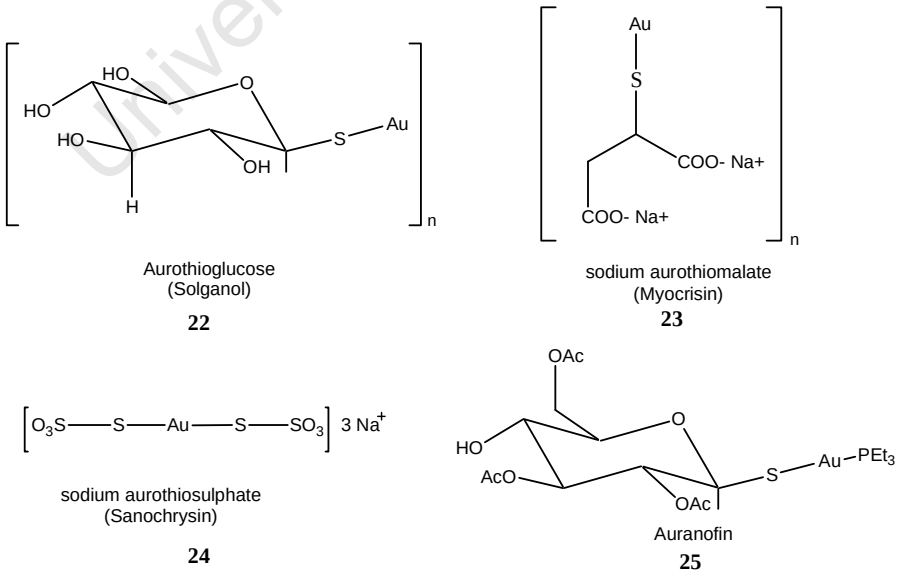

Aurothioglucose (Solganol) **22**

sodium aurothiomalate (Myocrisin) **23**

sodium aurothiosulphate (Sanochrysin) **24**

Auranofin **25**

Figure 1.12 Gold(I) complexes used in anti-arthritis therapy

Aurothioglucose (solganol) **22** is neutral, and the charged species aurothiomalate (myocrysin) **23**, aurothiosulphate (sanocrysin) **24**, and aurothiopropanol sulphonate (allocrysin) all feature gold in the +I oxidation state. The structures are thought to feature linear -S-Au-S-geometries and are also polymeric. The gold(I) thiolates, being water soluble owing to the presence of solubilising groups and/or charge, are administered parenterally. The gold compounds are functioning as pro-drugs, providing a means of delivering 'gold' to sites of inflammation [90].

More than 60 gold(I) compounds were evaluated against both B16 melanoma and P388 leukemia cells and this work showed that a wide variety of phosphine gold(I) thiolates display significant cytotoxicity and the presence of a phosphine ligand was very important as was shown by the fact that the gold thiolates, i.e. without phosphine, had significantly reduced potency [92, 93, 94, 95, 96]. Mirabelli *et al* proved that removal or replacement of the acetyl groups in the thiosugar of auranofin (**25**) or a change to other thiosugars did not significantly influence the potency [97] e.g chloro(triethylphosphine)gold(I) (**27**), an analogue of auranofin, in which the thiosugar is replaced by chlorine. Chlorotriethylphosphine gold(I) (TEPAu) (**27**) is an organo-gold compound that has therapeutic activity in animal models of rheumatoid arthritis. Initial studies have suggested that TEPAu is a potent cytotoxic compound *in vitro* against a variety of cultured cell types and isolated hepatocytes. Preliminary experiments have indicated that triethylphosphine gold chloride (TEPAu) may induce the peroxidative decomposition of cellular membrane lipids [98].

Promising anticancer results were achieved with a series of digold phosphine complexes. The lead compound was [$(AuCl)_2$ dppe] (**28**) (Figure 1.13). The dppe

ligand itself exhibits antitumour activity, and it has been suggested that the gold serves to protect the ligand from oxidation and aids in the delivery of the active species. There is substantial evidence to support a direct role for the gold in the anticancer activity of this complex [99]. The digold phosphine complex was shown to rearrange to give the tetrahedral complex $[Au(dppe)]^+$ **29** (Figure 1.13) [100]. The tetrahedral complex is more stable as the chelate effect stabilises the compound, and the phosphine ligand is more inert to substitution by the types of thiolate ligands that could be encountered in a biological environment.

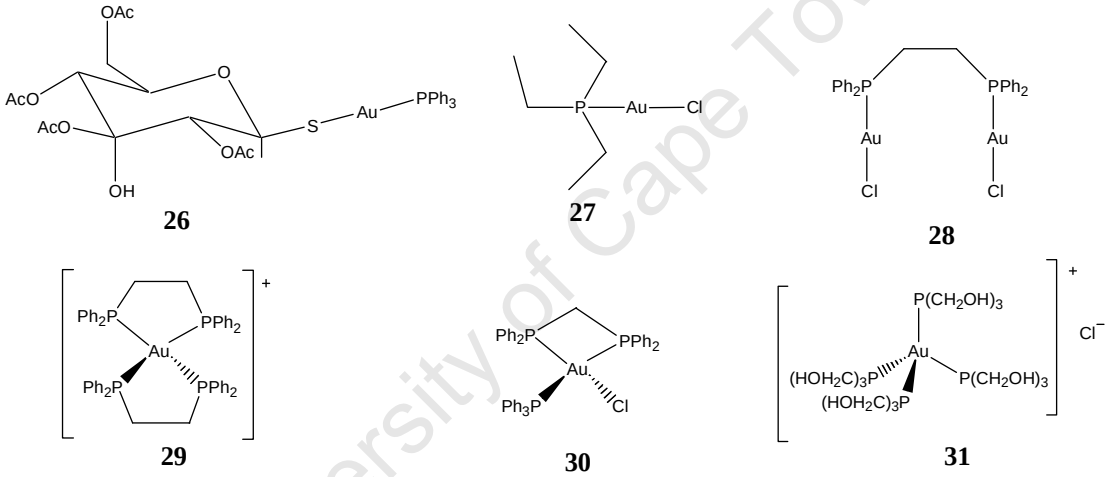

Figure 1.13 Examples of gold(I) phosphine complexes

Gold complexes with bis(diphenylphosphino)ethane ligands such as cationic tetrahedral four coordinated $[Au(dppe)_2]Cl$ (**30)** (Figure 1.13) were found to be cytotoxic to tumour cells, produced DNA-protein cross links and DNA strand breaks in cells and inhibited protein, DNA and RNA synthesis. $[Au(dppe)_2]Cl$ changed the inner mitochondrial membrane potential, increased mitochondrial respiration, swelling and permeability [101]. Recently, a hydrophilic tetrakis((tris(hydroxymethyl))phophine)gold(I) complex (**31**) was reported to be cytotoxic to several tumor cell lines. With HCT-15 cells, derived from human colon

carcinoma, cell cycle studies revealed that inhibition of cell growth may result from elongation of the G1 phase of the cell cycle [102].

A big step in the development of gold compounds as anticancer drugs may be the observation that the gold(I) complexes auranofin (**25**) and aurothioglucose (**22**) significantly inhibit the enzyme thioredoxin reductase [103, 104]. Thioredoxin reductase is a selenoenzyme involved in physiological processes and many that are involved in cancer cell growth like nucleotide biochemistry [105]. This prevents the repair of mitochondrial enzymes damaged by oxidation. More importantly, an excess of the oxidized form of thioredoxin is a crucial signal promoting mitochondrion-mediated apoptosis [106].

1.6 Gold(III) compounds

Whereas the majority of gold(I) compounds feature gold in a coordination geometry defined by 'soft' (i.e. easily polarisable) sulphur and/or phosphorus atoms, gold(III) compounds generally feature 'hard' atom donors such as nitrogen, oxygen and carbon. Four-coordinate gold(III) is found in square planar geometries and in this regard resembles the situation found for cisplatin and thus gold in the +III oxidation state is isoelectronic with platinum(II) and forms similar square-planar complexes. Ligand exchange kinetics are relatively slow in both cases, although faster in gold(III) complexes.

Since gold(III) complexes have similar chemical characteristics to platinum(II) compounds they have been considered as candidates for development and testing as potential anticancer drugs, but unfortunately their relatively poor chemical stability in

solution heavily hindered such studies for a long time. Thus, until the mid-90's, only a few reports existed in the literature describing the cytotoxic properties and the *in vivo* antitumor effects of gold(III) complexes [107, 108]. Given that the mammalian environment is generally reducing, compounds containing gold(III) may be expected to be reduced *in vivo* to gold(I) and metallic gold. There is a rich literature of anti-tumour/cytotoxicity investigations for these species.

Through implementation of appropriate ligand selection strategies, a number of gold(III) compounds have been obtained, exhibiting sufficient stability under physiological-like conditions and manifesting, in some cases, relevant cytotoxic properties *in vitro* [109]. The mononuclear gold(III) complexes that have been characterized include: gold(III) polyamines [110], gold(III) polypyridines [111,112], gold(III) porphyrins [113], various organogold(III) compounds, and gold(III) dithiocarbamate complexes [114, 115].

1.6.1 Structural features of some gold(III) complexes

Organogold(III) compounds bearing the bipyridyl moiety have also been synthesised by the group of Giovanni Minghetti in Sassari (Italy) and typical compounds of this family are shown in Figure 1.14.

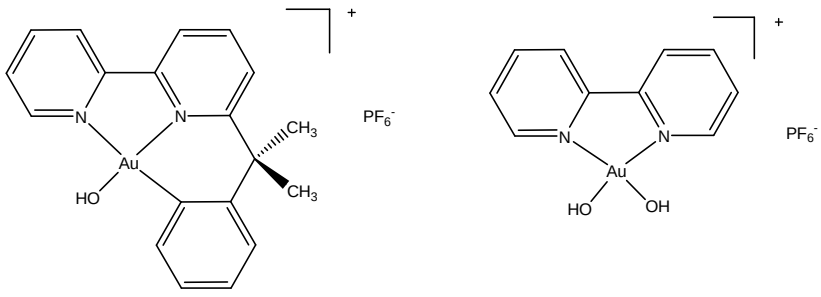

Figure 1.14 Organogold(III) complexes having a bipyridyl moiety

These complexes are characterized by the presence of a bipyridyl ligand within a square planar arrangement of the gold(III) center. In $[Au(bipy)(OH)_2][PF_6]$, two coordination positions of the square planar environment are occupied by two nitrogens of the bipyridyl ligand, the remaining positions being occupied by two hydroxide groups. $[Au(bipy\text{-}H)(OH)][PF_6]$ is an organogold(III) complex (bipy) 6-(1,1 dimethylbenzyl)-2,2'-bipyridine).

The *in vitro* cytotoxic properties of these gold(III) complexes were first evaluated toward the human ovarian carcinoma cell line A2780 either sensitive (A2780/S) or resistant (A2780/R) to cisplatin. Both bipyridyl gold(III) complexes show significant cell killing effects with IC_{50} values falling in the micromolar range. $[Au(bipy\text{-}H)(OH)][PF_6]$ is the most active with a cytotoxic activity 2 times higher than cisplatin in the A2780/R cell line. The cytotoxic properties of the free 2,2' bipyridyl ligand were also tested; this ligand is virtually devoid of toxicity toward the A2780/S cell line while it showed some cytotoxicity at high concentrations in SKOV3 cells. (another ovarian cancer cell line) [109].

The interactions of the bipyridyl gold(III) complexes with calf thymus DNA were analyzed by a variety of techniques Although some small effects on DNA conformation and stability were detected, results suggested that the gold(III) chromophore was not significantly modified and that binding of these gold(III) complexes to calf thymus DNA was relatively weak and DNA conformation was not largely affected. The authors were convinced that since DNA damage was relatively modest it was therefore very unlikely to account for the observed cytotoxic properties. They deduced that other DNA independent mechanisms were probably operative and

this was what lead to the observed biological effects. It was observed that binding of these complexes to model proteins was tight and might represent the molecular basis of the biological action of these gold(III) complexes.

New gold(III) compounds have been synthesised and characterised that show sufficient stability under physiological conditions. Such stability has generally been achieved by the selection of appropriate ligands and in most cases those bearing nitrogen atoms as donor groups. Some of these gold(III) complexes are shown in Figure 1.15.

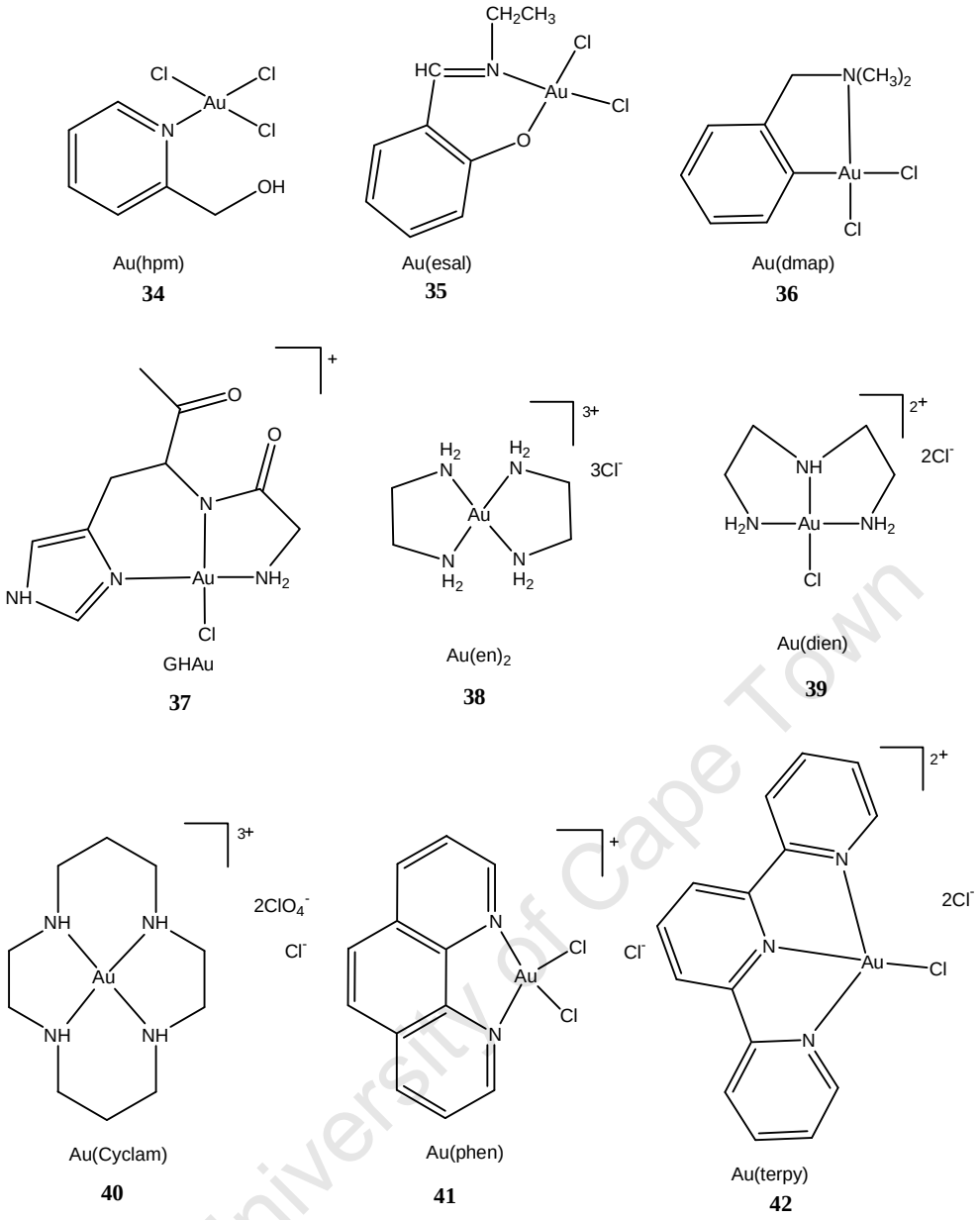

Figure 1.15 Examples of some gold(III) complexes [110]

Given their reasonable stability under physiological conditions, the cytotoxic properties of the gold(III) complexes were also evaluated toward the established A2780 ovarian human cell line either sensitive (A2780/S) or resistant (A2780/R) to cisplatin. The order of the cytotoxic potency of the investigated gold(III) complexes from experiments [116] was found to be the following: Auterpy ≥ Auphen > Auen, Audien ≥ Aucyclam. Remarkably Auen, Auphen, Auterpy, and Audien retain most of

their cytotoxic properties when tested on the cisplatin-resistant line. They also tested the cytotoxic properties of the free ligands and found that terpyridine and *o*-phenanthroline also exhibit important cytotoxic properties, whereas the other three ligands (ethylenediamine, diethylenetriamine, and cyclam) are virtually devoid of any intrinsic cytotoxicity. These results strongly support the view that cytotoxicity, for Auen and Audien, can be safely ascribed to the presence of the gold(III) center. One approach has been to synthesize complexes with a mono-negative bidentate ligand, damp, (2-[(dimethylamino)methyl]phenyl), and two monodentate anionic ligands e.g. CI or acetate (OAc) (Figure 1.16).

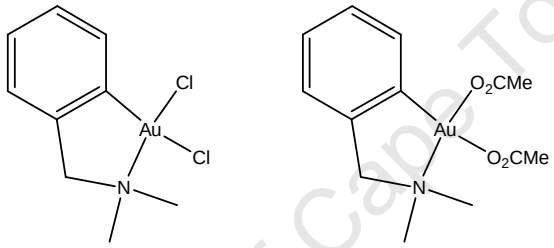

43 **44**

Figure 1.16 The structures of gold(III) compounds with antitumour activity; (**43**) [$AuCI_2$(damp)], (**44**) [$Au(OAc)_2$(damp)] [117].

The damp ligand forms part of a five-membered chelate ring in which the nitrogen of the amine group and the carbon of the aryl ring bond to the metal. The monodentate ligands are readily hydrolysed and are available for substitution. Biochemical studies [117] indicate that these compounds have a mechanism of action significantly different to that of cisplatin suggesting that this is a potentially important novel class of metal-containing antitumour agents.

When the two chloride ligands are replaced by acetate or malonate anions, the resulting complexes also exhibited good, selective cytotoxicities *in vitro* against a

panel of tumour cell lines and displayed *in vivo* antitumor activity in human tumor xenograft models [118]. These results open the possibility that the substitution of the chloride ligands by other anions could lead to new active complexes. In this sense, the thiosemicarbazonate anion (TSC^-) is a good option because some thiosemicarbazones themselves exhibit antineoplastic activity [119]. Preliminary tests showed that [Au(damp-C1; N)Cl_2] derivatives containing bi- or tridentate thiosemicarbazonate ligands showed antitumor activity against human MCF-7 breast cancer cells [120, 121].

1.6.2 Structure/function relationships of gold(III) complexes

Analysis of the cytotoxicity data of the gold(III) complexes permitted formulation of some preliminary structure/function relationships. The cytotoxicity of these gold(III) complexes is associated with the presence of the gold(III) center. The $[Au(en)_2]^{3+}$ and $[Au(dien)]^{3+}$ complexes are significantly more cytotoxic than the corresponding platinum compounds. The presence of hydrolysable chloride groups which are good leaving groups on the gold(III) center does not represent an essential requirement for cytotoxicity. Excessive stabilization of the gold(III) center results in loss of biological activity as seen in the $[Au(cyclam)]^{3+}$ complex, with the gold(III) center tightly bound to the macrocycle cage, is not cytotoxic, probably as a consequence of its low reactivity. The amount of gold that enters cells is roughly proportional to the exposure time, at least during the first hours. Thus, at least qualitatively, the longer the exposure time, the lower the drug concentration required to kill cells [116].

Most of the gold(III) compounds are able to overcome to a large extent resistance to cisplatin as witnessed by the relatively low resistance index values, suggesting a different mechanism of action with respect to cisplatin.

1.7 Titanium complexes

The first non-platinum complex tested in clinical trials was *cis*-$[Ti(IV)(CH_3CH_2O)_2(bzac)_2]$ (Figure 1.17), it was used against a wide variety of ascites and solid tumors [122,123,124].

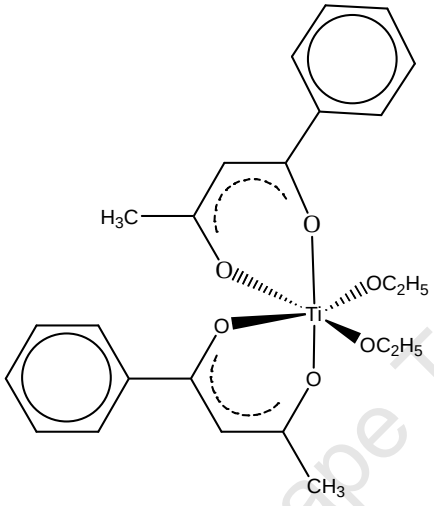

45

Figure 1.17 Structure of a *cis* isomer of $[Ti(IV)(CH_3CH_2O)_2(bzac)_2]$ complex.

However, the medicinal properties of transition metal organometallic complexes were not explored until 1979, when Köpf-Maier and Köpf published the first metallocene with antitumor activity, titanocene dichloride, Cp_2TiCl_2 (Figure 1.18) [125].

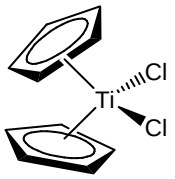

46

Figure 1.18 Structure of titanocene dichloride.

Cp_2TiCl_2 was the most active complex, showing its best activity against colon, lung and breast cancers [126]. In contrast to platinum complexes, titanocene dichloride showed no evidence of nephrotoxicity or myelotoxicity [127, 128]. It was found that

titanocene dichloride inhibited DNA synthesis, bound covalently to the DNA and induced apoptosis [129]. Based on these medicinal properties, titanocene dichloride then went on clinical trials [130, 131, 132, 133, 134]. Unfortunately, the efficacy of Cp_2TiCl_2 in Phase II clinical trials in patients with metastatic renal-cell carcinoma [132] or metastatic breast cancer [135] was too low to be pursued. The mechanism and biological action of Cp_2TiCl_2 seems to be different from that of cisplatin and any other metal-containing drug.

Little synthetic effort has been employed to overcome the mentioned efficacy problems. Therefore the research of Tackes' group focussed on the synthesis of substituted titanocene dichloride anti-cancer drugs. By using a novel method starting from titanium dichloride and fulvenes [136, 137, 138, 139] highly substituted ansa-titanocenes [140, 141, 142, 143, 144, 145, 146, 147], containing a carbon-carbon bridge, have been synthesised, such as [1,2-bis(cyclopentadienyl)-1,2- bis-(4-N,N dimethylaminophenyl)-ethanediyl] titanium dichloride.

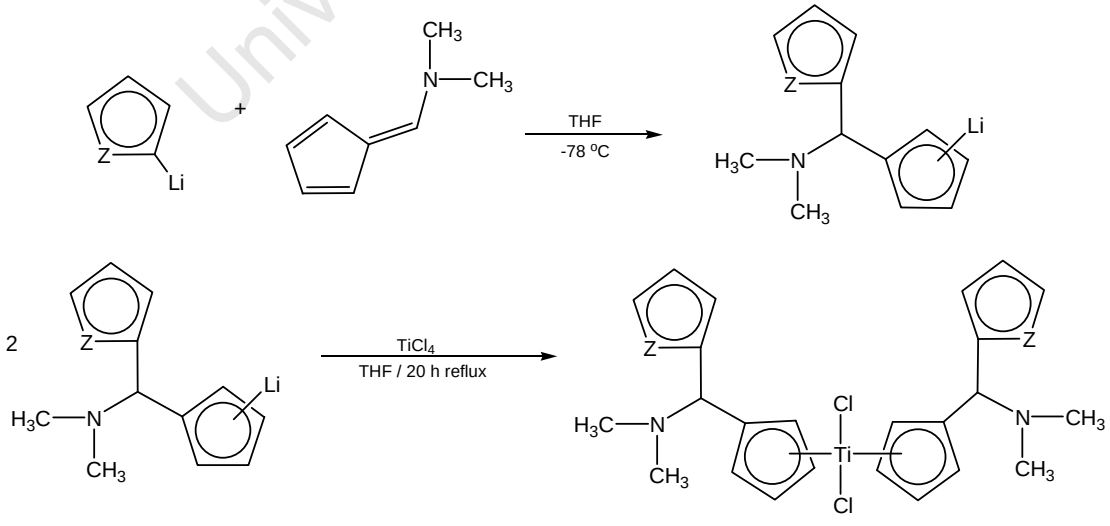

47

Scheme 1.1 Synthesis of titanocenes (Z = S, O, N–CH_3).

The main disadvantages of titanocene compounds, which lead to low activities are their poor solubilities in aqueous media and their hydrolytic instability under physiological conditions [148, 149]. More recently Allen *et al* [150] have reported a number of new ionic titanocenes and evaluated their cytotoxic properties, which are shown to have significantly better activity and stability than their non-functionalised counterparts.

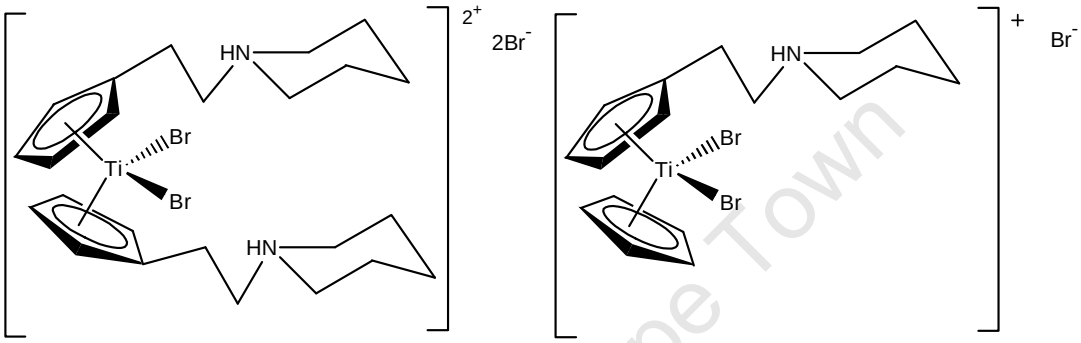

48 **49**

Figure 1.19 Structures of ionic titanocenes evaluated for cytotoxic activity

In particular they exhibit a potent cytotoxic effect on cisplatin-resistant ovarian tumour cell lines. The addition of two trimethylsilyl groups, shown in Scheme 1.2 yields a highly potent amino-functionalised titanocene dichloride.

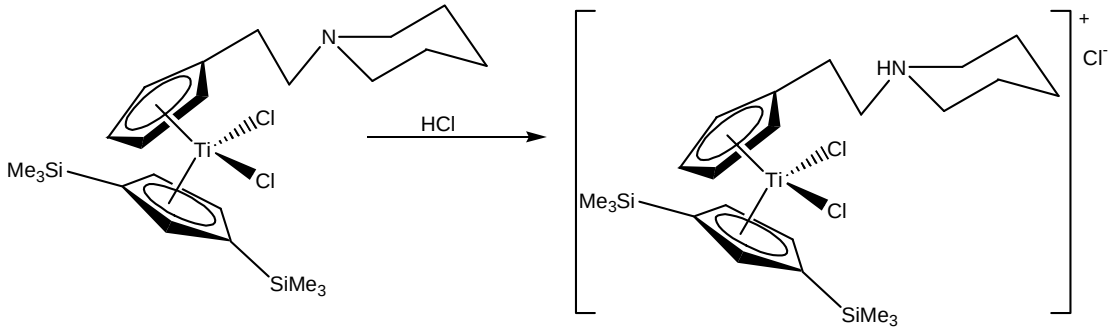

50

Scheme 1.2 Synthesis of a functionalised titanocene dichloride

The potency of the functionalised titanocenes is not greatly effected by the addition of one trimethylsilyl group, However, the addition of two trimethylsilyl groups, has a dramatic effect, increasing the cytotoxic activity significantly against several cell lines. The mechanism of action is still unknown for this class of drugs but from the experiments carried out it, can be seen that the compounds form interstrand crosslinks with cellular DNA [150].

1.8 Ferrocene compounds

Ferrocene has long been recognized as an important constituent in the biomedical applications of organometallic chemistry [151, 152]. However, ferrocene itself does not exhibit anticancer activity [128]. Ferrocene complexes have been investigated for their potential biological activity, but these studies have been hampered because ferrocene is insoluble in aqueous systems [126]. The insolubility of ferrocene has been overcome to some extent by the preparation of the ferrocenium cation or through the preparation of ferrocenyl inclusion complexes with cyclodextrin [153] but this does not bring about effective anticancer properties [154]. Anticancer activity is however, well documented for the oxidized form of ferrocene, the ferrocenium cation [154]. Earlier, several cisplatin-type ferrocenyl platinum complexes were prepared and their potential antitumour activity investigated (see for example Figure 1.20 below) [155].

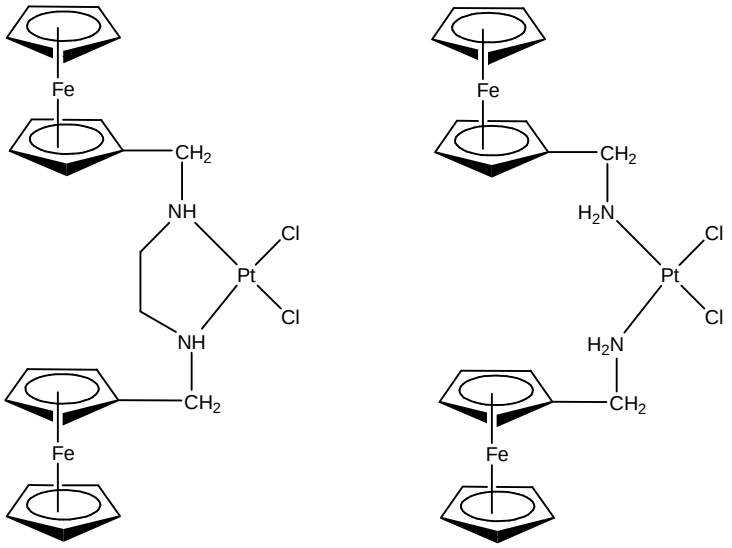

51 **52**

Figure 1.20 Cisplatin-type ferrocenyl platinum complexes [155]

Ferrocene has also been incorporated into water soluble polymers [156], tethered to DNA intercalators [157], phosphino compounds [158], vitamin B1 [159], and other biomolecules [160]. A variety of other small ferrocenyl molecules [161] have also been investigated for anticancer activity. Cytotoxic pathways involving DNA have been suggested for the activity of ferrocenyl compounds [162].

Work by Osella *et al.* [163, 164] illustrated considerable cytotoxic activity of the ferrocenium cation and its more stable decamethylferrocenium derivative against Ehrlich ascites tumour cell lines and breast cancer MCF- 7 cell lines, respectively. Mechanistic studies indicate that the anticancer activity of the ferrocenium cation can be linked to its reactivity with molecular oxygen (or superoxide anions) that causes generation of reactive oxygen species (ROS) including •OH radicals. These radicals are responsible for DNA degradation and strand-breakage. Results reported by Tamura and Miwa [165] confirm these observations and suggest the possibility of DNA cleavage caused by the activity of ferrocenium cations. Addition of thiourea (which is

known as an •OH scavenger) to a ferrocenium cation DNA mixture decreases cleavage and addition of dithiothreitol (DTT) triggers an enhanced scission. Thus, it is clear that the ferrocenium cations, where the iron atom is in the +3 oxidation state, are cytotoxic and efficient DNA cleaving agents.

Some simple ferrocene compounds show excellent cytotoxicities *in vitro* and inhibit the development of tumors *in vivo* [166]. A more widespread approach pioneered by Jaouen is to append biologically active molecules to the ferrocenyl unit which increases the potency of the overall compound, possibly due to the combined action of the organic molecule with Fenton chemistry of the Fe center [167]. Ferrocene has also been linked to both platinum [168, 169] and gold [170] centers in order to achieve synergistic effects between the two active metals.

1.9 Ruthenium compounds

Early reports in the 1970s and 1980s indicated antitumour potential of ruthenium complexes [171, 172, 173]. Medicinal ruthenium chemistry was reviewed in 2001 [174] and the early work of Clarke was reviewed in 2003 [175]. Recent excellent work from the Trieste groups on the NAMI-class compounds [176] which are the new antitumour metastasis inhibitor (NAMI)- type compounds. As octahedral complexes the NAMI-A complexes, differ structurally significant from the square planar platinum(II) drugs. The NAMI-type compounds all contain Ru(III), and it is believed that prior to biological, cytostatic action, reduction to Ru(II) may take place [175]. Despite the inactivity *in vitro* NAMI-A type complexes displayed significant anticancer activity *in vivo* [177] and this was attributed to anti-metastatic properties of these agents [178]. The mechanism of action of the ruthenium compounds is poorly known, and even the fact

that DNA is an important target is not sure as yet [179]. Although the kinetics of ruthenium coordination chemistry are comparable to those of platinum, and even though a number of active ruthenium compounds do react with DNA and DNA fragments, the mechanism of action for the ruthenium compounds is currently far less understood. Targets other than DNA may play a role as well here.

Also of interest are the azopyridine compounds, where different isomers show significantly different cytostatic activity. The structures and activity indicators are given in Figure 1.21 [17].

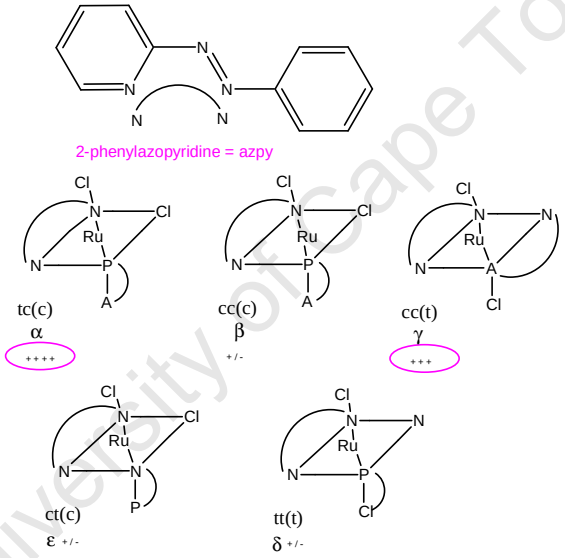

Figure 1.21 Five different isomers of a $Ru(azpy)_2Cl_2$ complex and their relative cytostatic activity (++++ = very active; t = trans; c = cis for each pair of ligand atoms (anions in parentheses).

Octahedral ruthenium(II) and ruthenium(III) complexes have shown antineoplastic properties on a number of experimental tumors. Tetraammine-, pentaammine-, heterocycle-, and dimethylsulfoxide-coordinated ruthenium complexes have been synthesized and shown to have high affinity for nitrogen donor ligands *in vitro* and as a result exhibit anticancer action *in vivo* [180, 181].

Many ruthenium complexes with oxidation state +2 or +3 display anti-tumour activity, especially against metastatic cancers. The Ru(III) complex *trans* [Na][Ru(Im)(Me_2SO)Cl_4] (Im = Imidazole) and its analogue, *trans* [ImH][Ru(Im)(Me_2SO)Cl_4], (Figure 1.22) are currently in clinical trials [175]. For Ru(III) compounds, *in vivo* reduction to Ru(II) is required for activity. This facilitates its binding to the highly electrostatically charged DNA molecule. Cellular uptake of many ruthenium complexes appears to be mediated by the iron transport protein transferring process (stimulated by protein transferrin) into the tumor cells where upon it is reduced.

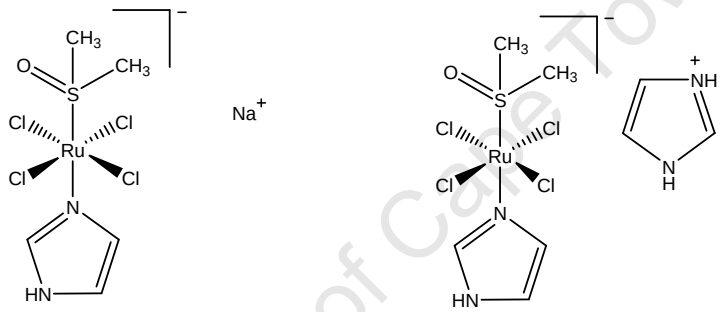

53 **54**

Figure 1.22 Structures of *trans*-[Na][Ru(Im)(Me_2SO)Cl_4] and *trans* [ImH][Ru(Im)(Me_2SO)Cl_4] complexes active against metastatic cancers

In general, the cytotoxicity of ruthenium complexes and other metals correlates with their ability to bind DNA following intracellular activation by their reduction. However other researchers have reported complexes that have shown a different mode of action. No conclusive explanation as to its mode of action is known but it is reported that it does not involve DNA binding but rather it interferes with type IV collagenolytic activity and reduces the metastatic potential of the tumors [175].

Ruthenium compounds exhibit low general toxicity compared to their platinum counterparts, which is probably due to two main reasons. Firstly, ruthenium

compounds specifically accumulate in rapidly dividing cells, such as tumors, due to the ability of ruthenium to mimic iron in binding to transferrin [182], the protein which delivers iron to cells, because transferrin receptors are overexpressed in cancer cells [183]. Secondly, the majority of ruthenium drugs comprise ruthenium in the +3 oxidation state, and it has been proposed that in this oxidation state ruthenium is less active and reduced *in vivo* to more active ruthenium(II) complexes, a process favored in the hypoxic environment of a tumor [183e, f]. It should however be noted that Ru(II) compounds also exhibit a low general toxicity. Since cancer cells can also become oxidising at certain stages of their growth cycle, oxidation of the ruthenium cannot be ruled out [184].

1.10 Vanadium compounds

Other significant metal complexes that have been studied are the vanadium complexes. Although speculation (which has been proven) that these metal complexes may possess anti-tumour activity had existed since the beginning of the 20th century, these complexes were not tested until 1967. The first evidence that vanadium may exert chemopreventive effects on experimental carcinogenesis was provided by Thompson *et al.* on 1-methyl-1-nitrosurea (MNU-1) -induced mammary carcinogenesisin female Sprague-Dewley rat [185]. They then proposed that the chemotherapeutic action of vanadium, in biological terms, was found to be mediated through inhibition of altered liver cell foci and hepatic nodule growth during the early stages of neoplastic transformation as reported elsewhere by Bishaye and Chatterjee [186].

Vanadocenes are organometallic complexes, with the vanadium(II) linked to organic ligands by direct carbon metal bonds. They have been found to exhibit significant antitumour properties both *in vitro* and *in vivo*. Bis-(cyclopentadienyl)vanadium(II)chloride, $[(\eta_5\text{-}C_5H_5)_2VCl_2]$ (Figure 1.23), which belongs to the metallocene class of antitumour agents, has turned out to be one of the most promising compounds as a drug among the various non-platinum metal complexes.

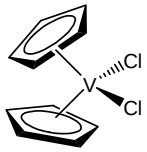

55

Figure 1.23 Bis(cyclopentadienyl)vanadium(II) chloride (vanadocene dichloride)

Vanadocene dichloride has been shown to be a potent antitumour agent against mouse tumours and its activity is due to its ability to interact at a molecular level with nucleic acids, especially DNA. Furthermore, the antitumor effects of vanadocene dichloride against human colon and lung carcinomas were shown to be due to the vanadium accumulation in nucleic acid-rich regions and to the inhibition of DNA and RNA synthesis in tumor cells suggesting the binding of this compound to the DNA [187].

1.11 Other metal-based anticancer compounds

Other transition metals have been used as anticancer drugs, including bismuth(III) labelled antibodies for systemic radio immunotherapy [188, 189], rhenium(I) complexes as DNA-binding agents [190], a $Zn^{2+}(MTR)_2$ complex that induces cancer cell death by binding to chromatin [191], and a Cu^{2+} compound chlorophyllin has been shown to

initiate apoptosis in human colon cancer cells through caspase-8 and apoptosis-inducing factor (AIF) activation in a cytochrome *c*-independent manner [192].

Rh(I), Rh(II) and Rh(III) complexes have shown interesting anticancer properties. Some rhodium metallointercalators exhibit specific DNA binding, suggesting that they represent a new type of DNA-targeting agents [193]. One binds specifically to destabilized regions near base pair mismatches and is able to recognize a single mismatch in a 2725-base pair plasmid DNA. The most common systemic side-effect of rhodium is nephrotoxicity. Its mechanism of action has not yet been studied systematically. However, it is possible that the inhibition of DNA synthesis is mediated by the inhibition of essential enzymes.

Dimeric μ-acetato dimers of rhodium(II) as well as monomeric square planar rhodium(I) and octahedral rhodium(III) complexes have shown interesting antitumour properties. The dirhodium tetraacetate complex, $[Rh_2(CH_3COO)_4(H_2O)_2]$, (Figure 1.24) is much more inhibitory towards *Escherichia coli* DNA polymerase I and exhibits good antitumour activity against P388 lymphocytic leukemia and sarcoma 180 but little activity against L1210 and B16 melanoma [194]. Recent structural studies suggest that the antitumour activity of di-rhodium(II) carboxylates may bear analogy to that of cisplatin by binding to adjacent guanines on DNA [195]. Antitumour activity has also been found to increase in the series $[Rh_2(RCOO)_4(H_2O)_2]$ (R = alkyl group) with the lipophilicity of the R group and is independent of its reduction potential [194].

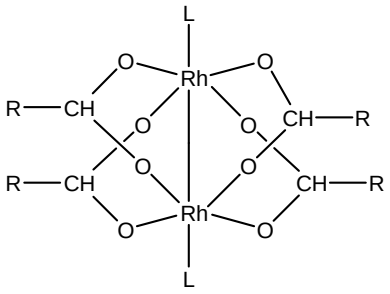

56

Figure 1.24 Six-coordinate cage complex of rhodium(II) carboxylates, $[Rh_2(RCOO)_4L_2]$, R = alkyl group, L = H_2O or other donor solvent.

Thus rhodium(II) acetate (R = CH_3), propionate (R = CH_3CH_2), butyrate (R = $CH_3CH_2CH_2$), pentanoate (R = $CH_3CH_2CH_2CH_2$) show a considerable variation in their antitumour activity against Ehrlich ascites tumour cells in mice, with the pentanoate complex being the most active. Lengthening the carboxylate alkyl (R) chain beyond the pentanoate was found to reduce the drugs' therapeutic efficacy.

Recently, Rajput *et al* [196, 197] reported the preparation of a series of complexes of the type (1,5-cyclooctadiene)(chloro)(L)rhodium(I) with L a substituted pyridine. They place particular emphasis on ferrocenyl, phenyl and other aromatic systems as substituents on the pyridine ring. The antitumor activity of the complexes was compared based on structural differences, see Figure 1.25.

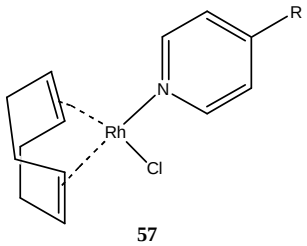

57

R = H, Ph, $(C_6H_4)Fc$, $(C{=}N)(C_6H_4)Fc$

Figure 1.25 Rhodium complexes [RhCl(COD)L] investigated as antitumor agents

The role played by the position and nature of substituent on the pyridyl ligand was evaluated. Several rhodium complexes showed significant activity for both the

WHCO1 and ME180 cancer cell lines. The authors report that it appears that derivitisation of the pyridyl ligand is related to enhanced toxic activity. However the major drawback was that the rhodium complexes were only partially soluble in aqueous environment.

1.12 Concluding remarks

An enormous amount of work has been done on metals and metal compounds, some can induce cancer while others can treat cancer and some can have both properties. It appears that research on some metals that had been abandoned for some time is being reactivated. The efficacy of cisplatin has given an impetus to research for new metal compounds. The results are not yet satisfactory and a great deal of work remains to be done. Approximately two-thirds of cancers could be avoided by life style changes (cigarettes, alcohol, nutrition, sexual behaviour, etc.). Therefore it is statistically easier to avoid cancer than to cure it. It would also be more efficient to protect our cells from mutations, rather than focussing exclusively on curing cancer.

Recent advances in medicinal inorganic chemistry demonstrate significant prospects for the utilization of Au(I) and Au(III) and their coordination complexes as drugs, presenting an interesting arena for inorganic chemistry. Significant progress in gold-based anticancer agents has been achieved, based in part on a mechanistic understanding of the pharmacological effects of classical antitumor drugs. There are quite a number of results indicating that gold coordination compounds might be developed into future drugs, but it will be a long time before their pharmacological potential can be realised. It will take even longer to have a suitable candidate turned into a clinically acceptable drug. The future development of medicinal inorganic

chemistry of Au(I) and Au(III) and their coordination complexes requires an understanding of the physiological processing of gold complexes, to provide a rational basis for the design of new gold-based drugs.

1.13 Aims of the project

This thesis addresses the preparation and anticancer activity of novel platinum group metal complexes containing phosphorus and nitrogen-donor groups. Since the preparation of cisplatin was first reported [13], numerous reports have appeared describing the biological activity of other transition metal complexes. Preliminary investigations of the activity of several complexes prepared in this study have been carried out and comparison made with related complexes reported in the literature but not tested for anticancer activity.

The primary aim of this project is to identify the metal compounds with promising anticancer activity, focusing on three metal centres; gold(I), platinum(II) and palladium(II). The choice of palladium as one of the metals is based on the fact that it is a homologue of platinum and thus is expected to show similar activity, and it is relatively cheap. Several complexes especially platinum containing, with *N*-heterocyclic ligands such imidazole, thiozole, benziimidazole, benzoxazole and benzothiozole have been reported. However it is noted that little has been done on complexes based on *N* and *P* donor ligands. The choice of gold was based on the fact that no complexes of gold have been reported in the literature with these types of iminophosphine ligands.

1.14 Objectives of the project

The major goal of the project is to identify and characterise novel compounds that can be used in the treatment of oesophageal cancer, using cultured oesophageal cancer cells as a model system. Oesophageal cancer has a high prevalence in South Africa and it causes a great number of mortalities and as such there is need for novel chemotherapeutic agents to help treat this disease.

1) The project focused on the design, synthesis and characterisation of a series of new iminophosphine ligands.

2) The iminophosphine ligands were then complexed with palladium, platinum and gold to give novel organometallic complexes.

3) The biology aspect of the project involved evaluating the effect of the complexes on cell growth. We determined IC_{50} values for the different compounds in two different oesophageal cancer cell lines, WHCO1 and KYSE450. The activity of the complexes was also evaluated against DMB cells which are primary fibroblasts derived from a skin biopsy obtained from a normal subject.

4) We also investigated whether the compounds induce apoptosis by employing the PARP cleavage assay and also their ability to bind DNA.

1.15 References

[1] Parkin D. M, Whelan S. L, Ferlay J, Storm H, in Cancer incidence in five continents, *IARC CancerBase No 7*, **2005**.

[2] Ahmed N, Cook P, *Br. J. Cancer*, **1969**, 23, 302.

[3] Gatei D. G, Odhiambo P. A, Orinda D. A, Muruka F. J, *Cancer Res*., **1978**, 38, 2. 303.

[4] Roth J, Putman A , Allen S. L, Aslene A. F: *Cancer*: Principles and Practise of Oncology: 4th Edition **1993**.

[5] Evans C. W, *The Mestatic Cell: Behaviour and Biochemistry*, **1991**, 2nd Ed., Chapman and Hill, London.

[6] Boyle P, Levin B, in *World Cancer Report 2008*, 15.

[7] Balandrin N. F, Kinghorn A. D, Farnsworth N. R, in *Human Medicinal Agents from Plants,* Kinghorn, A. D, Balandrin, N. F, Eds., *ACS Symposium Series,* **1993,** 534, 2.

[8] Cragg G. M, Boyd M. R, Cardellina J. H Grever M. R, Schepartz S. A, Snader K. M, Suffness M, Kinghorn A. D, Balandrin M.F, *Eds*., *ACS Symposium Series*, **1993**, 534, 81.

[9] Gerzon K, in *Anticancer agents Based on Natural Products Models,* Cassady J. M, Douros J. D, Eds., Academic Press, **1980**, 271.

[10] Jardine I. in *Anticancer Agents Based on Natural Products Models*, Cassady, J. M, Eds, Academic Press, **1980**, 319.

[11] Bair K. W, Tuttle R. L, Knick V. C, Cory M, McKee D. D, *J. Med. Chem*., **1990**, 33, 2385.

[12] Abdulla M, Gruber P, *Biofactor*s, **2000**, 12, 45.

[13] Peyrone, M. *Ann. Chem. Pharm*., **1845**, 51, 1.

[14] Trzaska S, *Chemical & Engineering News*, **2005**, 53.

[15] Rosenberg B, Van Camp L, Krigas T, *Nature*, **1965**, 205, 698.

[16] Desoize B, Madoulet C, *Critical Reviews in Oncology/Hematology*, **2002**, 42, 317.

[17] Reedjik J, *Plat. Met. Rev*., **2008**, 52, 2.

[18] Galanski M, Jakupec M. A, Keppler B. K, *Curr. Med. Chem.*, **2005**, 12, 2075.

[19] Kelland L, *Nature Reviews, Cancer*, **2007**, 7, 573.

[20] Giacchetti S, Perpoint B, Zidani R, Le Bail N, Faggiuolo R, Focan C, Chollet P, Llory J. F, Letourneau Y, Coudert B, Bertheaut-Cvitkovic F, Larregain-Fournier D, Le Rol A, Walter S, Adam R, Misset J. L, Levi F, *J. Clin. Oncol.*, **2000**, 18, 136.

[21] Woynarowski J. M, Faivre S, Herzig M. C. S, Arnett B, Chapman W. G, Trevino A. V, Raymond E, Chaney S. G, Vaisman A, Varchenko M, Juniewicz P. E, *Mol. Pharmacol*., **2000**, 58, 920.

[22] Hector S, Bolanowska-Higdon W, Zdanowick W, Hitt J, Pendyala S, *Cancer Chemother. Pharmacol*., **2001**, 48, 398.

[23] Rixe O, Ortuzar W, Alverez M. *Biochem. Pharmacol.*, **1996**, 52, 1855.

[24] Raymond B, Faivre S, Woynarowski J. M, *Semin. Oncol.*, **1998**, 25, 1.

[25] Schmidt W, Chaney S. G, *Cancer Res*., **1993**, 53, 799.

[26] Casazza A. M, Rose W. C, Comerski C, Oleson R, Fairchild C, *Proc. Am. Assoc. Canc*., **1992**, 33, 536.

[27] McKeage M. J, Morgan S. E, Boxall F. E, Hard G. C, *Ann. Oncol.*, **1992**, 111.

[28] McKeage M. J, Boxall F. E, Jones M, Harrap K. R, *Cancer Res.*, **1994**, 1.

[29] Raynaud F. I, Mistry P, Donaghue A, Poon G. K, Kelland L. R, Barnard C. F. J, Murrer B. A, Harrap K. R, *Cancer Chemother. Pharmacol.*, **1996**, 38, 155.

[30] Talman E. G, Kidani Y, Mohrmann L, Reedijk J, *Inorg. Chim. Acta*, **1998**, 283,

251.

[31] Holford, J, Raynaud F, Murrer B.A, Grimaldi K, Hartley J. A, Abrams M, Kelland L. R, *Anti-Cancer Drug Des.*, **1998**, 13, 1.

[32] Allardyce C. S, Dorcier A, Scolaro C, Dyson P. *J. Appl. Organomet. Chem.*, **2005**, 19, 1.

[33] Radulovic S, Tesic Z, Manic S, *Curr. Med. Chem.*, **2002**, 9, 17, 1611.

[34] Wheate N. J, Collins J. G, *Curr. Med. Chem: Anti-Cancer Agents*, **2005**, 5, 3, 267.

[35] Chan H.-L, Ma D.-L, Yang M, Che C.-M, *J. Biol. Inorg. Chem.*, **2003**, 8, 7, 761.

[36] Wheate N. J, Collins J. G, *Coord. Chem. Rev.*, **2003**, 241, 133.

[37] Hegmans A, Berners-Price S. J, Davies M. S, Thomas D. S, Humphreys A. S, Farrell N, *J. Am. Chem. Soc.*, **2004**, 126, 2166.

[38] Kãspárková J, Zehnulova J, Farrell N, Brabec V, *J. Biol. Chem.*, **2002**, 277, 48076.

[39] Farrell N, *Met. Ions Biol. Syst.*, **2004**, 42, 251.

[40] Zehnulova J, Kãspárková J, Farrell N, Brabec V, *J. Biol. Chem.*, **2001**, 276, 22191.

[41] Perego P, Caserini C, Gatti L, Carenini N, Romanelli S, Supino R, Colangelo D, Viano I, Leone R, Spinelli S, Pezzoni G, Manzotti C, Farrell N, Zunino F, *Mol. Pharm.*, **1999**, 55, 528.

[42] Servidei T, Ferlini C, Riccardi A, Meco D, Scambia G, Segni G, Manzotti C, Riccardi R, *Eur. J. Cancer*, **2001**, 37, 930.

[43] Rauter H, di Domenico R, Menta E, Oliva A, Qu Y, Farrell N, *Inorg. Chem*., **1997**, 36, 3919.

[44] Cleare M. J, Hoeschele J. D, *Plat. Met. Rev.*, **1973**, 17, 3.

[45] Cleare M. J, Hoeschele J. D, *Bioinorg. Chem.*, **1973**, 2, 187.

[46] Rosenberg B, Van Camp L, *Cancer Res*., **1970**, 30, 1799.

[47] Kociba R. J, Sleight S. D, Rosenberg B, *Cancer Chemother. Rep.*, **1970**, 54, 325.

[48] Jamieson E. R, Lippard S. J, *Chem. Rev.*, **1999**, 99, 2467.

[49] Fuertes M. A, Castilla J, Alonso C, Pérez J. M, *Curr. Med. Chem.*, **2003**, 10, 257.

[50] Bancroft D. P, Lepre C. A, Lippard S. J, *J. Am. Chem. Soc*., **1990**, 112, 6860.

[51] Miller S. E, House D. A, *Inorg. Chim. Acta*, **1991**, 187,125.

[52] Go R. S, Adjei A. A, *J. Clin. Oncol.*, **1999**, 17, 409.

[53] Bancroft D. P, Lepre C. A, Lippard S. J, *J. Am. Chem. Soc.*, **1990**, 112, 6860.

[54] Payet D, Gaucheron F, Sip M, Leng, M, *Nucleic Acids Res.*, **1993**, 21, 5846.

[55] Barnham K. J, Berners-Price S. J, Frenkiel T. A, Frey U, Sadler P. J, *Angew. Chem. Int. Edit. Engl.*, **1995**, 34, 1874.

[56] Fuertes M. A, Castilla J, Alonso C, Pérez J. M, *Curr. Med. Chem: Anti-Cancer Agents*, **2002**, 2, 539.

[57] Zwelling L. A, Anderson T, Kohn K. W, *Cancer Res.*, **1979**, 39, 365.

[58] Auge P, Kozelka J, *Transit. Met. Chem.*, **1997**, 22, 91.

[59] Cohen S. M, Lippard S. J, *Prog. Nucleic Acid Res. Mol. Biol*., **2001**, 67, 93.

[60] González V. M, Fuertes M. A, Alonso C, Pérez J. M, *Mol. Pharmacol.*, **2001**, 59, 657.

[61] Kruidering M, van de Water B, Zhan Y, Baelde J. J, de Heer E, Mulder G. J, Stevens J. L, Nagelkerke J. F, *Cell Death Differ.*, **1998**, 5, 601.

[62] Lau A. H, *Kidney Int.*, **1999**, 56, 1295.

[63] Lempers E. L. M, Reedijk J, *Adv. Inorg. Chem.*, **1991**, 37, 175.

[64] Ishikawa T, Ali-Osman F, *J. Biol. Chem.*, **1993**, 268, 20116.

[65] Louie A. Y, Meade T. J, *Chem. Rev.*, **1999**, 99, 2711.

[66] Sartori D. A, Bierbach U, Miller B, Farrell N, *J. Inorg. Biochem.*, **1999**, 74, 286.

[67] Faraglia, G, Fregona D, Sitran S, Giovagnini L, Marzano C, Baccichetti F, Casellato U, Graziani R, *J. Inorg. Biochem.*, **2001**, 83, 31.

[68] Gill D. S, in: Hacker M. P, Douple E. B, Krakoff I. H, (Eds.), *Platinum Coordination Complexes in Cancer Chemotherapy*, Nijhoff, Boston, **1984**, 267.

[69] Navarro M, Pena, N P, Colmenares I, Gonzalez T, Arsenak M, Taylor P, *J. Inorg. Biochem.*, **2006**, 100, 152.

[70] Budzisz E, Krajewska U, Rozalski M, Szulawska A, Czyz M, Nawrot B, *Eur J. Pharm.*, **2004**, 502, 59.

[71] Friebolin W, Schilling G, Zoller M, Amtmann, E, *J. Med. Chem.*, **2005**, 48, 7925.

[72] Gonzalez M. L, Tercero J. M, Matilla A, Niclos-Gutierrez J, Fernandez M. T, Lopez M. C, Alonso C, Gonzalez S, *Inorg. Chem*., **1997**, 36, 1806.

[73] Kascatan-Nebioglu A, Melaiye A, Hindi K, Durmus S, Panzner M. J, Hogue L. A, Mallett R. J, Hovis C. E, Coughenour M, Crosby S. D, Milsted A, Ely D. L, Tessier C. A, Cannon C. L, Youngs W. J, *J. Med. Chem.*, **2006**, 49, 6811.

[74] Barnard P. J, Wedlock L. E, Baker M. V, Berners-Price S. J, Joyce D. A, Skelton B. W, Steer J. H, *Angew. Chem., Int. Ed.*, **2006**, 45, 5966.

[75] Ozdemir I, Denizci A, Ozturk H. T, Cuetinkaya B, *Appl. Organomet. Chem.*, **2004**, 18, 318.

[76] (a) Lin I. J. B, Vasam C. S, *Coord. Chem. Rev.*, **2007**, 251, 642;

(b) Garrison J. C, Youngs W. J, *Chem. Rev.*, **2005**, 105, 3978;

(c) Peris E, Crabtree R. H, *Coord. Chem. Re*v., **2004**, 248, 2239;

(d) Arnold P. L, *Heteroat. Chem.*, **2002**, 13, 534;

(e) Herrmann W. A, *Angew. Chem., Int. Ed.*, **2002**, 41, 1290.

[77] Ray S, Mohan R, Singh J. K, Samantaray M. K, Shaikh M. M, Panda D, Ghosh P, *J. Am. Chem. Soc*., **2007**, 129, 15042.

[78] Mostafa S. I, *Transition Met. Chem.*, **2007**, 32, 6, 769.

[79] Mostafa S. I, Badria F. A, *Metal-Based Drugs*, **2008**, 1.

[80] Lebwohl D, Canerra R, *Eur. J. Cancer*, **1998**, 34, 10, 1522.

[81] Keter F. K, Kanyanda S, Lyantagaye S. S. L, Darkwa J, Rees D. J. G, Meyer M, *Cancer Chemother. Pharmacol*., **2008**, 63, 127.

[82] Rauterkus M. J, Fakih S, Mock C, Puscasu I, Krebs B, *Inorg. Chim Acta*, **2003**, 350, 355.

[83] Cotton F. A Wilkinson G, *Advanced Inorganic Chemistry*, **1972**, Wiley & Sons, New York.

[84] Gumus F, Algul O, Eren G, Eroglu H, Diril N, Gur S, Ozkul A, *Eur. J. Med. Chem.*, **2003**, 38, 473.

[85] Bhuyan B. K, Loughman B. E, Fraser T. J, Day K. *J. Exp. Cell Res.*, **1996**, 97, 275.

[86] Simon T. M, Kunishima D. H, Vilbert G. J, Lorber A, *Cancer*, **1979**, 44, 1965.

[87] Mirabelli C. K, Johnson R. K, Faucette L, Sung C. M. *Proc. Am. Assoc. Cancer Res*., **1984**, 25, 367.

[88] Mirabelli C. K, Johnson R. K, Faucette L, Sung C. M. *Cancer Res*., **1985**, 45, 32.

[89] Sadler P. J, Sue R. E, *Metal-Based Drugs*, **1994**, 1, 107.

[90] Shaw C. F, *Chem. Rev.*, **1999,** 99, 2589.

[91] Tiekink E. R. T, *Critical Reviews in Oncology/Hematology*, **2002**, 42, 225.

[92] Mirabelli C. K, Jensen B. D, Mattern M. R, *Anti-Cancer Drug Des*., **1986**, 1, 223.

[93] Mirabelli C. K, Hill D T, Faucette L. F, *J. Med. Chem.*, **1987**, 30, 2181.

[94] Berners-Price S. J, Johnson R. K, Mirabelli C. K, Faucette L. F, McCabe F. L, Sadler P. J, *Inorg Chem.*, **1987**, 26, 3383.

[95] Berners-Price S. J, Johnson R. K, Giovenella A. J, Faucette L. F, Mirabelli C. K, Sadler P. J, *J. Inorg. Biochem*., **1988**, 33, 285.

[96] Snyder R. M, Mirabelli C. K, Johnson R. K, *Cancer Res.*, **1986**, 46, 5054.

[97] Mirabelli C. K, Johnson R. K, Hill D T, Faucette L. F, *J. Med. Chem*., **1986**, 29, 218.

[98] Rush G. F, Smith P. F, Alberts D. W, Mirabelli C. K, Snyder R. M, Crooke S. T, Sowinski J, Jones H. B, Bugelski P, *J. Toxicol. Appl. Pharmacol*., **1987**, 90, 377.

[99] Ni Dhubhghaill O. M, Sadler P. J, *Weinheim*, **1993**, 221.

[100] Mirabelli C. K, Johnson R. K, Crooke S. T, Mattern M. R, Mong S. M, Sung C. M, Rush G, Berners-Price S. J, Jarrett P. S, Sadler P. J, in *'5th International Symposium on Platinum and Other Metal Coordination Compounds in Cancer Chemotherapy'*, Padua, Italy, **1987**, 319.

[101] Smith P. F, Hoke G. D, Alberts D. W, Bugelski P. J, *J. Pharmacol. Exper. Ther*., **1989**, 249, 944.

[102] Pillarsetty N, Katti K. K, Hoffman T. J, Volkert W. A, Katti K. V, Kamei H, Koide T, *J. Med. Chem.*, **2003**, 46, 1130.

[103] Hill K. E, McCollum G. W, Boeglin M. E, Burk R. F, *Biochem. Biophys. Res. Commun*., **1997**, 234, 293.

[104] Gromer S, Arscott L. D, Williams C. H, Schirmer R. H, Becker K, *J. Biol. Chem*., **1998**, 273, 20096.

[105] Becker K, Gromer S J. Schirmer R. H, Muller S, *Eur. J. Biochem*., **2000**, 267, 6118.

[106] Marzano C, Gandin V, Folda A, Scutari G, Bindoli A, Rigobello M. P, *Free Radic. Biol. Med*., **2007**, 42, 872.

[107] Abbate F, Orioli P, Bruni B, G. Marcon, Messori L, *Inorg. Chim. Acta*, **2000**, 311, 1.

[108] Marcon G, O'Connell T, Orioli P, Messori L, *Metal-Based Drugs*, **2000**, 7, 253.

[109] Casini A, Cinellu M. A, Minghetti G, Gabbiani C, Coronnello M, Mini E,

Messori L, *J. Med. Chem.*, **2006,** 49, 5524.

[110] Messori L, Abbate F, Marcon G, Orioli P, Fontani M, Mini E, Mazzei T, Carotti S, O'Connell T, Zanello P, *J. Med. Chem.*, **2000,** 43, 3541.

[111] Coronnello M, Mini E, Caciagli B, Cinellu M. A, Bindoli A, Gabbiani C, Messori L, *J. Med. Chem.*, **2005**, 48, 21, 6761.

[112] Messori L, Marcon G, Cinellu M. A, Coronnello M, Mini E, Gabbiani C, Orioli P, *Bioorg. Med. Chem.*, **2004**, 12, 23, 6039.

[113] Che C. M, Sun R. W, Yu W. Y, Ko C. B, Zhu N, Sun H, *Chem. Commun.*, **2003**, 14, 1718.

[114] Ronconi L, Giovagnini L, Marzano C, Bettio F, Graziani R, Pilloni G, Fregona D, *Inorg. Chem.*, **2005**,

[115] Giovagnini L, Ronconi L, Aldinucci D, Lorenzon D, Sitran S, Fregona D, *J. Med. Chem.* **2005**, 48, 1588.

[116] Messori L, Marcon G, Orioli P, *Bioinorg. Chem. Appl*., **2003**, 1(2), 177.

[117] Elsome A. M, PhD Thesis, King's College, London, **1995**.

[118] Buckley R. G, Elsome A. M, Fricker S. P, Henderson G. R, Theobald B. R. C, Parish R. V, Howe B. P, Kelland L. R, *J. Med. Chem*., **1996**, 39, 5208.

[119] Pandeya S. N, Dimmock J. R, *Pharmazie*, **1993,** 48, 659.

[120] Ortner K, Abram U, *Inorg. Chem. Commun.*, **1998**, 1, 251.

[121] Abram U, Ortner K, Gust R, Sommer K, *J. Chem. Soc., Dalton Trans.*, **2000**, 735.

[122] Keppler B K, Friesen C, Moritz H G, Vongerichten H, Vogel E, *Struct. Bonding*, **1991**, 78, 97, 127.

[123] Clarke M. J, Zhu F, Frasca D. R, *Chem Rev.*, **1999**, 99, 2511.

[124] Schilling T, Keppler B. K, Heim M. E, *Invest. New Drugs*, **1996**, 13, 327.

[125] Köpf H, Köpf-Maier P, *Angew. Chem. Int. Ed. Engl.*, **1979**, 18, 477.

[126] Köpf-Maier P, *Eur. J. Clin. Pharmacol.*, **1994**, 47, 1.

[127] Köpf-Maier P, Köpf H, *Struct. Bonding*, **1988**, 70, 103.

[128] Köpf-Maier P, Köpf H. *Chem. Rev.*, **1987**, 87,1137.

[129] Cristododoulou C. V, Eliopoulos A. G, Young L. S, Hodgkins L, *Br. J. Cancer*, **1998**, 77, 2088.

[130] Berdel W. E, Schmoll H. J, Scheulen M. E, *J. Cancer Res. Clin. Oncol.*, **1994**, 120, 172.

[131] Korfel A, Scheulen M. E, Schmoll H. J, *Clin. Cancer. Res*., **1998**, 4, 2701.

[132] Luemmen G, Sperling H, Luboldt H, Otto T, Rueben H. *Cancer Chemother. Pharmacol.*, **1998**, 42, 415.

[133] Christodoulou C. V, Ferry D. R, Fyfe D. W, *J. Clin. Oncol.*, **1998**, 16, 2761.

[134] Kröger N, Kleeberg U. R, Mross K, Sass G, Hossfeld D.K, *Onkologie*, **2000**, 23, 60.

[135] Pampillón C, Sweeney N. J, Strohfeldt K, Tacke M, *J. Organomet. Chem*., **2007**, 692, 2153.

[136] Teuber R, Linti G, Tacke M, *J. Organomet. Chem*., **1997**, 105, 545.

[137] Hartl F, Cuffe L, Dunne J. P, Fox S, Mahabiersing T, Tacke M, *J. Mol. Struct. Theochem*., **2001,** 559, 331.

[138] Tacke M, Dunne J. P, Fox S, Linti G, Teuber R, *J. Mol. Struct*., **2001,** 570, 197.

[139] Fox, S, Dunne J. P, Dronskowski D, Schmitz D, Tacke M, *Eur. J. Inorg. Chem*., **2002**, 3039.

[140] Eisch J. J, Xian S, Owuor F. A, *Organometallics*, **1998**, 17, 5219.

[141] Eisch J. J, Owuor F. A, Xian S, *Organometallics*, **1999**, 18, 1583.

[142] Kane K. M, Shapiro P. J, Vij A, Cubbon R, Rheingold A. L, *Organometallics*, **1997**, 16, 4567.

[143] Fox S, Dunne J. P, Tacke M, Gallagher J. F, *Inorg. Chim. Acta,* **2004**, 357, 225.

[144] Tacke M, Allen L. T, Cuffe L. P, Gallagher W. M, Lou Y, Mendoza O, Müller-Bunz H, Rehmann F. J. K, Sweeney N, *J. Organomet. Chem*., **2004**, 689, 2242.

[145] Rehmann F. J. K, Cuffe L. P, Mendoza O, Rai D, Sweeney N, Strohfeldt K, Gallagher W. M, Tacke M, *Appl. Organomet. Chem*., **2005**, 19, 293.

[146] Tacke M, Cuffe L.P, Gallagher W. M, Lou Y, Mendoza O, Müller-Bunz H, Rehmann F. J. K, Sweeney N, *J. Inorg. Biochem*., **2004**, 98, 1987.

[147] (a) Pampillón C, Mendoza O, Sweeney N, Strohfeldt K, Tacke M, *Polyhedron,* **2006**, 25**,** 2101;

(b) Pampillón C, Sweeney N, Strohfeldt K, Tacke M, *Inorg. Chim. Acta,* **2006** 359, 3969.

[148] Harding M. H, Mokdsi, G, *Curr. Med. Chem*., **2000**, 7, 1289.

[149] Melendez, E, *Crit. Rev. Oncol. Hematol*., **2002**, 42, 309.

[150] Allen O. R, Gott A. L, Hartley J. A, Hartley J. M, Knox R. J, McGowan P. C, *Dalton Trans.*, **2007**, 5082.

[151] van Staveren D. R, Metzler-Nolte N, *Chem. Rev.*, **2004**, 104, 5931.

[152] Bioorganometallics: Biomolecules, Labeling, Medicine, ed. G. Jaouen, Wiley-VCH, New York, **2006**.

[153] Osella D, Feralli M, Zanello P, Laschi F, Fontani M, Nervi C, Cavigiolio G, *Inorg. Chim. Acta*, **2000**, 42, 306.

[154] Tabbi G, Cassino C, Cavigiolio G, Colangelo D, Ghiglia A, Viano I, Osella D, *J. Med. Chem.*, **2002**, 45, 5786.

[155] Neuse E. W, Meirim M. G, Blom N. F, *Organometallics,* **1988**, 7, 2562.

[156] (a) Swarts J. C, Neuse E. W, Lamprecht G. J, *J. Inorg. Organomet. Polym.*, **1994**, 4, 143;

(b) Neuse E. W, *Macromol. Symp.*, **2001**, 172, 127;

(c) Swarts J. C, Swarts D. M, Maree D. M, Neuse E. W, La Madeleine C, Van Lier J. E, *Anticancer Res.*, **2001**, 21, 2033;

(d) Johnson M. T, Kreft E, N'Da D. D, Neuse E. W, van Rensburg C. E. J, *J. Inorg. Organomet. Polym.*, **2003,** 13, 255;

(e) Caldwell G, Meirim M. G, Neuse E. W, vanRensburg C. E. J, *Appl. Organomet. Chem.*, **1998**, 12, 793.

[157] Ong C. W, Jeng J. Y, Juang S. S, Chen C. F, *Bioorg. Med. Chem. Lett.*, **1992**, 2, 929.

[158] Bincoletto C, Terariol I. L. S, Oliveira C. R, Dreher S, Fausto D. M, Soufen M. A, Nascimento F. D, Caires A. C. F, *Bioorg. Med. Chem.*, **2005**, 13, 3047.

[159] Oparin D. A, Makhaev V. D, Vilchevskaya V. D, Zimatkina T. I, Motylevich Z. V, Zimatkin S. M, Zabrodskaya S. V, Krylova A. I, Gorelikova Y. Y, *Khim.-Farm. Zh.*, **1996**, 30, 11.

[160] Hartinger C. G, Nazarov A. A, Arion V. B, Giester G, Jakupec M, Galanski M, Keppler B. K, *New J. Chem.*, **2002**, 26, 671.

[161] (a) Kelly P. N, Pretre A, Devoy S, O'Rielly I, Devery R, Goel A, Gallagher J. F, Lough A. J, Kenny P. T. M, *J. Organomet. Chem.*, **2007**, 692, 1327;

(b) Wu X, Tiekink E. R. T, Kostetski I, Kocherginsky N, Tan A. L. C, Khoo S. B, Wilairat P, Go M. L, *Eur. J. Pharm. Sci.*, **2006**, 27, 175.

[162] Tabbi G, Cassino C, Cavigiolio G, Colangelo D, Ghiglia A, Viano I, Osella D, *J. Med. Chem.*, **2002**, 45, 5786.

[163] Osella D, Ferrali M, Zanello P, Laschi F, Fontani M, Nervi C, Cavigiolio G, *Inorg. Chim. Acta*, **2000**, 306, 42.

[164] Tabbi G, Cassino C, Cavigiolio G, Colangelo D, Ghiglia A, Viano I, Osella D, *J.*

Med. Chem., **2002**, 45, 5786.

[165] Tamura H, Miwa M, *Chem. Lett.*, **1997**, 1177.

[166] (a) Popova L. V, Babin V. N, Belousov Y. A, Nekrasov Y. S, Snegireva A. E, Borodina N. P, Shaposhnikova G. M, Bychenko O. B, Raevskii P. M. *Appl. Organomet. Chem.*, **1993**, 7, 85;

(b) Köpf-Maier P, Köpf H, Neuse E. W, *J. Cancer Res. Clin.*, **1984**, 108, 336.

[167] Hillard E, Vessieres, A, Le Bideau F, Plazùuk D, Spera D, Huché M, Jaouen G, *Chem. Med. Chem.*, **2006**, 1, 551 and references cited therein.

[168] Henderson W, Alley S. R, *Inorg. Chim. Acta*, **2001**, 322, 106.

[169] Rosenfeld A, Blum J, Gibson D, Ramu A, *Inorg. Chim. Acta*, **1992**, 201, 219.

[170] Viotte M, Gautheron B, Kubicki M. M, Nifant'ev I. E, Fricker S. P, *Met.-Based Drugs*, **1995**, 2, 311.

[171] Rudolph R, *Arch. Exp. Veterinaermed*., **1971**, 25, 925.

[172] Anghileri L. J, Z. *Krebsforsch. Klin. Onkol*., **1975,** 83, 213.

[173] Clarke M. J, *Met. Ions Biol. Syst.*, **1980**, 11, 231.

[174] Allardyce C. S, Dyson P. J, *Platinum Metals Rev*., **2001**, 45, 2, 62.

[175] Clarke M. J, *Coord. Chem. Rev*., **2003**, 236, 1, 207.

[176] A. Bergamo, S. Zorzet, B. Gava, A. Sorc, E. Alessio, E. Lengo and G. Sava, *Anti-Cancer Drugs*, **2000**, 11, 8, 665.

[177] Pluim D, van Waardenburg R. C. A. M, Beijnen J. H, Schellens J. H. M, *Cancer Chemother. Pharmacol.*, **2004**, 54, 71.

[178] Ang. W. H, Dyson P. J, *Eur. J. Inorg. Chem*., **2006**, 20, 4003.

[179] Bergamo A, Gava B, Alessio E, Mestroni G, *Int. J. Oncol*., **2002**, 21, 1331.

[180] Clarke M. J, Bitler S, Rennert D, Buchbinder M, Kelman A. D, *J. Inorg. Biochem*., **1980**, 12, 1, 79.

[181] Mishra L, Sinha R, Itokawa H, *Bioorg. Med. Chem.*, **2001**, 9(7), 1667.

[182] Pongratz M, Schluga P, Jakupec M. A, Arion V. B, Hartinger C. G, Allmaier G, Keppler B. K, *J. Anal. At. Spectrom*., **2004**, 19, 46.

[183] (a) Messori L, Gonzales Vilchez F, Vilaplana R, Piccioli F, Alessio E, Keppler B. K, *Met.-Based Drugs*, **2000**, 7, 335;

(b) Timerbaev A. R, Hartinger, C. G, Aleksenko, S. S, Keppler, B. K. *Chem. Rev*., **2006**, 106, 2224;

(c) Hartinger C. G, Ang W. H, Casini A, Messori L, Keppler B. K, Dyson P. J, *J. Anal. At. Spectrom.*, **2007**, 22, 960;

(d) Polec-Pawlak K, Abramski J. K, Semenova O, Hartinger C. G, Timerbaev A. R, Keppler B. K, Jarosz M. *Electrophoresis*, **2006**, 27, 1128;

(e) Clarke M. J, Bitler, S. Rennert D, Buchbinder M, Kelman A. D, *J. Inorg. Biochem.*, **1980**, 12, 79;

(f) Schluga P, Hartinger C. G, Egger, A, Reisner E, Galanski M, Jakupec M. A, Keppler B. K, *Dalton Trans.*, **2006**, 14, 1796.

[184] Dyson P. J, Sava G, *Dalton Trans*., **2006**, 1929.

[185] Thompson H. J, Chasteen D. N, Neeker L, *Carcinogenesis*, **1997**, 8, 51.

[186] Bishaye A, Chatterjee M, *Br. J. Cancer*, **1995**, 71, 1214.

[187] Angelos M. Evangelou, *Crit. Rev. Oncol. Hematol.*, **2002**, 42, 249.

[188] Kotzerke J, Bunjes D, Scheinberg D. A, *Bone Marrow Transplantation*, **2005**, 36, 12, 1021.

[189] Beaumier P. L, Venkatesan P, Vanderheyden J. L, *Cancer Research*, **1991**, 51, 2, 676.

[190] Ma D.-L, Che C.-M, Siu F.-M, Yang M, Wong K.-Y, *Inorg. Chem.*, **2007**, 46, 3, 740.

[191] Das S, Dasgupta D, *J. Inorg. Biochem.*, **2005**, 99, 3, 707.

[192] Dıaz G. D, Li Q, Dashwood R. H, *Cancer Research*, **2003**, 63, 6, 1254.

[193] Desoize B, *Critical Reviews in Oncology/Hematology*, **2002**, 42, 213.

[194] Howard R. A, Kimball A. P, *Cancer Res*., **1979**, 39, 2568.

[195] Dunbar K. R, Matonic J. H, Saharan V. P, Crawford C. A, Christou G, *J. Am. Chem. Soc*., **1994,** 116, 2201.

[196] Rajput J, Moss J. R, Hutton A. T, Hendricks D. T, Arendse C. E, Imrie C. *J. Organomet. Chem.*, **2004**, 689, 1553.

[197] Rajput, J, Hutton A. T, Moss J. R, Su H, Imrie C, *J. Organomet. Chem.,* **2006,** 691, 4573.

CHAPTER 2

SYNTHESIS OF IMINOPHOSPHINE , TETRADENTATE, AND SCHIFF BASE LIGANDS AND THEIR COMPLEXATION WITH PALLADIUM, PLATINUM AND GOLD PRECURSORS

CONTENT

2.1 INTRODUCTION

During recent years there has been a growing interest in the chemistry of ligands with both 'hard' nitrogen and 'soft' phosphorus donor atoms [1a-c]. Metal complexes with N and P donor atoms display a variety of coordination possibilities beyond those of P-P or N-N ligands [2]. The hard ligand components can readily dissociate from the soft metal centre generating a vacant site on the metal ion for substrate binding. These ligands show a particular behaviour in binding to soft metal centres such as palladium(II) and platinum(II) that make their complexes good precursors in catalytic processes [3a-d]. Among the most studied ligands with this characteristic are the pyridylphosphines and iminophosphines which have been widely reported in complexes with ruthenium [4], palladium [5], rhodium [10a] and iridium [11b].

The use of 2-(diphenylphosphino)benzaldehyde as a building block for iminophosphines was first reported in the Schiff-base condensation with ethylene-diamine [6,7] and has since been extended to a wide variety of other amines [8]. It has been well documented that primary amines can react with aldehydes and ketones to yield imines. The process is often acid catalysed, involving the nucleophilic attack of the amine on the carbonyl group, followed by the proton-transfer from nitrogen to oxygen to yield a neutral carbinolamine. Upon the protonation of the carbinolamine oxygen by the acid catalyst, the hydroxyl is converted into a good leaving group, so that the E1 type loss of water generates an iminium ion. The final imine is formed after loss of a proton to regenerate the acid catalyst (Scheme 2.1).

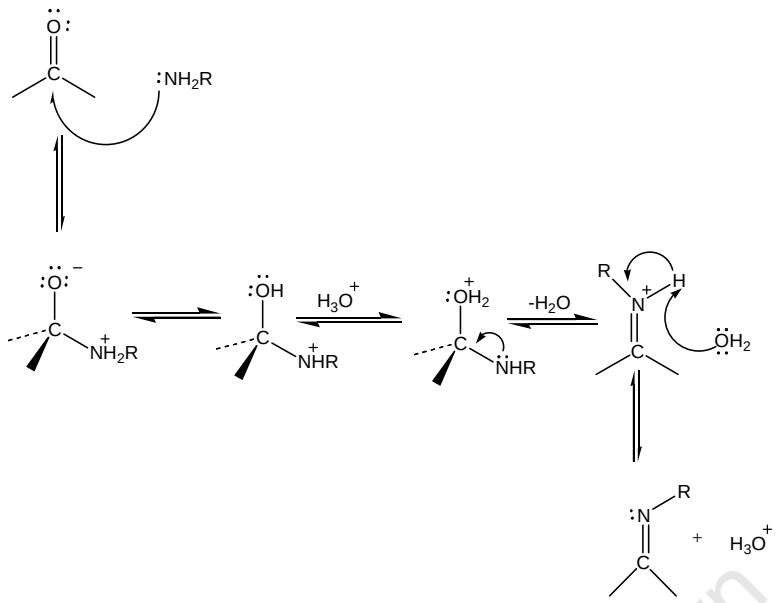

Scheme 2.1 Mechanism of acid catalysed imine formation

Since *o*-diphenylphosphinobenzaldehyde is a well known precursor it was decided to use this phosphine as a starting material for the synthesis of a range of iminophosphines.

The general method we employed is shown for synthesis of a primary amine, propylamine (Scheme 2.2). The reaction was left to stir at room temperature for *ca* 16 hours, in the absence of an acid catalyst. The iminophosphine was obtained in high yield (85%) without oxidation taking place.

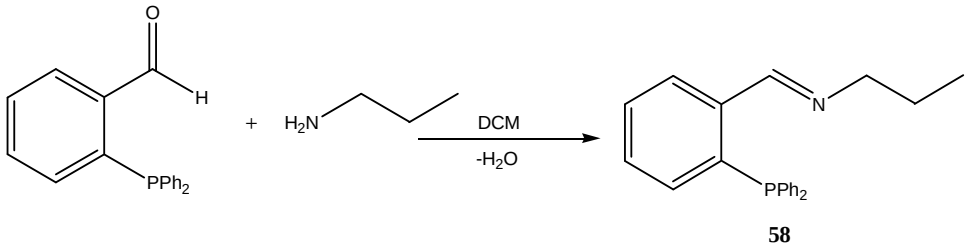

58

Scheme 2.2 Synthesis of an iminophosphine ligand

2.2 RESULTS AND DISCUSSION

2.2.1 Preparation and characterisation of the iminophosphine ligands

The 2-(diphenylphosphino)benzylidene)amines were synthesised in high yields from the Schiff-base condensation reaction of 2-(diphenylphosphino)benzaldehyde with the appropriate primary amine in dichloromethane at room temperature (Scheme 2.3).

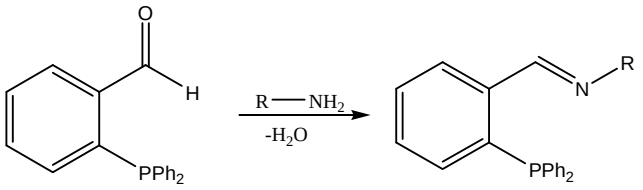

$R = (CH_2)_2CH_3$	**58**
$R = (CH)(CH_3)_2$	**59**
R = 2,6 ^{i}Pr C_6H_3	**60**
$R = (CH_2)C_6H_5$	**61**
$R = (CH_2)C_5H_4N$	**62**
$R = (CH_2)C_4H_3O$	**63**
$R = (CH_2)C_4H_3S$	**64**

Scheme 2.3 Synthesis of iminophosphine ligands

Under these conditions, the reaction proceeds smoothly to completion and does not require any heating at higher temperature (e.g. refluxing ethanol [6]), or the presence of a drying agent (e.g. molecular sieves [9,10]), or the use of a large excess of the amine (e.g. neat *tert*-butylamine [11a,b]).

The resultant iminophosphine ligands shown in Table 2.1 were obtained in good yields (≥ 75%).

Table 2.1 Iminophosphine ligands synthesised

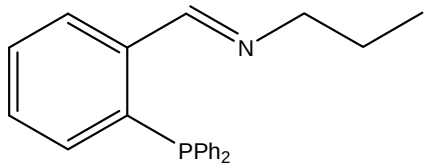 **58**	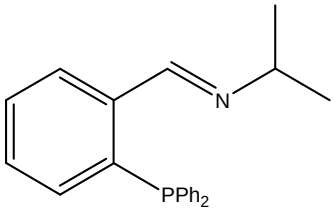 **59**
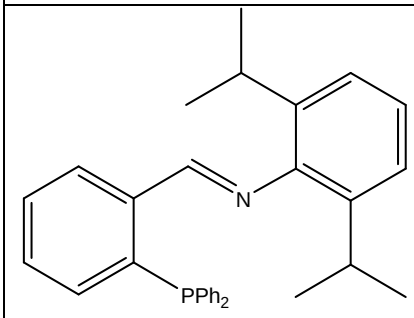 **60**	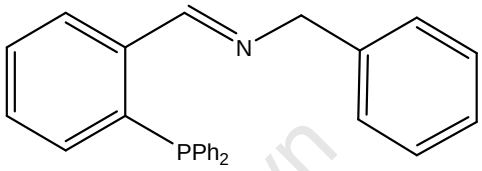 **61**
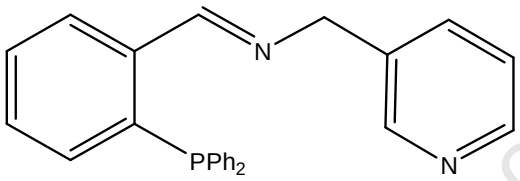 **62**	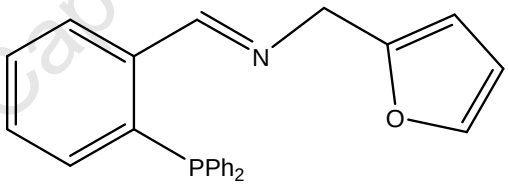 **63**
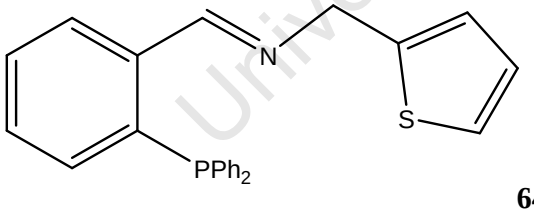 **64**	

2.2.1.1 ^{1}H NMR studies of the iminophosphine ligands

^{1}H NMR spectra of the ligands were consistent with the proposed structures and were also in agreement with ^{1}H NMR data reported in the literature for related ligands [12, 13]. The disappearance of the aldehyde proton and appearance of an imine signal

confirmed that a condensation reaction had taken place between the respective aldehyde and amine. The chemical shift of aldehyde protons is normally in the region of 9.7 – 10 ppm on a ^{1}H-NMR spectrum [14]. In the case of ligands **58** – **64**, a characteristic doublet for the aldehyde proton was present at a chemical shift of 8.9 – 9.1 ppm and with coupling constants of $J_{P\text{-}H}$ = 4.9 – 5.8 Hz. The appearance of the signal as a doublet is the consequence of a long-range coupling of phosphorus with the imine proton – similar to that of phosphorus with corresponding imine protons [15]. The chemical shift of imine-protons was observed to be more upfield shifted in comparison with the corresponding aldehyde and resonated in the region of 8.9 – 9.1 ppm.

2.2.1.2 ^{31}P NMR data of the iminophosphine ligands

The ^{31}P NMR spectra of the iminophosphine ligands displayed singlet resonances as shown in Table 2.2.

Table 2.2 ^{31}P NMR data of **58** to **64**

Ligand	δ (ppm) ($CDCl_3$)
58	-13.4
59	-13.2
60	-15.8
61	-13.6
62	-13.2
63	-13.9
64	-13.8

The analysis of starting material and iminophosphine ligands by ^{31}P-NMR analysis provided sound and precious information about the samples of concern. Phosphorus

has characteristic chemical shifts for its +3 and +5 oxidation states. In the low P(III) oxidation state, high field signals are usually expected, and when oxidised, low field signals are present. The characteristic for phosphorus in the staring material 2-diphenylphosphinobenzaldehyde is a singlet at -11.7 ppm. The iminophosphine ligands **58** – **64** exhibited singlets in the region -13.2 – 15.8 ppm. This downward shift has been well documented in the literature for related iminophosphine ligands [16,17]. The appearance of a singlet in the ^{31}P NMR is also an indication that only one product has been formed.

2.2.1.3 Infrared spectroscopy and elemental analysis for the iminophosphine ligands

The elemental analysis data obtained for the ligands were in agreement with the proposed formulations depicted in Scheme 2.3 (Table 2.3). The ligands show a distinctive stretching frequency, ν(C=N) at 1637 cm^{-1} (as KBr plates) which agrees with previously reported values for iminophosphine ligands [11a]. Upon complexation, this peak shifts to lower frequencies than in the ligands. This is due to increased electron density on the metal upon coordination of the imine moiety to the metal centre.

Table 2.3: Elemental analysis and IR data for iminophosphine ligands **58** – **64**

Ligand	M.p. (°C)	Formula	Anal Found (Calcd.)			IR (cm^{-1})[a]
			C	H	N	ν(C=N)
58	70 - 71	$C_{22}H_{22}NP$	79.59 (79.74)	6.82 (6.69)	4.12 (4.23)	1637
59	107 - 108	$C_{22}H_{22}NP$	79.88 (79.74)	6.52 (6.69)	4.52 (4.23)	1634
60	108 - 110	$C_{31}H_{32}NP$	82.69 (82.82)	7.12 (7.17)	3.32 (3.12)	1629
61	80 - 82	$C_{26}H_{21}N_2P$	82.49 (82.30)	5.62 (5.84)	3.72 (3.69)	1636
62	79- 82	$C_{25}H_{21}N_2P$	78.82 (78.93)	5.62 (5.56)	7.52 (7.36)	1632
63	77 - 78	$C_{24}H_{20}NOP$	78.19 (78.03)	5.22 (5.46)	3.72 (3.79)	1635
64	70- 72	$C_{24}H_{20}NPS$	74.59 (74.78)	5.12 (5.23)	3.72 (3.63)	1636

[a]Recorded as KBr plates

Table 2.4: Selected[1]H-NMR[a] chemical shifts δ (ppm) for iminophosphine ligands **58 - 64**

Ligand	HC=N	Ar-H	N-(CH_2)	N-(CH_2CH_3)/Py-H	Fur-H /Thio-H
58	8.91 (d, 1H, *J* = 4.8 Hz)	8.01 (dd, 1H, *J* = 7.8, 4.2 Hz), 7.39 – 7.22 (m, 12H), 6.90 (dd, 1H, *J* = 7.2, 5.4 Hz)		3.50 (t, 2H, *J* = 6.8 Hz), 1.54-1.44 (m, 2H), 1.21-1.07 (m, 2H), 0.82 (t, 3H, *J* =7.2 Hz)	-
59	8.51 (s, 1H)	6.92 (m, 1H, *J* = 8.4 Hz); 7.2 – 7.4 (m, 7H, *J* = 7.6 Hz)	-	-	-
60	8.60 (s, 1H)	6.9 – 7.2 (m, 4H, *J* = 2.2 Hz); 7.4 (m, 3H, *J* = 2.2 Hz)	1.29 (s, 9H)	-	-
61	9.03 (d, 1H, *J* =5.8 Hz)	8.10 (m, 1H), 7.19 – 7.43 (m, 15H), 7.09 (m, 2H) 6.94 (ddd, 1H, *J* = 7.7, 4.7, 1.2 Hz)	4.67 (s, 2H)	-	-
62	9.02(d,1H, *J* =4.9 Hz)	8.01(ddd,1H, *J*=1.4, 3.9, 7.6 Hz), 7.24 – 7.43 (m, 13H), 7.12 (ddd, 1H, *J* = 0.8, 4.8,7.8 Hz), 6.90 (ddd, 1H, *J* = 7.7, 4.7, 1.7 Hz)	4.67(s,2H)	8.45(dd,1H, *J* =1.7,4.8z),8.42(d,1H,*J* =1.7Hz)	-
63	9.01(d, *J* = 5.1 Hz)	8.07(ddd, 1H, *J* =7.7, 4.0,1.4 Hz), 7.25 – 7.42 (m, 13H)	4.65(s,2H)	3.07 (m, 2H, *J* = 6.8 Hz)	6.91(m, 1H),6.27(m,1H), 6.05 (dd, 1H, *J* =3.3, 0.7 Hz)
64	9.02 (br d,1H, *J*=4.9 Hz)	8.11 (m, 1H), 7.25 – 7.45 (m, 12H), 7.59 (d, 1H, *J* = 2.6 Hz)	4.86(s,2H)	3.11 (m, 2H, *J* = 6.6 Hz)	1.25 (d, 12H, , *J* = 7.0 Hz)

[a] Spectra obtained in $CDCl_3$; s, singlet; d, doublet; t, triplet; dd, doublet of doublets; m, multiplet

2.2.1.4 Mass spectra of the iminophosphine ligands

Fragmentation patterns of the ligands were obtained by EI mass spectrometry. Normally the mass spectral fragmentation of the compound is found to give a characteristic pattern. Each kind of fragment has a particular ratio of mass to charge, or m/z value. For most ions, the charge is 1, so that m/z is simply the mass of the fragment. Thus for ligand **63** it exhibited a systematic fragmentation pattern (Scheme 2.4). It gave a molecular ion peak of m/z =369 with a corresponding base peak (the most intense peak signifying a stable fragment) of m/z =287.79 attributed to the loss a thiophenyl unit in the ligand.

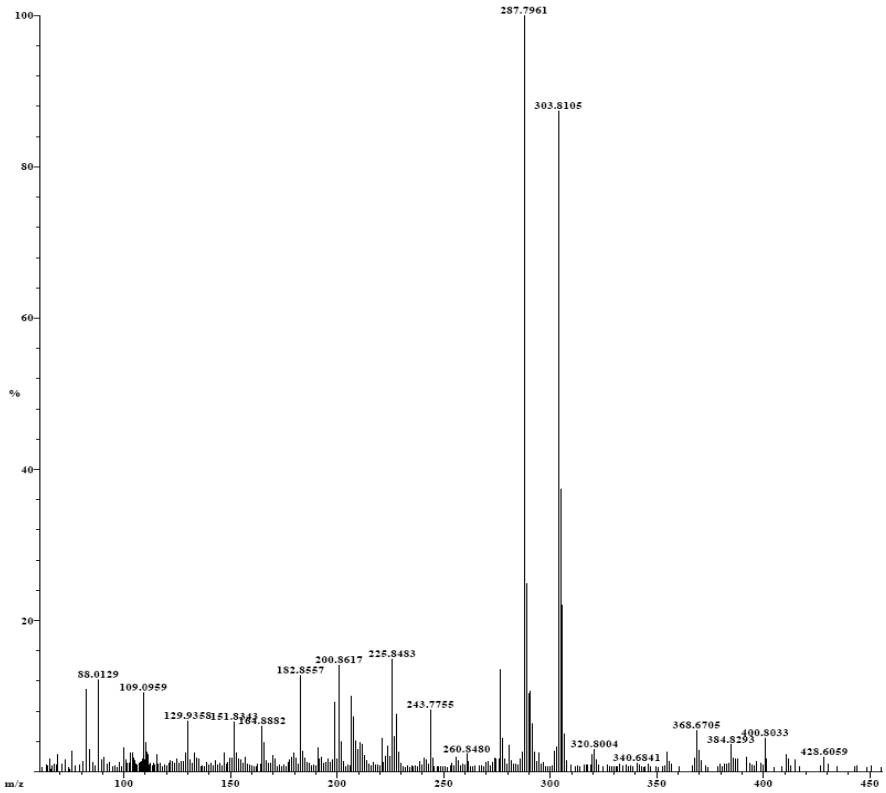

Figure 2.1 Mass spectrum (EI) of ligand **63**

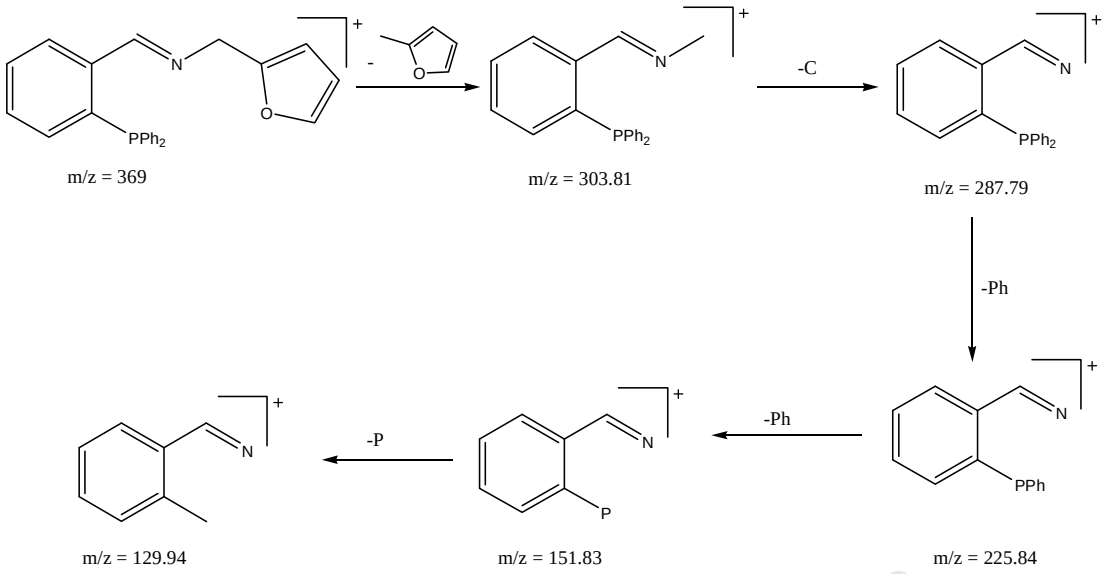

Scheme 2.4 Possible fragmentation pattern of **63**

The mass spectra data of the iminophosphine ligands are shown in Table 2.5. The molecular ion peaks are in good agreement with their empirical formula as indicated from elemental analysis. The mass spectra of all the ligands exhibited similar fragmentation patterns

Table 2.5 Mass spectra data of the iminophosphine ligands **58**-**64**

Ligand	Calculated molar mass (g/mol)	Molecular fragment	Assignment
58	331.39	331.22	$[M]^+$
59	331.39	331.24	$[M]^+$
60	449.57	449.56	$[M]^+$
61	379.43	379.78	$[M]^+$
62	380.42	380.80	$[M]^+$
63	369.40	369.61	$[M]^+$
64	385.46	385.32	$[M]^+$

2.2.2 Tetradentate ligands

The chemistry of bidentate compounds (i.e α-diimines and β-diimines) has been well explored [18, 19]. A few reports on unconjugated diimines describing their use as catalysts [20] and in bio-inorganic chemistry [21] have appeared in literature. Westcott and co-workers have prepared unconjugated diimines with boronate esters, and complexed them with platinum (Scheme 2.5), to synthesise platinum complexes which can be used as anticancer agents [22].

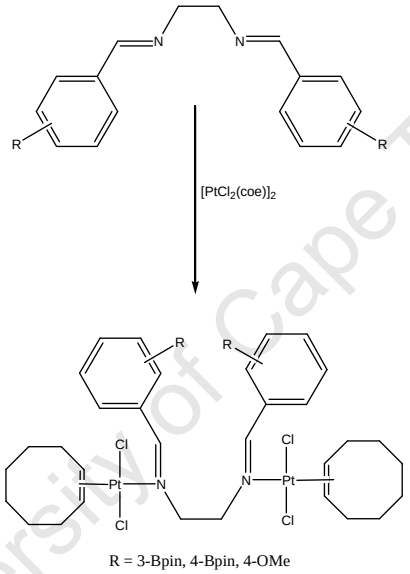

Scheme 2.5 Synthesis of unconjugated diimine platinum complexes

The next section discusses the tetradentate ligands that we prepared their characterisation data and attempts to complex them with palladium and platinum precursors.

2.3.1 Synthesis and characterization of tetradentate ligands

Symmetrical ligands **65** to **68** (Table 2.6) are usually prepared upon condensation of dialdehydes with amines [23]. Ligands **65** to **68** were characterised by IR spectroscopy as well as ^{1}H, ^{13}C NMR, X-ray crystallography and mass spectrometry.

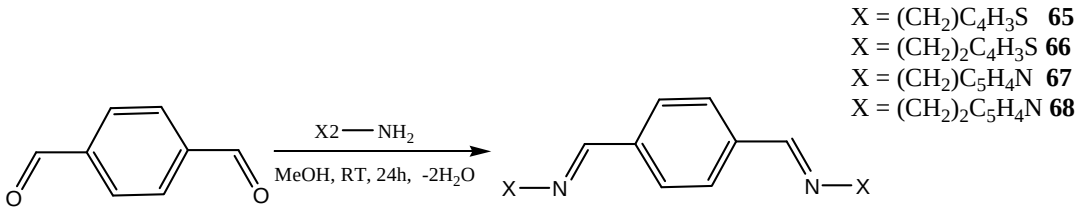

Scheme 2.6: Synthetic route to tetradentate ligands *via* a Schiff base reaction

Table 2.6: Tetradentate ligands synthesised

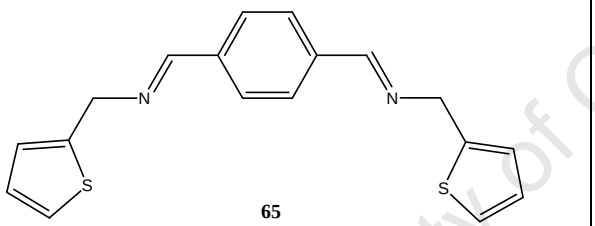 **65**	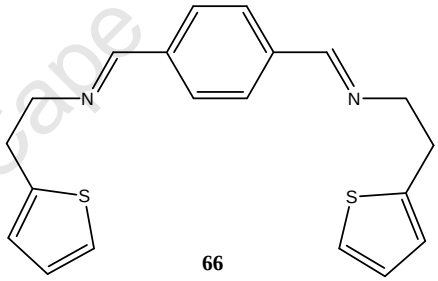 **66**
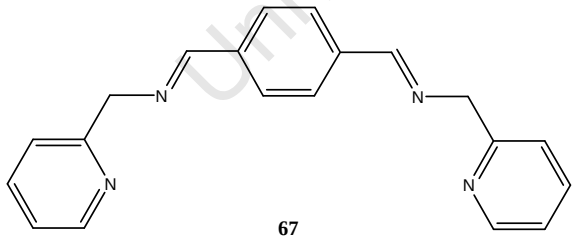 **67**	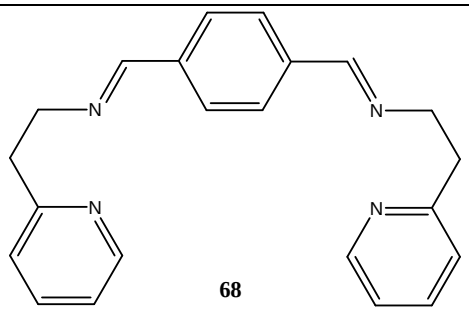 **68**

2.3.1.1 ^{1}H NMR spectra for tetradentate ligands

In the ^{1}H NMR spectra of the tetradentate ligands **65 - 68** the imine protons appear as singlets in the range 8.23 – 8.57 ppm, the chemical shifts for the methylene (-CH_2-) protons appear at 5.00 ppm for **65** and **67** but at *ca* 3 - 4 ppm for **66** and **68**. The ^{1}H NMR spectra of the ligands **65** to **68** displayed peaks for the aromatic protons in the region of 7.45 - 7.95 ppm. The signals for the pyridyl and thiophenyl rings occur at between 6.9 – 7.2 ppm for all the ligands respectively.

The NMR spectra of the ligands indicate that each half of the ligand is equivalent due to the presence of internal symmetry. In view of the observed NMR pattern, it may be considered that the *trans* configuration of the ligands is predominant in solution or that there is a fast equilibrium between the *cis* and *trans* isomers of the ligands.

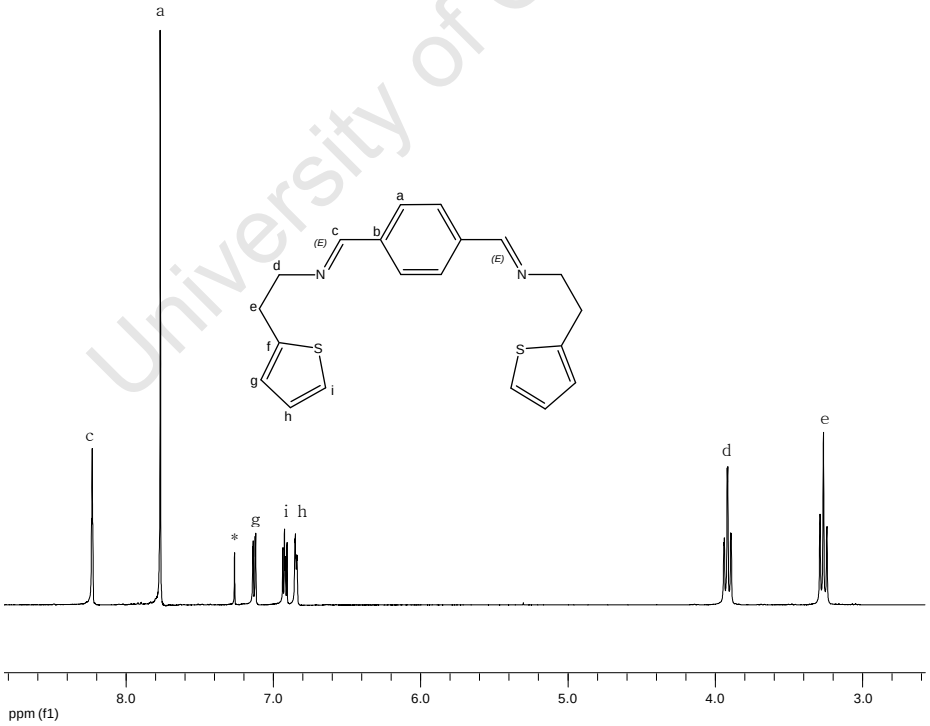

Figure 2.2 ^{1}H NMR spectrum of ligand **66** in $CDCl_3$ (* residual solvent peak)

The ^{13}C NMR spectra of ligand **63** in $CDCl_3$ exhibits 9 distinct carbon peaks as expected. The imine carbon appears at 161.27 ppm. The thiophenyl ring carbons appear at 142.28, 128.34, 125.18 and 123.61 ppm respectively. The phenyl ring carbons appear at 126.72 ppm and the -CH_2 carbon signal separately at the upfield region at 31.42 ppm.

The assignments in the ^{13}C NMR spectra are consistent with those reported for related ligands. By use of selective proton decoupling, the ^{13}C NMR assignments could generally be ascertained.

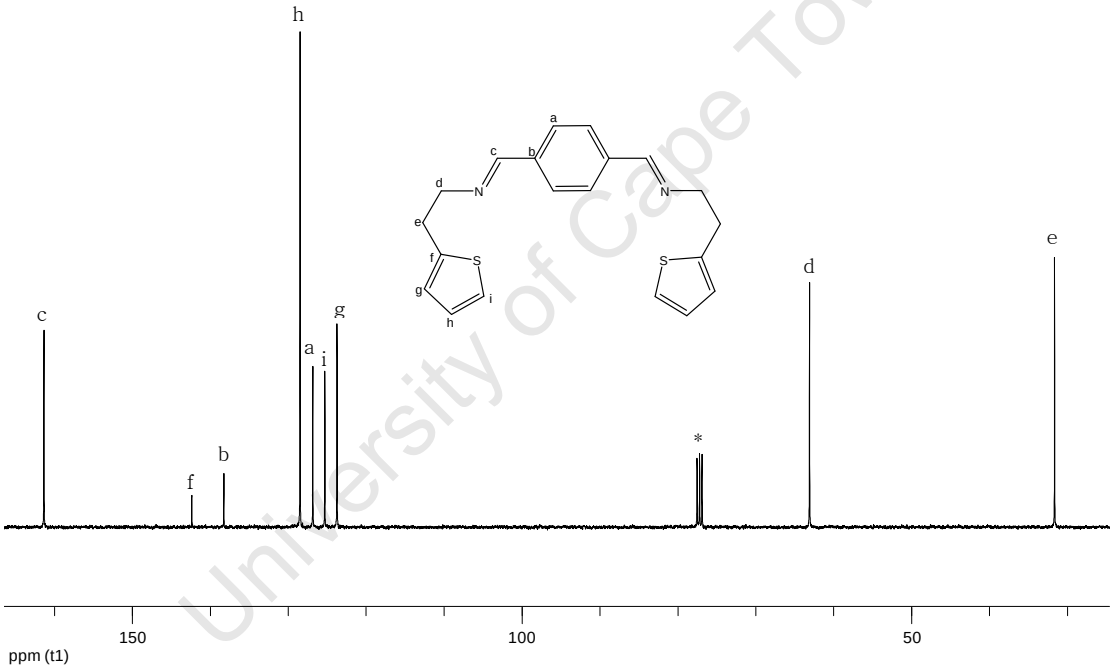

Figure 2.3 ^{13}C NMR spectra of ligand **66** in $CDCl_3$ (* residual solvent peak)

2.3.1.2 Physical properties of tetradentate ligands

Ligands **65** to **68** were all air stable solids and were obtained in good yields ranging between 70 – 85 % (Table 2.7). The ligands were isolated as white solids with the exception of **68** which was cream. Ligand **67** had the lowest melting point range between 126 – 128 $^{\circ}C$ and **68** the highest between 185-187 ºC.

Table 2.7 Yields and physical properties of ligands **65** to **68**

Ligand	Yield (%)	Colour of Solid	Melting point (°C)
65	85	White	180-182
66	80	White	140-142
67	72	White	126-128
68	70	Cream	185-187

2.3.1.3 Mass spectra of the tetradentate ligands

The mass spectral data of the tertradentate ligands are given in Table 2.8. The molecular ion peaks are in good agreement with their empirical formula as indicated from elemental analysis. The other peaks represent fragments of the molecular ion.

Table 2.8 Mass spectra data of the tetradentate ligands **65**-**68**

Ligand	Calculated molar mass (g/mol)	Molecular fragment	Assignment
65	324.47	103.30	$[M\text{-}2C_5H_5SN]^+$
66	352.52	254.89	$[M\text{-}C_5H_8S]^+$
67	314.38	221.84	$[M\text{-}C_6H_6N]^+$
68	342.44	249.90	$[M\text{-}C_6H_6N]^+$

2.3.1.4 Single crystal X-ray determination of ligand 65

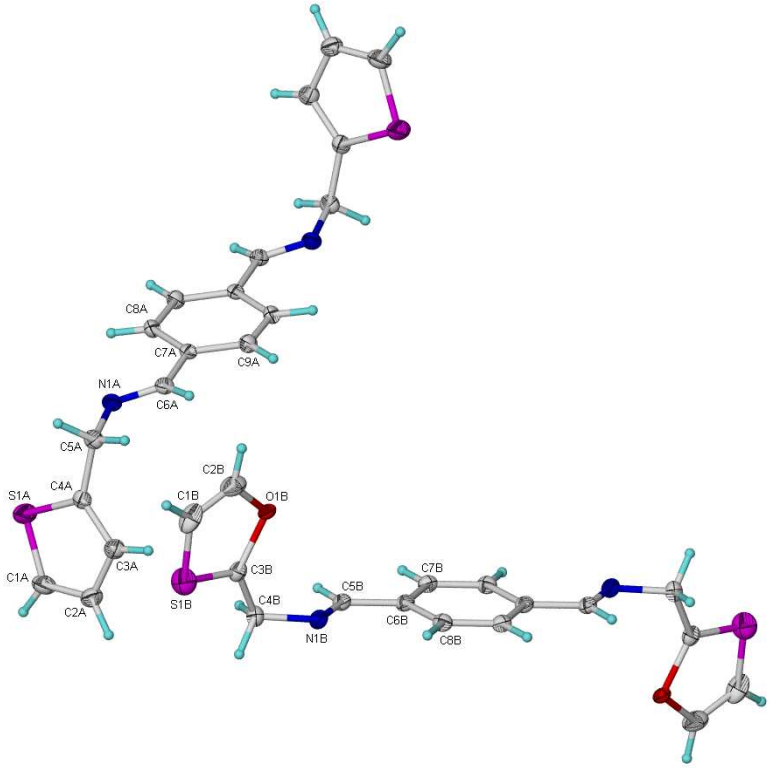

Figure 2.4 The ORTEP plot of the molecular structure of **65** showing the atomic numbering. All non-hydrogen atoms were presented with ellipsoidal model with probability level 40%. Only half of the molecule for each are labelled and another half are generated via centre of symmetry (symmetry code: 2-x, 1-y, 1-z for molecule A; symmetry code: -x, 2-y, 2-z fro molecule B).

For structure **65**, all non-hydrogen atoms, except those of ethanol solvent, were refined anisotropically. The solvent molecule showed high thermal motion and was refined isotropically with bond length constraints. C8A, C9A, C11A, C12A, C11B and C12B also showed high thermal motions, so they were refined with anisotropic displacement parameters equal to those of their neighbouring atoms with bond length constraints. All hydrogen atoms, except the ethanol hydroxyl hydrogen, were positioned geometrically with C-H = 0.94 – 0.99 Å and refined as riding on their parent atoms with U_{iso} (H) = 1.2 - 1.5 U_{eq} (C). The ethanol hydroxyl hydrogen was located in the difference electron density maps and refined with fixed isothermal temperature factor and fixed bond length.

Table 2.9 Selected bond distances and angles for ligand **65**

Bond Distances (Å)		**Bond Angles(º)**	
S(1A)-C(1A)	1.704(4)	C(1A)-S(1A)-C(4A)	92.42(18)
S(1A)-C(4A)	1.720(3)	C(6A)-N(1A)-C(5A)	117.2(3)
N(1A)-C (6A)	1.267(4)	C(2A)-C(1A)-S(1A)	111.9(3)
N(1A)-C(5A)	1.467(4)	N(1A)-C(5A)-C(4A)	109.3(3)
C(3A)-C(4A)	1.381(5)	N(1A)-C(6A)-C(7A)	121.5(3)
C(4A)-C(5A)	1.498(5)		

The crystal structure reveals that **65** exists as discrete molecules. The C(9)-N(1) distance of 1.267 Å is consistent with a C=N double bonding.

*2.3.1.5 Single crystal X-ray determination of ligand **66***

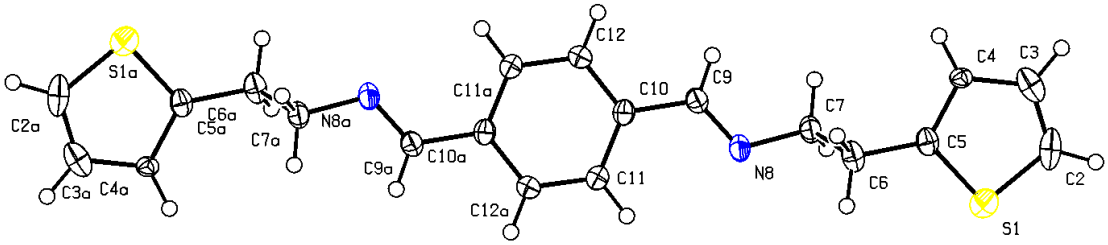

Figure 2.5 Molecular structure of ligand **66** showing the atomic numbering scheme. All non-hydrogen atoms were presented with ellipsoidal model with probability level 40%. Only half of the molecule is labelled as the other half is generated through a symmetry operator (symmetry code: 3/2-x, 5/2-y, 1-z).

Table 2.10 Selected bond distances and angles for ligand **66**

Bond Distances (Å)		**Bond Angles(º)**	
S(1)-C(2)	1.691(3)	C(2)-S(1)-C(5)	93.56(12)
S(1)-C(5)	1.693(2)	C(7)-N(8)-C(9)	117.3(2)
N(8)-C (7)	1.455(3)	S(1)-C(2)-C(3)	111.6(2)
N(8)-C(9)	1.266(3)	S(1)-C(5)-C(6)	121.91(17)
C(5)-C(6)	1.502(3)	N(8)-C(9)-C(10)	122.84(19)
C(6)-C(7)	1.520(3)		
C(9)-C(10)	1.473		

The crystal structure reveals that **66** exists as discrete molecules. The C(9)-N(1) distance of 1.266 Å is consistent with a C=N double bonding.

*2.3.1.6 Single crystal X-ray determination of ligand **68***

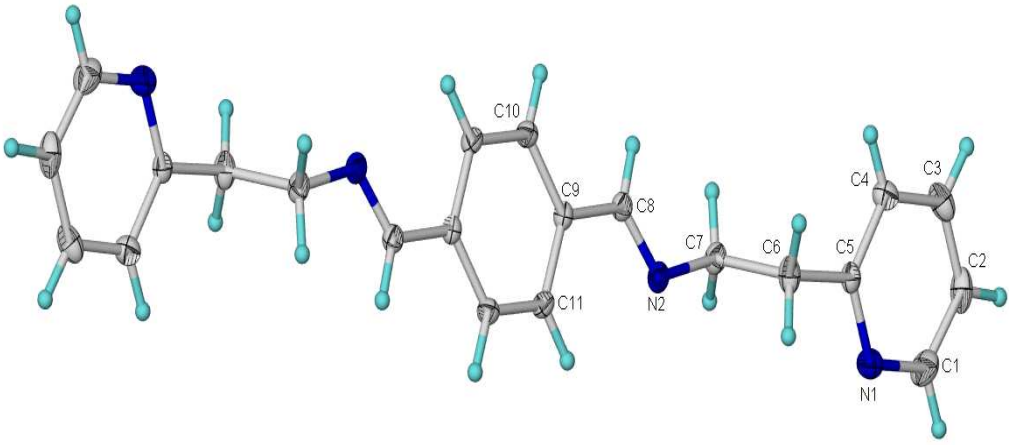

Figure 2.6 The ORTEP plot of the molecular structure of **68** showing the atomic numbering All non-hydrogen atoms were presented with ellipsoidal model with probability level 40%. Only half of the molecule is labelled and another half of the molecule is generated via centre of symmetry (symmetry code: -x, -y, -z).

Table 2.11 Selected bond distances and angles for ligand **68**

Bond Distances (Å)		**Bond Angles(º)**	
N(1)-C(5)	1.3344(15)	C(5)-N(1)-C(1)	117.33(10)
N(1)-C(1)	1.3395(17)	N(1)-C(1)-C(2)	124.19(12)
N(2)-C (8)	1.2628(14)	C(8)-N(2)-C(7)	117.17(9)
N(2)-C(7)	1.4609(13)	N(1)-C(5)-C(4)	122.27(10)
C(5)-C(6)	1.5023(15)	N(1)-C(5)-C(6)	116.12(10)
C(6)-C(7)	1.5204(16)	N(2)-C(8)-C(9)	122.66(9)
C(8)-C(9)	1.4748(14)		

The crystal structure reveals that **68** exists as discrete molecules. The N(2)-C(8) distance of 1.2628 Å is consistent with a C=N double bonding.

The ligands **65**, **66** and **68** exhibit short C=N bonds with lengths of 1.2628 Å to 1.276 Å and longer N-C bonds with lengths of 1.455 Å to 1.467 Å. The C=N-C angles in the three ligands range from 117.2° to 117.33°, slightly less than the idealised angle of 120°, as is seen in other structurally characterised imines [24, 25]. Bond distances and angles around the sulphur atoms for ligands **65** and **66** are similar to those in related compounds [24].

2.4 Synthesis and characterization of other Schiff base ligands

The new Schiff base ligands **69** – **72** (Table 2.12) were prepared by condensation of aldehydes with diamines. They were characterised by IR spectroscopy as well as ^{1}H (Table 2.13) and by ^{13}C NMR (Table 2.14).

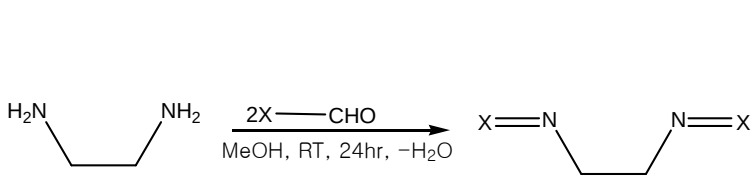

X = $CH_3O(C_6H_3)Cl$ **69**
X = $ClNO_2(C_6H_2)$ **70**
X = $(CH_3O)_2(C_6H_3)$ **71**
X = $(CH_3O)_3(C_6H_2)$ **72**

Scheme 2.7 Synthetic route to Schiff base ligands

The Schiff base ligands **69** – **72** were prepared according to literature procedures and are shown in Table 2.12.

Table 2.12 Schiff base ligands prepared

69 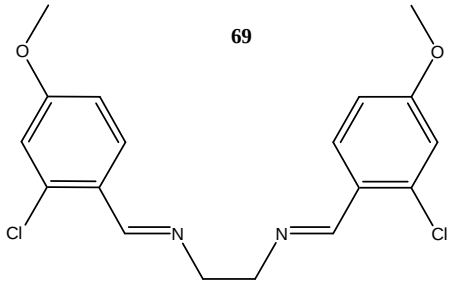	**70** 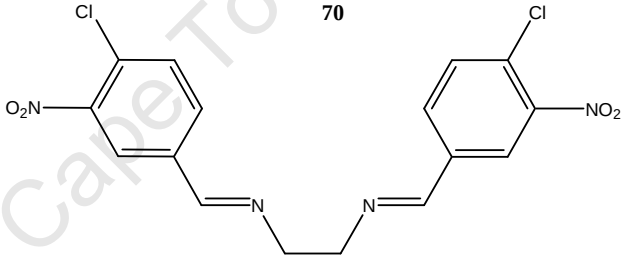
71 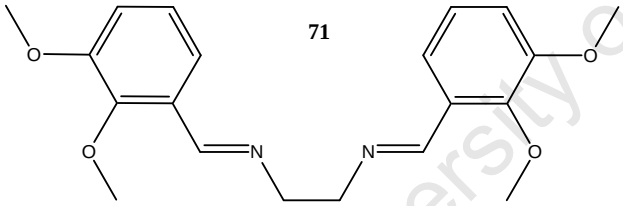	**72** 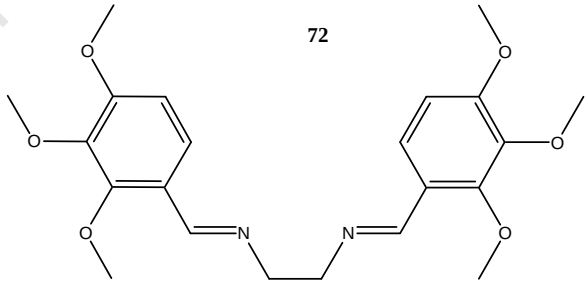

Ligands **69** – **72** where fully characterised by IR spectroscopy as well as ^{1}H, ^{13}C NMR, melting points and mass spectroscopy as shown in Tables 2.13 – 2.16.

Table 2.13 ^{1}H-NMR[a] chemical shifts δ (ppm) and microanalytical data for Schiff base ligands **69**-**72**

Ligand	HC=N	Ar-H	$N(CH_2)_2$	$O(CH_3)$	[b]IR(cm^{-1})
69	8.64 (s, 2H)	7.95 (d, 2H, *J*=8.5Hz), 7.24 (dd, 2H, *J*=0.7Hz, *J*=2.0Hz), 7.27 (dd, 2H, *J*=0.6Hz, *J*=2.1Hz)	4.01 (s, 4H)	2.17 (s, 6H)	1617
70	8.30 (s, 2H)	8.22 (s, 2H),7.83 (d, 2H, *J*=8.3Hz), 7.58 (d, 2H, *J*=8.3Hz)	4.03 (s, 4H)	-	1614
71	8.65 (s, 2H)	7.51 (d, 2H, *J*=1.6Hz), 7.03 (t, 2H, *J*=7.8Hz), 6.92(d, 2H, *J*=1.6Hz, *J*=2.1Hz)	4.00 (s, 4H)	3.85 (s, 6H) 3.77 (s, 6H)	1618
72	8.52 (s, 2H)	7.66 (s, 2H), 6.66 (s, 2H), 3.93 (s, 4H)	-	3.87 (s, 6H), 3.85 (s, 6H), 3.83 (s, 6H)	1625

[a]Spectra obtained in $CDCl_3$
[b]Recorded as KBr plates

^{1}H NMR data suggests that the four ligands have symmetrical structure with two imine groups. Four methylene protons are found at *ca* 4.00 ppm as singlets. Methylene protons on the methoxy substituant are observed as sharp singlets at around 3.77 – 3.87 ppm for ligands **71** and **72** but for ligand **69** the signal is observed at 2.17 ppm. The multiplets in the region 6.92 – 7.95 ppm are due to aromatic protons and the singlets observed at 8.30 – 8.65 ppm are assigned to the C=N protons.

The infrared spectra of the four ligands show stretching vibrations, (C-H) of the phenyl groups are in the region 3115 – 3015 cm^{-1}, while, (C-H) vibrations of the =CH- groups are observed as expected in the region 2970-2860 cm^{-1} [26]. Also strong bands appeared at about 1613 cm^{-1} and these bands are attributed to the C=N stretching vibration [27].

Table 2.14 ^{13}C-NMR[a] chemical shifts δ (ppm) for Schiff base ligands **69**-**72**

Ligand	H<u>C</u>=N	Ar-<u>C</u>	N(<u>C</u>H$_2$)$_2$	O(<u>C</u>H$_3$)
69	158.45	129.52, 129.27, 127.49,	61.34	55.65
70	158.81	135.92, 132.14, 128.82, 124.53	61.11	-
71	158.54	152.89, 149.69, 130.09, 124.04, 118.88, 114.25	61.91	55.85
72	158.09	122.17, 107.70	62.00, 61.81, 60.87	56.03

[a]Spectra obtained in $CDCl_3$

2.4.1 Physical properties of Schiff base ligands

Ligands **69** - **72** were isolated as crystalline solids which were all air stable solids and obtained in very good yields ranging between 83 – 92 % (Table 2.15).

Table 2.15 Yields and physical properties of ligands **69** to **72**.

Ligand	Yield (%)	Colour of Solid	Melting point (°C)
69	83	White	125-127
70	85	yellow	135-137
71	88	yellow	145-147
72	92	yellow	154-155

The mass spectra of Schiff base ligands are given in Table 2.16. The molecular ion peaks are in agreement with that calculated from their respective elemental analysis and fragmentation starts by loss of the methoxy group for ligands **69**, **71** and **72** but by initial loss of a chloride for ligand **70**.

Table 2.16 Mass spectra[a] data of Schiff base ligands **69-70**

Ligand	Calculated molar mass (g/mol)	Molecular fragment	Assignment
69	365.24	336.74	$[M\text{-}CH_3O]^+$
70	395.20	363.66	$[M\text{-}Cl]^+$
71	356.42	326.69	$[M\text{-}CH_3O]^+$
72	416.47	386.44	$[M\text{-}CH_3O]^+$

[a]EI-MS

2.5 Synthesis and characterization of palladium(II) complexes

2.5.1 Palladium dichloride complexes

Palladium dichloride complexes were obtained from the reaction of ligands **58-64** with $Pd(COD)Cl_2$ in CH_2Cl_2 at room temperature as shown in Scheme 2.9

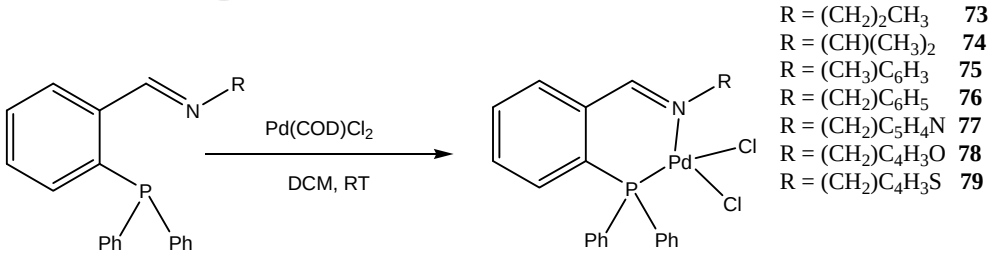

Scheme 2.8 Synthesis of palladium dichloride complexes

The palladium dichloride complexes were not very soluble in most organic solvents and thus proved to be very difficult to characterize due to their insoluble nature.

Table 2.17 Characterization data for palladium (II) dichloride complexes **73 – 79**.

Complex	Formula	M^+ (calcd) m/z	Anal Found (Calcd.)			IR spectra (cm^{-1})[a]	
			C	H	N	ν(C=N)	ν(C=N)[f]
73	$C_{22}H_{22}Cl_2NPPd$	[b,e]437.31 (508.72)	51.69(51.94)	4.12(4.36)	2.72(2.75)	1632	1637
74	$C_{22}H_{22}Cl_2NPPd$	[c,e]474.68 (508.72)	51.79(51.94)	4.12(4.36)	2.52(2.75)	1634	1634
75	$C_{31}H_{32}Cl_2NPPd$	[c,e]591.44 (626.89)	59.19(59.39)	5.12(5.15)	2.42(2.23)	1624	1629
76	$C_{26}H_{22}Cl_2NPPd$	[c,e]531.31 (556.76)	56.26(56.09)	3.72(3.98)	2.72(2.52)	1627	1636
77	$C_{25}H_{21}Cl_2N_2PPd$	[d,e]557.71 (557.75)	53.69(53.84)	3.92(3.80)	4.92(5.02)	1626	1632
78	$C_{24}H_{20}Cl_2NOPPd$	[d,e]546.71 (546.72)	52.59(52.72)	3.42(3.69)	2.72(2.56)	1630	1635
79	$C_{24}H_{20}Cl_2NPPdS$	[d,e]562.71 (562.79)	51.48(51.22)	3.32(3.58)	2.72(2.49)	1628	1636

[a]Recorded as KBr pellets

[b]Represents m/z for the fragment $[M-2Cl]^+$

[c]Represents m/z for the fragment $[M-Cl]^+$

[d]Represents m/z for the fragment $[M]^+$

[e]EI-MS

[f]Ligand absorption bands

*2.5.2 Single crystal X-ray determination of a palladium complex **74***

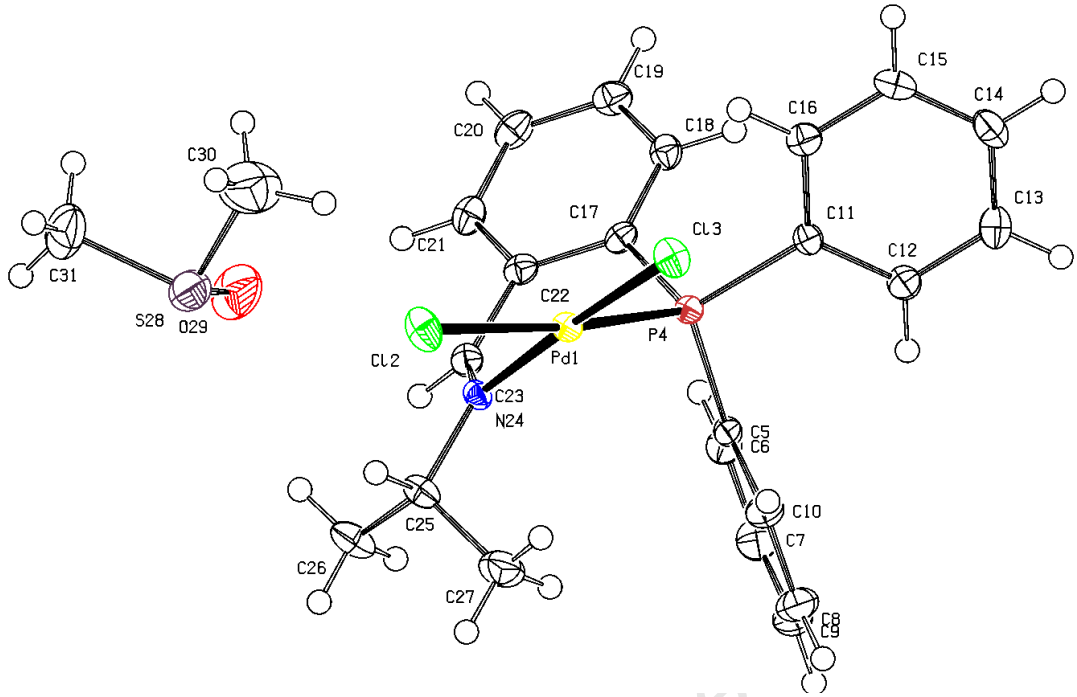

Figure 2.7 Molecular structure of **74** showing the atomic numbering scheme. All non-hydrogen atoms were presented with ellipsoidal model with probability level 40%. The asymmetric unit contains the organometallic compound and a dmso solvent molecule.

Table 2.18 Selected bond distances and angles for the palladium complex **74**

Bond Distances (Å)		**Bond Angles(º)**	
Pd(1)-Cl(2)	2.3838(6)	Cl(2)-Pd(1)-Cl(3)	90.74(2)
Pd(1)-Cl(3)	2.2826(6)	Cl(2)-Pd(1)-P(4)	172.6(2)
Pd(1)-N(24)	2.0726(17)	Cl(2)-Pd(1)-N(24)	91.07(5)
Pd(1)-P(4)	2.2189(6)	Cl(3)-Pd(1)-P(4)	92.31(2)
P(4)-C(11)	1.811(2)	Cl(3)-Pd(1)-N(24)	177.29(5)
P(4)-C(17)	1.820(2)	P(4)-Pd(1)-N(24)	86.13(5)
N(24)-C(23)	1.268(3)		

Selected bond distances and angles of **74** are presented in Table 2.18. The coordination around the palladium is slightly distorted from the ideal square planar

geometry. The main distortion is the NPdP bite angle of 86.13(5)° similar to other palladium complexes with iminophosphines [28]. The Pd-P distance (2.2189(6) Å) is within the expected range and the length of the carbon-nitrogen double bond is also within the expected range.

2.5.3 Single crystal X-ray determination of a palladium complex ***79***

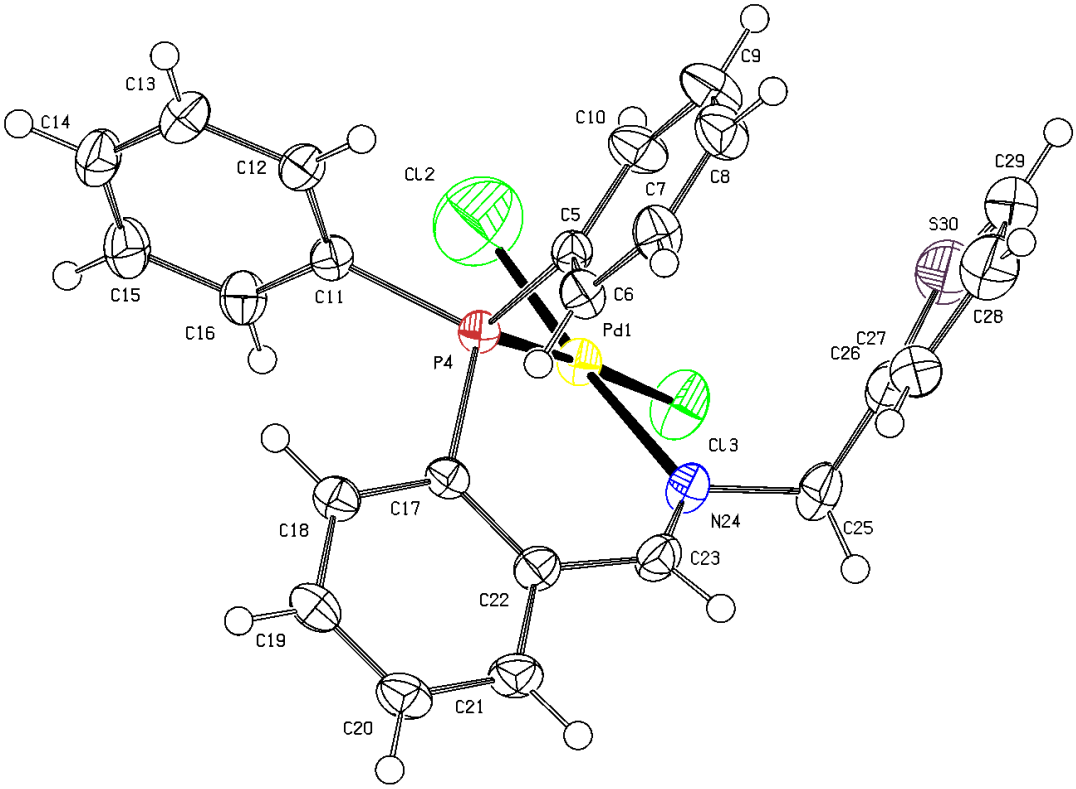

Figure 2.8 The ORTEP plot of the molecular structure of **79** showing the atomic numbering.

The solid state structure of **79** was obtained by X-ray diffraction (Figure 2.8). Pale yellow crystals suitable for single crystal X-ray diffraction were obtained by slow evaporation of a dmso-d_6-CH_2Cl_2 solution of the complex. The atomic labels of the asymmetric unit are given in the ORTEP picture in Figure 2.8. All non-hydrogen atoms were refined anisotropically and all hydrogens are placed geometrically with idealized riding models. Selected bond lengths and angles are listed in Table 2.19.

Table 2.19 Selected bond distances and angles for the palladium complex **79**

Bond Distances (Å)		**Bond Angles(º)**	
Pd(1)-Cl(2)	2.149(3)	Cl(2)-Pd(1)-Cl(3)	88.82(8)
Pd(1)-Cl(3)	2.3930(12)	Cl(2)-Pd(1)-P(4)	91.49(8)
Pd(1)-P(4)	2.1904(9)	Cl(2)-Pd(1)-N(24)	174.37(11)
Pd(1)-N(24)	2.135(3)	Cl(3)-Pd(1)-P(4)	176.40(4)
P (4)-C(5)	1.820(3)	P(4)-Pd(1)-N(24)	86.38(9)
P(4)-C(11)	1.812(3)	Pd(1)-P(4)-C(5)	111.55(11)
P(4)-C(17)	1.823(3)	Pd(1)-P(4)-C(11)	120.74(11)
N(24)-C(23)	1.276(5)	Pd(1)-P(4)-C(17)	109.32(11)

The molecular structure revealed a slightly distorted square planar geometry around the palladium metal center. The ligand was shown to bind in the expected κ^2-P^N fashion with a bite angle P(4)-Pd(1)-N(24) of 86.38(9)°. The angle deviated slightly from the expected 90°, presumably due to the strain imposed by the six-membered chelate ring P(4)-C(17)-C(22)-C(23)-N(24)-Pd(1). This reduction in the bite angle was compensated for by an increase in the Cl(2)-Pd(1)-P(4) angle of 91.49(8)°. This deviation of the bite angle from 90° has been observed for similar complexes with iminophosphines [28].

*2.5.4 Synthesis of palladium methylchloride complexes **80-83***

Palladium methylchloride complexes **80 - 83** were obtained from the reaction of ligands **61 - 64** with PdMe(COD)Cl as shown in the Scheme 2.9.

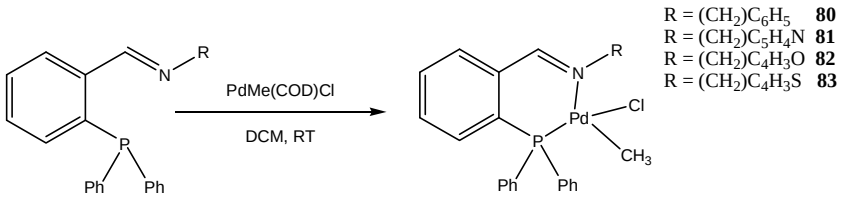

Scheme 2.9 Synthesis of palladium methylchloride complexes

The reaction was allowed to stir in dry CH_2Cl_2 at room temperature for 8 hours. The solvent was reduced and product precipitated out with Et_2O. Further precipitation was achieved by allowing the products to crystallize slowly at – 16 °C giving pale yellow crystals in reasonable yields. These complexes are much more soluble than the palladium dichloride complexes.

2.5.4.1 ^{1}H NMR and ^{31}P NMR data of complexes 80 - 83

The ^{1}H NMR spectra of complexes **80** – **83**, showed imine protons in the region δ 8.63 – 8.81 ppm. The observed upfield shifts of 0.21 – 0.28 ppm with respect to the free ligands further confirmed coordination of the imine nitrogen to the metal center. A downfield shift of δ 0.18 – 0.25 ppm was also observed for the methylene signals, due to the coordination of the adjacent imine nitrogen thereby deshielding these protons. No significant chemical shifts were observed for the olefinic signals of the furyl and the thiophenyl with respect to those of the free ligands, suggesting that these groups did not participate in bonding with the metal center. The ^{31}P NMR spectra of complexes **80** – **83** showed the expected downfield shift to δ 37.4 – 38.5 ppm with respect to the free ligands which appeared at δ -13.2 to -13.9 ppm, due to coordination of the phosphine moiety to the palladium metal center. The appearance of one signal in the ^{31}P NMR spectra also suggests that only one species had been formed.

Table 2.20 Characterization data for palladium methylchloride complexes **80 – 83**.

Complex	Formula	M^+ (calcd) m/z	Anal Found (Calcd.)			IR spectra (cm^{-1})[a]	
			C	H	N	ν(C=N)ligand	ν(C=N)
80	$C_{27}H_{25}ClNPPd$	[b]521.75 (536.34)	60.72(60.46)	4.51(4.70)	2.81(2.61)	1636	1628
81	$C_{26}H_{24}ClNPPd$	[c]537.13 (537.33)	58.19(58.12)	4.12(4.50)	5.54(5.21)	1632	1628
82	$C_{25}H_{23}ClNOPPd$	[c]526.03 (526.30)	57.19(57.07)	4.12(4.40)	2.72(2.66)	1635	1631
83	$C_{25}H_{23}ClNPPdS$	[b]531.8 (542.37)	55.15(55.36)	4.08(4.27)	2.38(2.58)	1636	1629

[a]IR obtained using KBr pellets

[b]Represents m/z for $[M\text{-}CH_3]^+$

[c]Represents m/z for $[M\text{-}Cl]^+$

*2.5.5 Single crystal X-ray determination of a palladium complex **80***

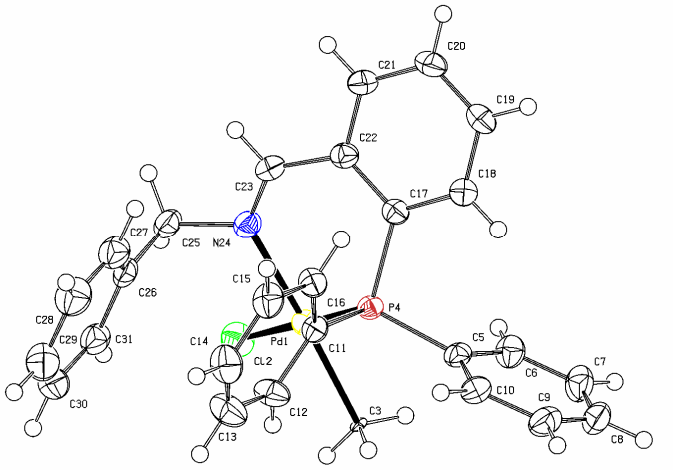

Figure 2.9 Molecular structure of **80** showing the atomic numbering scheme. All non-hydrogen atoms were presented with ellipsoidal model with probability level 40%.

The slow evaporation of a CH_2Cl_2-dmso-d_6 solution of **80** at room temperature afforded pale yellow single crystals suitable for X-ray diffraction.

Table 2.21 Selected bond distances and angles for the palladium complex **80**

Bond Distances (Å)		**Bond Angles(º)**	
Pd(1)-Cl(2)	2.4035(9)	Cl(2)-Pd(1)-P(4)	178.09(8)
Pd(1)-P(4)	2.1940(7)	Cl(2)-Pd(1)-N(24)	94.38(8)
Pd(1)-N(24)	2.151(2)	Cl(2)-Pd(1)-C(3)	88.10(6)
Pd(1)-C(3)	2.1232(19)	P(4)-Pd(1)-N(24)	86.76(6)
P (4)-C(5)	1.821(3)	P(4)-Pd(1)-N(24)	86.38(9)
P(4)-C(11)	1.824(3)	Pd(1)-P(4)-C(5)	111.55(11)
N(24)-C(23)	1.280(4)	Pd(1)-P(4)-C(17)	109.32(11)
N(24)-C(25)	1.486(4)		

The Pd-P distances 2.1940(7) Å is within the expected range and close to the values determined for the monohalide complex [PdMeCl(L)] (2.1925(9) Å and in the dihalide complexes of the same ligand studied by Coleman *et al* [29, 37]. The Pd-N distances are similar to those found for Pd(II) complexes in the same series. The methyl group is *trans* to the nitrogen atom of the ligand. The torsion angle Pd(1)-P(4)-C(17)-C(22) = 39.9(2) Å indicates that the $=CHC_6H_4$- unit lies above the PdMeCl(P,N) plane.

2.6 Synthesis and characterization of platinum(II) complexes

2.6.1 Platinum dichloride complexes

Platinum dichloride complexes were obtained from the reaction of ligands **60-64** with either $[Pt(COD)Cl_2]$ or $[Pt(DMSO)_2Cl_2]$ as shown in Scheme 2.11.

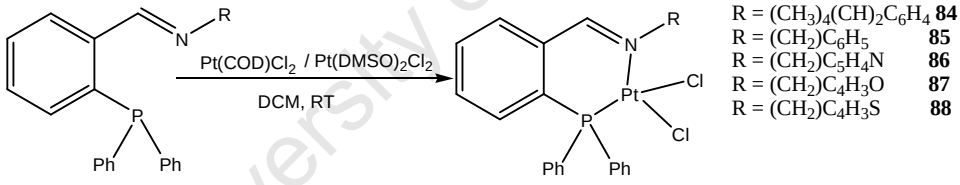

Scheme 2.10 Synthesis of platinum dichloride complexes

The reagents were taken up in CH_2Cl_2 and stirred at room temperature for 2 hours. The solvent was reduced and the complexes precipitated out on addition of hexane before washing with Et_2O affording pale yellow complexes in reasonable yields

*2.6.1.1 ^{31}P NMR spectra of platinum complexes **84-88***

The platinum complexes **84** to **88** displayed sharp singlets flanked by platinum satellites in their ^{31}P NMR spectra (Table 2.22).

Table 2.22 ^{31}P NMR of complexes **84-88**

Ligand	δ (ppm)	Pt complex	δ (ppm)	^{1}J (Pt-P) Hz
60	-15.8	**84**	5.83	3661
61	-13.6	**85**	8.09	3668
62	-13.2	**86**	8.44	3469.9
63	-13.9	**87**	5.86	3777.6
64	-13.8	**88**	8.06	3758.5

($CDCl_3$, RT, internal standard: H_3PO_4)

The ^{31}P NMR spectra of platinum complexes provides a sensitive probe for the structures of complexes. The one-bond coupling ^{1}J(Pt-P) is characteristic of these complexes and those which contain Cl atoms *trans* to phosphorus atoms have been found to possess coupling constants greater than 3500 Hz [30].

There were downfield shifts of approximately 20 ppm from ligand to complex, with the most significant shift arising from formation of complex **88**.

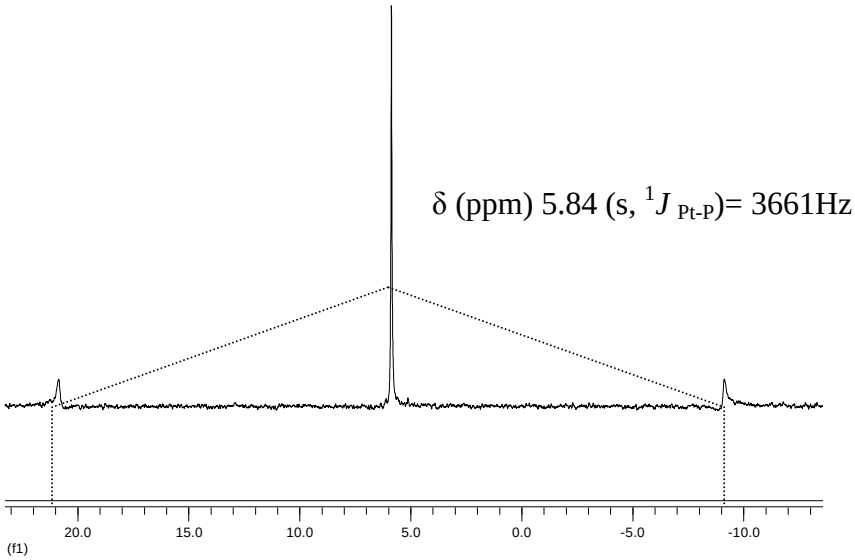

Figure 2.10 ^{31}P NMR spectrum of **84** ($CDCl_3$, RT, internal standard: H_3PO_4).

^{31}P NMR data for the complexes **84-88** show a downfield shift of between 19.76 and 21.86 ppm on complexation of the ligands to the metal centre, with the most significant shift arising from formation of complex **88** as shown in Table 2.22 indicating that the P centre of the ligand is coordinated to the metal. The coordination chemical shift observed for complexes **84-88** is comparable to that reported previously [32]. There is a strong similarity in chemical shift observed among all the complexes *e.g* δ_p values for the platinum complexes are almost identical, indicating that the substituents on the aldehyde constituent of the iminophosphine ligand have little influence on the value of the shift. This observation is also consistent with previous reports of similar types of ligands [32]. The signal due to the P centre in the platinum complexes is shifted *ca* 20 ppm upfield. This trend was also noted previously for platinum complexes of the [P, N, O] ligand 2-$[Ph_2PC_6H_4CH{=}N]C_6H_3OH$ [31]. The presence of Pt satellites in the spectra of complexes **84-88**, Table 2.22, is further evidence of coordination by the P centre.

2.6.1.2 Mass spectra

Figure 2.11 shows the mass spectrum (EI) obtained for complex **84.** The spectrum shows a strong peak corresponding to the parent ion with loss of a chloride ion (Table 2.23). The complex fragments by loss of the remaining chloride ion(m/z = 640.46) and subsequent loss of a two isopropyl units (m/z = 562.50). This is followed by sequential loss of the phenyl group (m/z = 453.47).

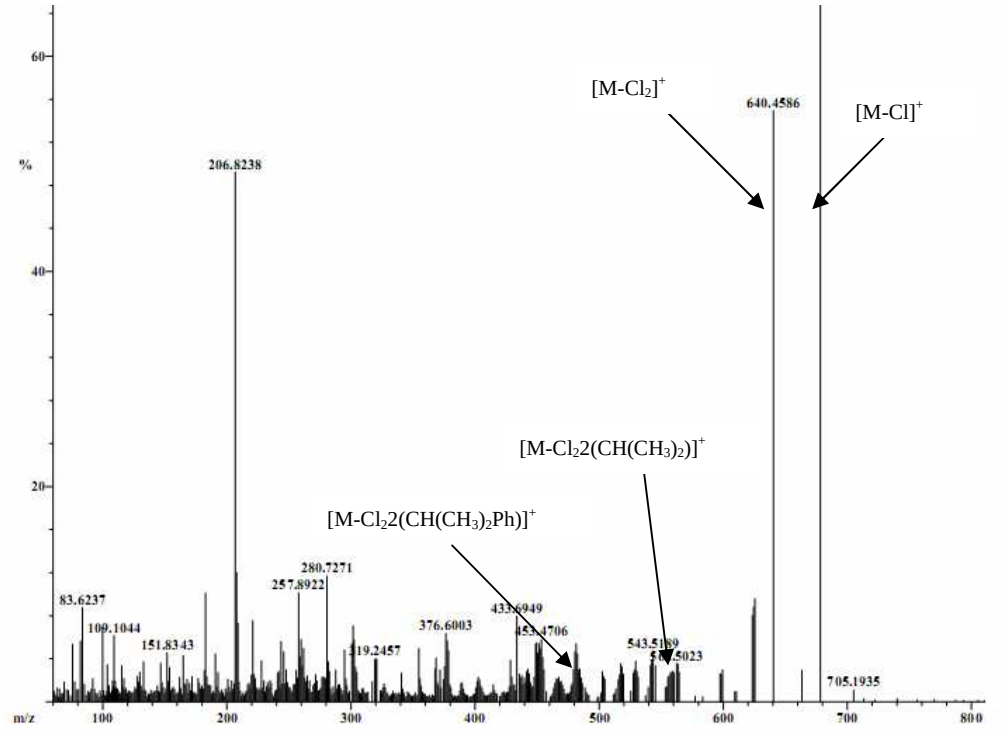

Figure 2.11 Mass Spectrum (EI) of **84**

Table 2.23 Assignment of fragment ions in the mass spectrum of **84**

Fragment ion	m/z
$[M\text{-}Cl]^+$	678.34
$[M\text{-}Cl_2]^+$	640.46
$[M\text{-}Cl_2 2(CH(CH_3)_2)]^+$	562.50
$[M\text{-}Cl_2 2(CH(CH_3)_2Ph)]^+$	453.47

2.6.1.3 Physical properties of platinum dichloride complexes

The platinum dichloride complexes **84** to **88** were all air stable, yellow solids which did not melt or decompose below 250 °C. The data obtained agrees with those previously reported [20]. Experimental yields obtained varied between 68 to 72 % as shown in Table 2.24.

Table 2.24 Yields and physical properties of platinum complexes **84-88**

Complex	Yield (%)	Colour	Melting point (^{o}C)
84	72	yellow	272-273
85	68	Light yellow	>300
86	70	Dark orange	258-260
87	71	Yellow/orange	>300
88	70	Pale yellow	>300

2.6.1.4 IR spectroscopy

The elemental analysis data obtained for the ligands were in agreement with the proposed formulations depicted in Scheme 2.11. The most informative peak in the IR spectra of iminophosphine complexes of platinum is that of the C=N group occurring in the 1600 cm^{-1} region, Table 2.25. Comparison of the position of this peak in complexes **84**-**88** with that of the corresponding ligands **60**-**64** shows a shift to lower wavenumber on complexation of between 5 and 9 cm^{-1}. The direction and magnitude of this shift is in agreement with previous observations on metal complexes of similar types of ligands [32]. A shift to lower wavenumbers indicates a weakening of the bond between C and N, in this case due to the coordination of the imine to the metal centre. The largest shift is seen for complex **84**.

Table 2.25 Elemental analysis and IR data for platinum complexes **84** – **88**

Complex	Formula	Anal Found (Calcd.)			IR (cm^{-1})[a]
		C	H	N	ν(C=N)
84	$C_{31}H_{32}C_{l2}NPPt$	52.19 (52.03)	4.74 (4.51)	1.99 (1.96)	1624
85	$C_{26}H_{22}Cl_2NPPt$	48.19 (48.38)	3.12 (3.44)	2.17 (2.47)	1632
86	$C_{25}H_{21}Cl_2N_2PPt$	46.45 (46.19)	3.27 (3.12)	4.33 (4.72)	1630
87	$C_{24}H_{20}Cl_2NOPPt$	48.83 (48.69)	3.77 (3.52)	2.28 (2.52)	1633
88	$C_{24}H_{20}Cl_2NPPtS$	44.19 (44.25)	3.12 (3.09)	2.42 (2.15)	1631

[a]IR obtained using KBr pellets

*2.6.1.5 Single crystal X-ray determination of platinum dichloride complex **84***

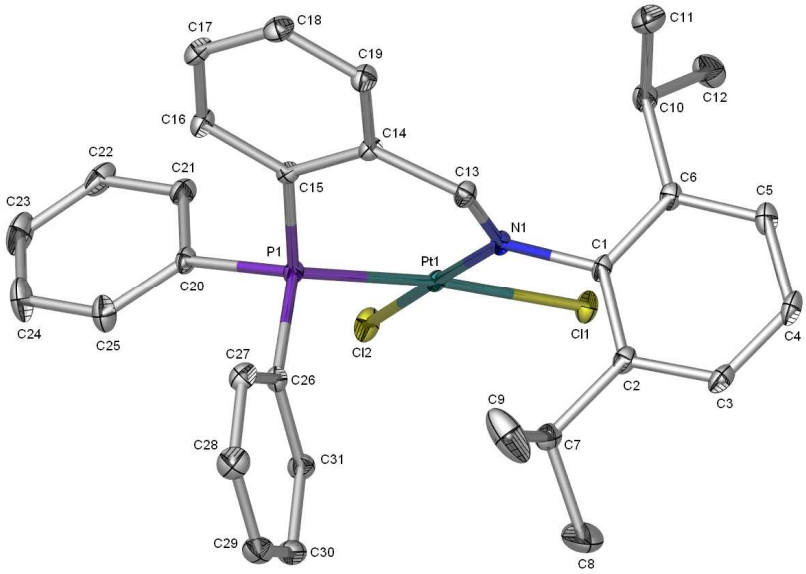

Figure 2.12 The ORTEP plot of the molecular structure of **84** showing the atomic numbering. All the H atoms are omitted for clarity and are presented with ellipsoidal model with probability level 35%.

The slow evaporation of a CH_2Cl_2 solution of **84** at room temperature afforded pale yellow single crystals suitable for X-ray diffraction (Figure 2.12).

The platinum complex is of distorted square planar geometry with the P–Pt–N angle at 89.80(5)° and the corresponding angle between the chloride ligands has also been reduced to 87.92(2)°. As phosphorus ligands have higher *trans* influence than amine ligands, the Pt – Cl bond *trans* to P is slightly elongated compared to the chloride bound *cis* to P [33].

Selected bond lengths and angles are listed in Table 2.26

Table 2.26 Selected bond distances and angles for the platinum complex **84**

Bond Distances (Å)		**Bond Angles(º)**	
Pt(1)-N(1)	2.0421(18)	N(1)-Pt(1)-P(1)	89.80(5)
Pt(1)-P(1)	2.2128(6)	N(1)-Pt(1)-Cl(2)	178.85(5)
Pt(1)-Cl(2)	2.2901(6)	P(1)-Pt(1)-Cl(2)	91.25(2)
Pt(1)-Cl(1)	2.3512(6)	N(1)-Pt(1)-Cl(1)	90.98(5)
P(1)-C(15)	1.809(2)	P(1)-Pt(1)-Cl(1)	174.20(2)
P(1)-C(26)	1.816(2)	Cl(2)-Pt(1)-Cl(1)	87.92(2)
N(1)-C(13)	1.287(3)		

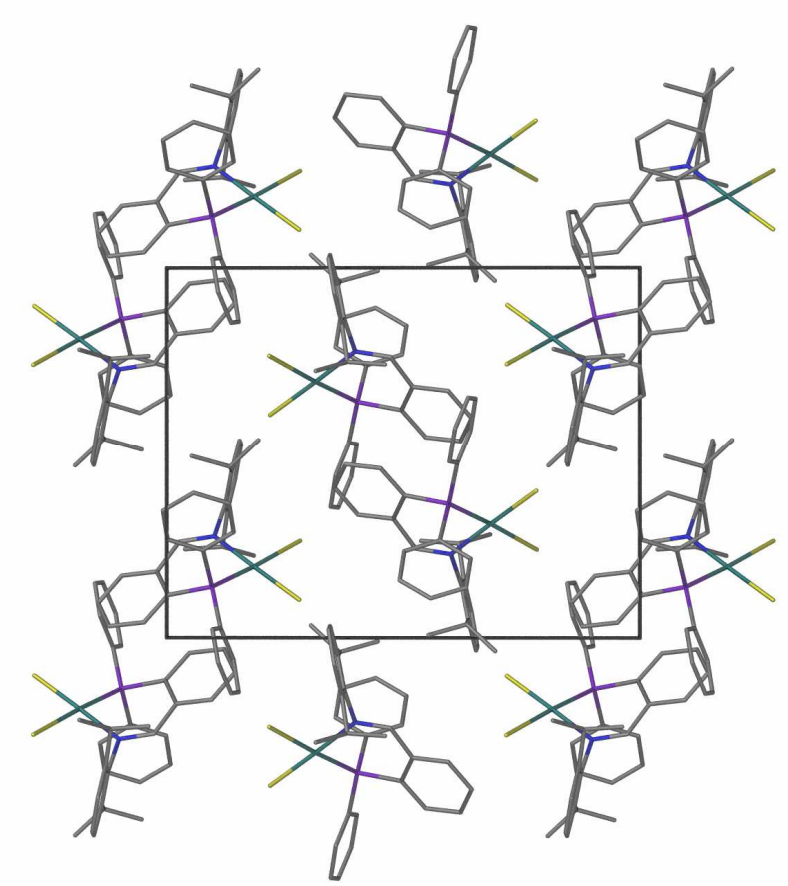

Figure 2.13 Projection of **84** viewed along [100]. All H atoms are omitted for clarity.

A similar geometrical arrangement of the ligands was observed by McIsaac *et al* [34] for novel iminophosphino rhodium(I) complexes including [Rh(κ^2-*o*-$Ph_2PC_6H_4CH$=N-2,6-$^iPr_2C_6H_3$)(μ-Cl)]$_2$. In comparison to the related compound *o*-$Ph_2PC_6H_4CH=NC_6H_4OMe$-*o* [35], both iminophosphines have a very similar arrangement with planar C(14)–C(19)=N(20)–C(21) imino units with an *E* configuration with respect to the diphenylphosphine group. These structures are in contrast to *o*-$Ph_2PC_6H_4CH=NC_6H_4OH$-*o* [36] where the nitrogen is closer to the phosphorus atom as the molecule assumes a *Z* configuration. The N(1)=C(13) double bond of complex **84** is 1.287(2) Å is well within the range observed for these types of compounds [36]. There is little variation observed in the bond lengths of the ligand upon chelation to Pt(II), for the free ligand the length is 1.2668 (19) Å. The ligand

backbone carbon-carbon distances for the complex are comparable with that of the free ligand. The average Pt-N and Pt-P bond lengths of 2.0421(18) and 2.2128(6) Å, respectively are in the range expected for iminophosphine platinum(II) complexes [37]. The torsion angle Pt(1)-P(1)-C(15)-C(14) = -35.5(2)° indicates that the $=CHC_6H_4$- unit lies below the $PtCl_2$(P,N) plane.

*2.6.1.6 Single crystal X-ray determination of platinum complex **86***

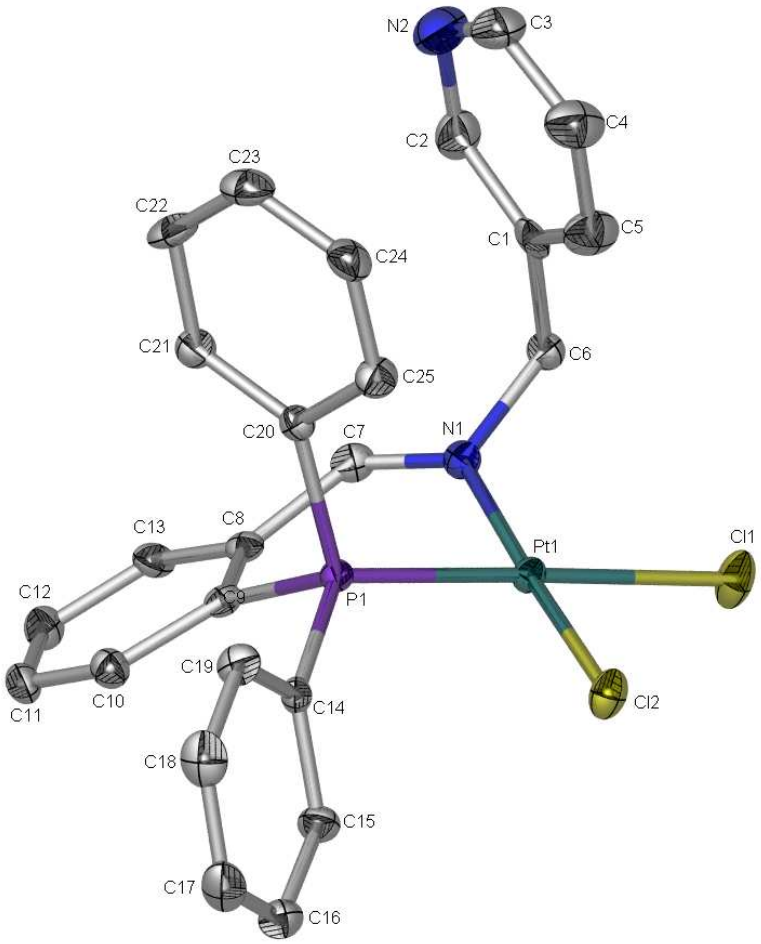

Figure 2.14 The ORTEP plot of the molecular structure of **86** showing the atomic numbering. All non-hydrogen atoms were presented with ellipsoidal model with probability level 40%. All hydrogen atoms are omitted for clarity.

The slow evaporation of a CH_2Cl_2 solution of complex **86** at room temperature afforded pale yellow single crystals suitable for X-ray diffraction.

Table 2.27 Selected bond distances and angles for the platinum complex **86**

Bond Distances (Å)		**Bond Angles(º)**	
Pt(1)-N(1)	2.040(4)	N(1)-Pt(1)-P(1)	88.47(12)
Pt(1)-P(1)	2.1999(13)	N(1)-Pt(1)-Cl(2)	176.70(12)
Pt(1)-Cl(2)	2.2840(12)	P(1)-Pt(1)-Cl(2)	91.76(5)
Pt(1)-Cl(1)	2.3806(14)	N(1)-Pt(1)-Cl(1)	91.27(12)
P(1)-C(20)	1.803(5)	P(1)-Pt(1)-Cl(1)	178.20(5)
P(1)-C(14)	1.815(5)	Cl(2)-Pt(1)-Cl(1)	88.60(5)

The platinum is in a square-planar environment and it is bound to the ligand using a κ^2-N,P interaction in a *cis* fashion, with the chlorides located at the two remaining sites. However the square-planar geometry of the platinum environment is distorted with the angles being less than 180°, N(1)-Pt(1)-Cl(2) and P(1)-Pt(1)-Cl(1) of 176.70(12)° and 178.20(5)°, respectively. The average Pt-N and Pt-P bond lengths of 2.040(4) and 2.1999(13) Å, respectively are in the range expected for iminophosphine platinum(II) complexes. The torsion angle Pt-P-C(9)-C(8) = -36.5(4)° indicates that the $=CHC_6H_4$- unit lies below the $PtCl_2$(P,N) plane.

*2.6.1.7 Single crystal X-ray determination of platinum complex **88***

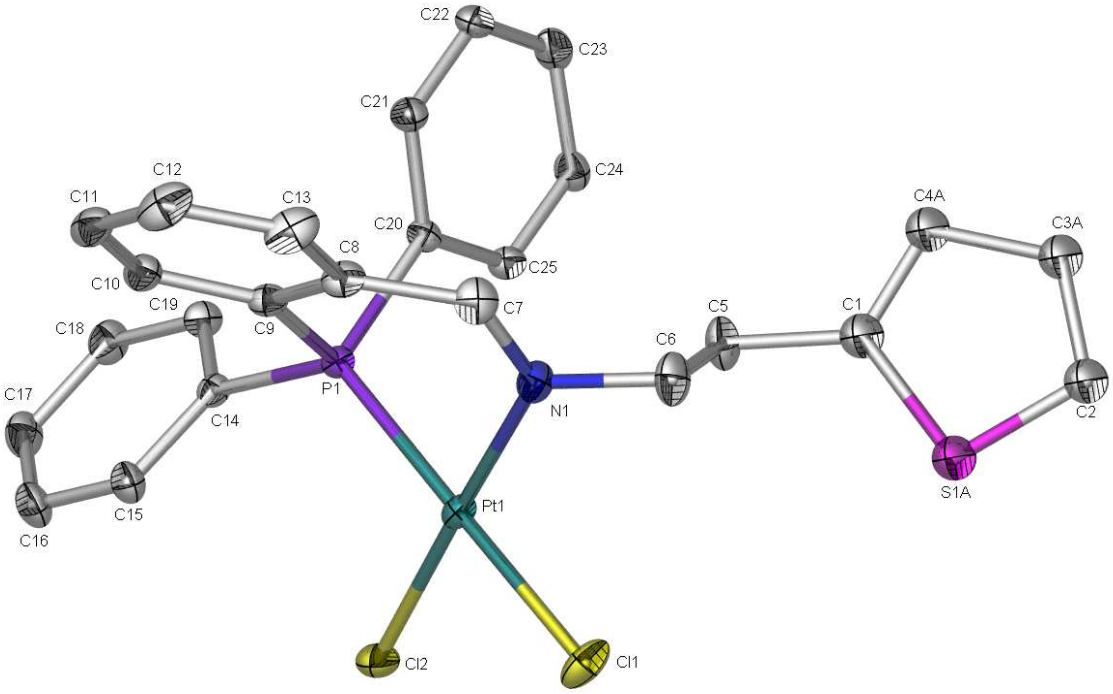

Figure 2.15 The ORTEP plot of the molecular structure of **88** showing the atomic numbering. All non-hydrogen atoms were presented with ellipsoidal model with probability level 40%. The thiophene ring was disordered over two places and only one ring is shown here. One solvent water molecule and all hydrogen atoms are omitted for clarity.

The slow evaporation of a CH_2Cl_2 solution of complex **88** at room temperature afforded pale yellow single crystals suitable for X-ray diffraction.

Selected bond lengths and angles of complex **88** are listed in Table 2.28.

Table 2.28 Selected bond distances and angles for the platinum complex **88**

Bond Distances (Å)		**Bond Angles(º)**	
Pt(1)-N(1)	2.032(5)	N(1)-Pt(1)-P(1)	86.13(14)
Pt(1)-P(1)	2.2084(13)	N(1)-Pt(1)-Cl(2)	178.42(14)
Pt(1)-Cl(2)	2.2901(15)	P(1)-Pt(1)-Cl(2)	95.36(5)
Pt(1)-Cl(1)	2.3639(14)	N(1)-Pt(1)-Cl(1)	89.48(14)
P(1)-C(20)	1.811(5)	P(1)-Pt(1)-Cl(1)	174.05(5)
P(1)-C(9)	1.823(5)	Cl(2)-Pt(1)-Cl(1)	89.06(6)

In complex **88** the ligand adopts a κP, κN coordination mode in a square-planar coordination geometry for the platinum center. The Pt(1)-N(1), Pt(1)-P(1), Pt(1)-Cl(2) and the Pt(1)-Cl(2) are in the normal range [38]. The Pt-Cl bond length *trans* to the P atom (2.3639(14) Å) is longer than that *trans* to the N atom (2.2901(15) Å) owing to the stronger *trans* influence of a tertiary phosphine with respect to an imine. The bond angle at the Pt(1) atom exhibits only minor deviations from a right angle. The torsion angle Pt(1)-P(1)-C(9)-C(8) = 44.8(5)° indicates that the $=CHC_6H_4$- unit lies above the $PtCl_2$(P,N) plane.

*2.6.1.8 Synthesis of platinum methylchloride complexes **89-90***

Platinum methylchloride complexes were isolated from the reaction of ligands **63-64** with PtClMe(COD) as shown in the Scheme 2.12.

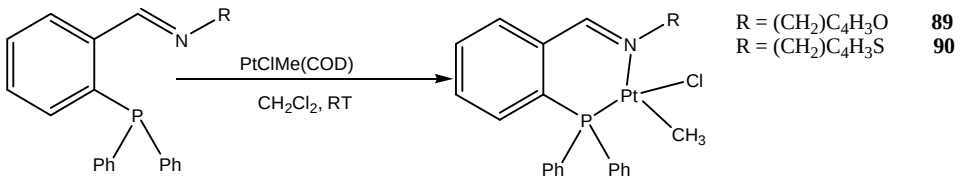

Scheme 2.11 Synthesis of platinum methylchloride complexes

The reagents were taken up in CH_2Cl_2 and stirred at room temperature for 2 hours. The solvent was reduced and the complexes precipitated out on addition of hexane, before washing with Et_2O affording pale yellow complexes in good yields. Spectroscopic and analytical data were in agreement with the proposed structures.

2.6.1.9 NMR data for platinum chloromethyl complexes

The ^{1}H NMR spectroscopy of **89** showed a doublet assignable to the group at δ 0.19 (*trans* to the PPh_2 moiety, J_{PH} = 73.9 Hz) respectively. Complex **90** exhibited a doublet at δ 0.38 *cis* to PPh_2, J_{PH} = 3.8 Hz). As expected, the Pt-H coupling is larger for the MePt trans to PPh_2 than for the MePt *cis* to P. The signal for the azomethine proton in the ^{1}H NMR spectra of the complexes is shifted downfield from that of the free ligand, indicating that imine nitrogen is coordinated to the metal centre. Previous data for almost similar complexes reported the azomethine peaks as singlets; in the present work, the spectra were obtained at a slight higher field with Pt satellites J_{PtH} = 101.3 Hz and J_{PtH} = 109.8 Hz. The ^{1}H NMR spectra of the complexes shows a set of resonances in the region 6.90 – 7.99 ppm arising from the aromatic protons of the iminophosphine ligand

The ^{31}P NMR spectroscopy in dmso-d_6 of **89** exhibited a singlet at δ 9.28, showing that the Pt-coordinated phosphine is considerably de-shielded compared to the free ligand **63**. The singlet has two pairs of ^{195}Pt satellites ascribed to isomers in solution with coupling constants J_{PtP} = 2322.7 Hz and J_{PtP} = 3782.6 Hz. The presence of platinum satellites in the spectra of the complexes **89** and **90** is further evidence of

coordination by the P centre. Furthermore the J_{PtP} coupling constants are of the order of magnitude expected in such complexes.

Table 2.29 Characterization data for platinum complexes **89** – **90**

Complex	Formula	M^+ (calcd) m/z	Anal Found (Calcd.)		
			C	H	N
89	$C_{25}H_{23}ClNOPt$	[a]598.94 (614.96)	47.29(47.44)	3.69(3.98)	2.08(2.21)
90	$C_{25}H_{23}ClNPPtS$	[b]595.45 (631.03)	48.26(48.58)	3.83(3.67)	2.28(2.15)

[a]Represents m/z for $[M\text{-}CH_3]^+$
[b]Represents m/z for $[M\text{-}Cl]^+$

2.6.1.10 Mass spectrometry of complex 90

The complex displays a peak corresponding to the parent ion (m/z = 630.32, $[M]^+$) with loss of a chloride ion (m/z = 595.45, $[M–Cl]^+$. The complex fragments by initial loss of the chloride ion and subsequent loss of the methyl group (m/z = 580.54, $[M–Cl–CH_3]^+$) This is followed by sequential loss of one phenyl group (m/z = 502.62, $[M–Cl–CH_3–Ph]^+$ and loss of the other phenyl group (m/z = 428.60, $[M–Cl–CH_3–(Ph)_2]^+$).

Table 2.30 Assignment of fragment ions in the mass spectrum of complex **90**

Fragment ion	m/z
$[M]^+$	630.32
$[M–Cl]^+$	595.45
$[M–Cl–CH_3]^+$	580.54
$[M–Cl–CH_3–Ph]^+$	502.62
$[M–Cl–CH_3–(Ph)_2]^+$	428.60

2.6.1.11 Infrared spectroscopy of platinum chloromethyl complexes

Ligands **63** and **64** show distinctive stretching frequencies, ν(C=N) at 1635 and 1633 cm^{-1} (KBr plates) which agrees with previously reported values for iminophosphine ligands [11]. Upon complexation, these peaks shift to 1625 and 1627 cm^{-1}. This is due to increased electron density on the metal upon coordination of the imine moiety to the metal centre. The direction and magnitude of this shift is in agreement with previous observations on metal complexes of similar types of ligands [11]. A shift to lower wavenumbers indicates a weakening of the bond between C and N, in this case due to the coordination of the imine nitrogen to the metal centre.

2.7 Synthesis and characterization of gold(I) complexes

2.7.1 Synthesis of gold(I) chloride complexes

Gold(I) chloride complexes were obtained from the reaction of ligands **60, 62-64** with Au(tht)Cl as shown in Scheme 2.13.

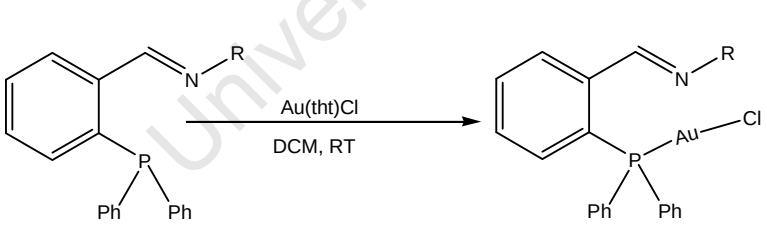

R = $(CH_3)C_6H_3$ **91**
R = $(CH_2)C_5H_4N$ **92**
R = $(CH_2)C_4H_3O$ **93**
R = $(CH_2)C_4H_3S$ **94**

Scheme 2.12 Synthesis of gold(I) chloride complexes

Reagents were dissolved in CH_2Cl_2 and stirred at room temperature for 2 hours before reducing the solvent and precipitating out the complex with hexane and then washing with Et_2O before drying under vacuum for 4 hours. Complex **95** was obtained from

the reaction of an equimolar amount of triphenylphosphine with Au(tht)Cl in CH_2Cl_2 at room temperature.

2.7.2 ^{1}H NMR spectroscopy of gold complexes

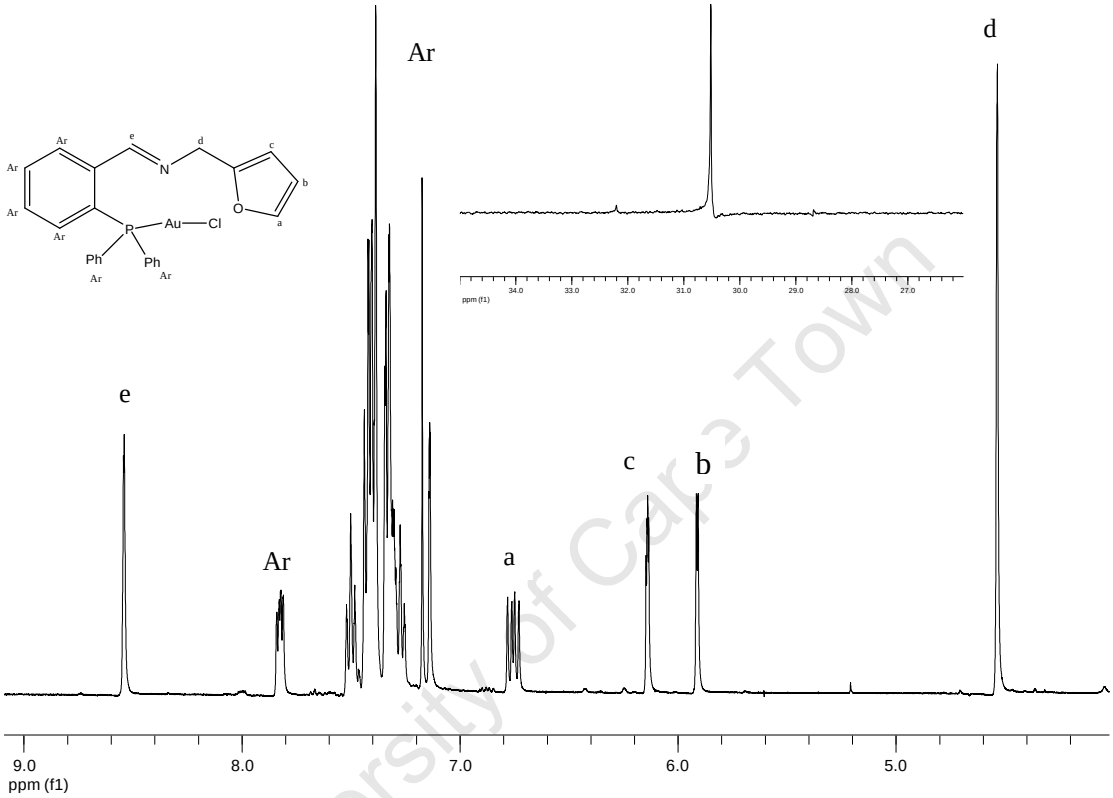

Figure 2.16 ^{1}H NMR and ^{31}P NMR spectrum of complex **93**

^{1}H NMR and ^{31}P NMR data of complexes 91 – 94

The ^{1}H NMR spectra of complexes **91** – **94**, showed imine protons in the region δ 8.54 – 8.90 ppm. The observed slight upfield shifts observed with respect to the free ligands further confirmed no coordination of the imine nitrogen to the metal center. This was also further unambiguously confirmed by the X-ray structural analysis of **91**, **93** and **95** shown in Figures 2.18, 2.19 and 2.20. No significant chemical shifts were observed for the olefinic signals of the furyl and the thiophenyl with respect to those

of the free ligands, suggesting that these groups did not participate in bonding with the metal center.

The free ligands manifested singlet resonances at -13.8 to -15.8 ppm respectively in their ^{31}P NMR spectra. Upon complexation, a significant downfield shift of these signals from 26.64 to 31.93 ppm for complexes **91 – 94**, respectively, was observed with the disappearance of the original free ligand, providing a diagnostic analytical tool by which the complexation process could be followed. The appearance of one signal in the ^{31}P NMR spectra of the complexes proved the formation of one species in all cases.

2.7.3 Mass spectrometry of complex gold complexes

The gold complexes display a peak corresponding to the parent ion $[M]^+$, a loss of a chloride ion $[M–Cl]^+$. The complexes then fragment by subsequent loss of the gold atom $[M–Cl–Au]^+$.

The mass spectra of the gold complexes are summarised in Table 2.31. The molecular ion peaks are in good agreement with their empirical formula as indicated by their elemental analysis. The other peaks represent fragments of the molecular ion.

Table 2.31 Fragmentation patterns of gold complexes **91-95**

[a]**Fragment ion m/z**	**Complex**				
	91	**92**	**93**	**94**	**95**
$[M]^+$	679.85	612.84	601.77	618.25	494.14
$[M–Cl]^+$	643.77	576.89	563.87	581.38	459.10
$[M–Cl–Au]^+$	449.31	379.89	367.44	385.73	262.10

[a]EI-MS

Figure 2.17 shows the mass spectrum (EI) obtained for complex **93.** The spectrum shows a peak corresponding to the molecular ion peak (m/z = 601.77). The complex fragments by loss of a chloride ion(m/z = 563.87) and finally by the subsequent loss of a gold atom (m/z = 376.44).

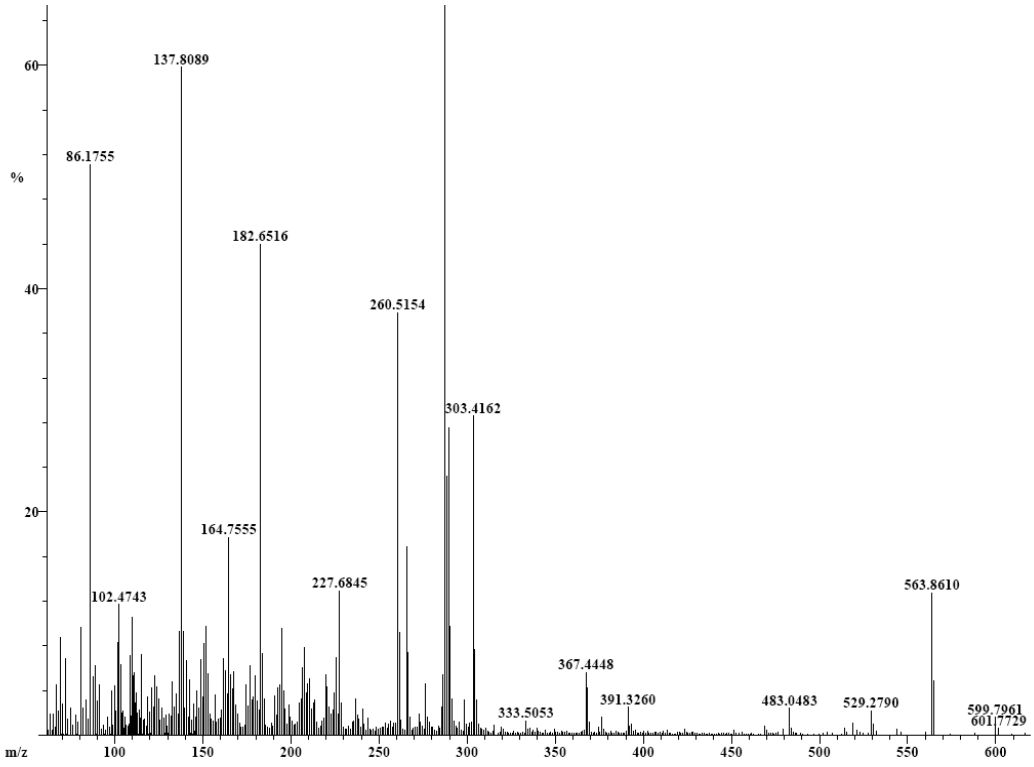

Figure 2.17 Mass spectrum (EI) of gold complex **93**

Table 2.32 Characterization data for gold complexes **91 – 95**

Complex	Formula	M^+ (calcd)[d] m/z	Anal Found (Calcd.)			IR spectra (cm^{-1})[a]	
			C	H	N	ν(C=N)ligand	ν(C=N)
91	$C_{31}H_{32}ClNPAu$	[b]449.31 (681.99)	54.88(54.60)	4.57(4.73)	1.97(2.05)	1629	1628
92	$C_{25}H_{21}ClN_2PAu$	[c]577.37 (612.82)	49.22(49.00)	3.23(3.45)	4.54(4.57)	1632	1630
93	$C_{24}H_{20}ClNOPAu$	[c]563.87 (601.81)	46.77(46.90)	3.48(3.35)	2.09(2.33)	1635	1634
94	$C_{24}H_{20}ClNPSAu$	[c]581.38 (617.88)	46.80(46.65)	3.42(3.26)	2.45(2.27)	1636	1634
95	$C_{18}H_{15}ClPAu$	[c]459.10 (494.70)	43.39(43.70)	3.12(3.06)	-	-	1625

[a]Recorded as KBr pellets
[b]Represents m/z for $[M\text{-}Cl\text{-}Au]^+$
[c]Represents m/z for $[M\text{-}Cl]^+$
[d]EI-MS

2.7.4 Infrared spectroscopy of gold(I) complexes

For the gold complexes **91**-**94** containing iminophosphine ligands the position of the ν(C=N) peak (*ca*. 1628 to 1635 cm^{-1} is comparable to that of the uncomplexed ligand suggesting that there is no interaction between this group and the metal center. For complex **95** the peak occurs at 1625 cm^{-1}. The peaks are shown in Table 2.32.

*2.7.5 Single crystal X-ray determination of gold complex **91***

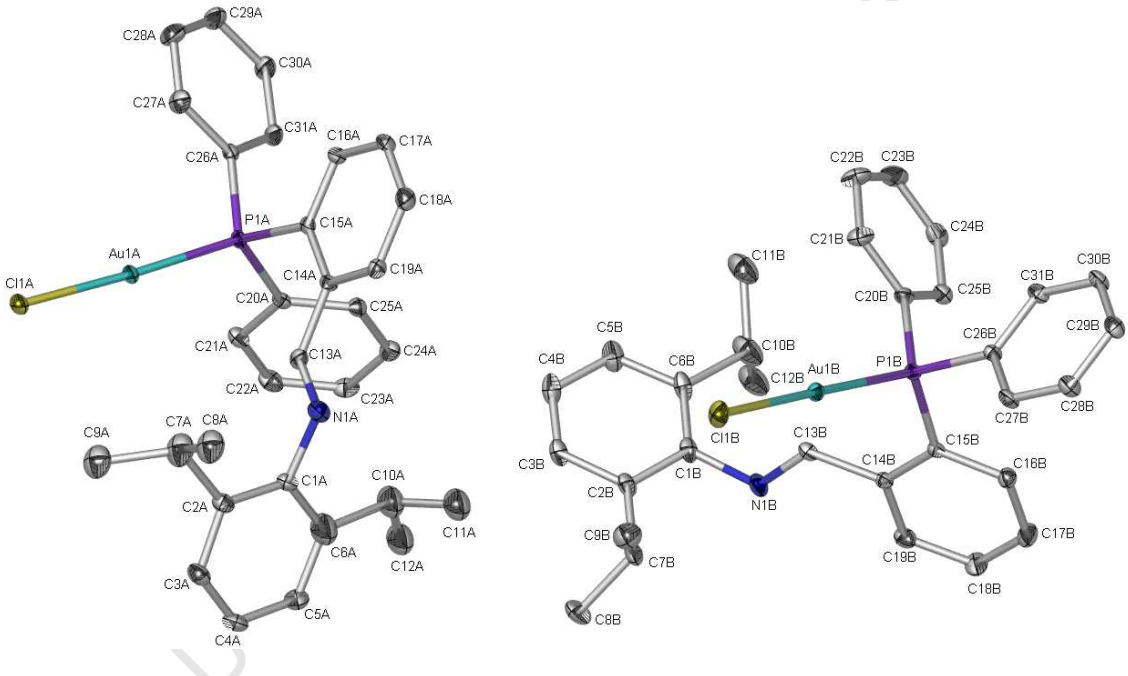

Figure 2.18 The ORTEP plot of the molecular structure of **91** showing the atomic numbering. There are two crystallographic independent molecules labelled as A and B in the asymmetric unit. All non-hydrogen atoms were presented with ellipsoidal model with probability level 25%. There is one solvent molecule ethanol and all hydrogen atoms are omitted from the picture.

The solid state structure of **91** was obtained by X-ray diffraction (Figure 2.18). Dark yellow crystals suitable for single crystal X-ray diffraction were obtained by slow evaporation of a CH_2Cl_2 solution of the complex at room temperature.

Table 2.33 Selected bond distances and angles for the gold complex **91**

	Bond Distances (Å)		**Bond Angles(°)**	
Molecule 1	Au(1A)-P(1A)	2.2350(13)	P(1A)-Au(1A)-Cl(1A)	177.17(5)
	Au(1A)-Cl(1A)	2.2783(14)	C(26A)-P(1A)-C(20A)	105.2(2)
	P(1A)-C(26A)	1.805(6)	C(26A)-P(1A)-C(15A)	105.3(2)
	P(1A)-C(20A)	1.825(6)	C(26A)-P(1A)-Au(1A)	110.80(18)
	P(1A)-C(15A)	1.834(6)	C(20A)-P(1A)-Au(1A)	116.84(17)
	N(1A)-C(13A)	1.231(7)		
Molecule 2	Au(1B)-P(1B)	2.2272(13)	P(1B)-Au(1B)-Cl(1B)	178.55(6)
	Au(1B)-Cl(1B)	2.2709(15)	C(26B)-P(1B)-C(20B)	106.4(2)
	P(1B)-Cl(26B)	1.810(5)	C(26B)-P(1B)-C(15B)	106.4 (2)
	P(1B)-Cl(20B)	1.814(6)	C(26B)-P(1B)-Au(1B)	110.01(17)
	P(1B)-C(15B)	1.828(5)	C(20B)-P(1B)-Au(1B)	115.51(19)
	N(1B)-C-(13B)	1.259(7)		

The crystallographic asymmetric unit contains two independent molecules which are essentially identical structurally. The main differences concern the arrangement of the phenyl groups. No unusual bond angles or distances were observed and the complex **91** showed a virtually linear P – Au – Cl system (bond angle of 177.17°)**.** Williams *et al* report the preparation and characterisation of three new complexes of gold(I) with bidentate P – N ligands where the ligand binds to gold(I) either in a mono- or bidentate fashion to form the corresponding gold(I) complexes [39]. For the $C_{23}H_{24}AuClNP$ complex they report bond lengths of 2.2916 Å and 2.2380 Å for the

Cl – Au and P – Au bonds and the complex had a linear P – Au – Cl geometry with a bond angle of 177°.

*2.7.6 Single crystal X-ray determination of gold complex **93***

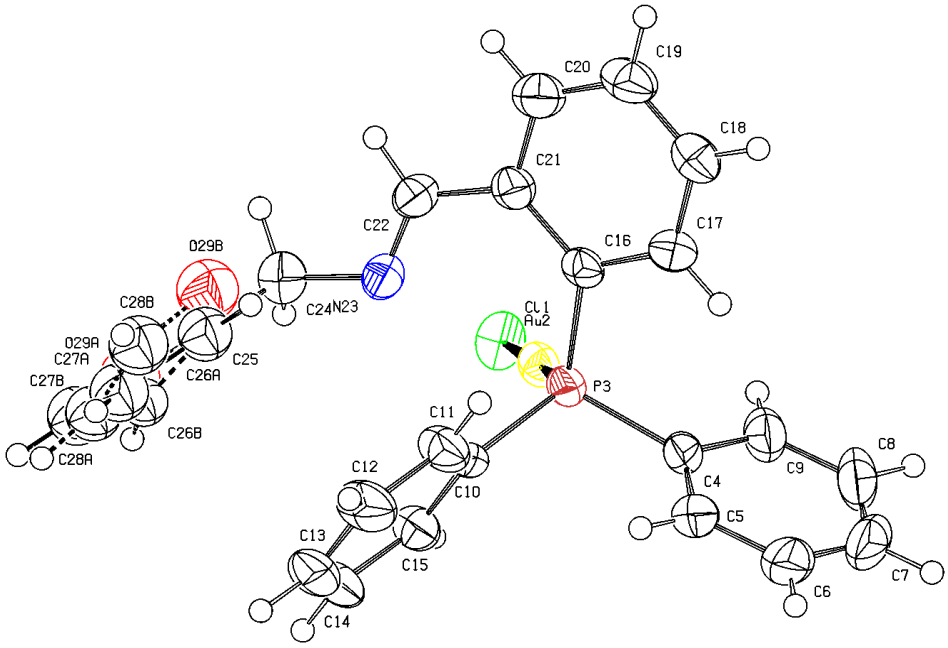

Figure 2.19 Molecular structure of **93** showing the atomic numbering scheme. All non-hydrogen atoms were presented with ellipsoidal model with probability level 40%.

The solid state structure of **93** was obtained by X-ray diffraction (Figure 2.19). Pale yellow crystals suitable for single crystal X-ray diffraction were obtained by slow evaporation of a CH_2Cl_2 solution of the complex at room temperature. Selected bond distances and angles are shown in Table 2.34.

Table 2.34 Selected bond distances and angles for the gold complex **93**

Bond Distances (Å)		**Bond Angles(º)**	
Au(2)-Cl(1)	2.2821(12)	Cl(1)-Au(2)-P(3)	176.54(4)
Au(2)-P(3)	2.2336(11)	Au(2)-P(3)-C(4)	112.50(13)
P(3)-C(4)	1.805(6)	Au(2)-P(3)-C(10)	112.51(14)
P(1A)-C(20A)	1.819(4)	Au(2)-P(3)-C(10)	112.53(14)
P(3)-C(10)	1.813(3)	C(4)-P(3)-C(10)	105.22(18)
P(3)-C(16)	1.8284(7)	C(4)-P(3)-C(16)	103.38(18)
N(23)-C(22)	1.252(5)		

Complex **93** showed a virtually linear Cl – Au – P system (bond angle of 176.54°) as is anticipated for two-coordinate Au(I) compounds. The Au – P bond distances of 2.2336(11) Å agrees with that reported by Williams *et al* [39] (2.244(2) Å). The length of the carbon-nitrogen bond (1.252(5) Å) is also within the expected range. The torsion angle Au(2)-P(3)-C(16)-C(21) = 52.2(3)° indicates that the $=CHC_6H_4$- unit lies above the AuCl(P,N) plane.

*2.7.7 Single crystal X-ray determination of gold complex **94***

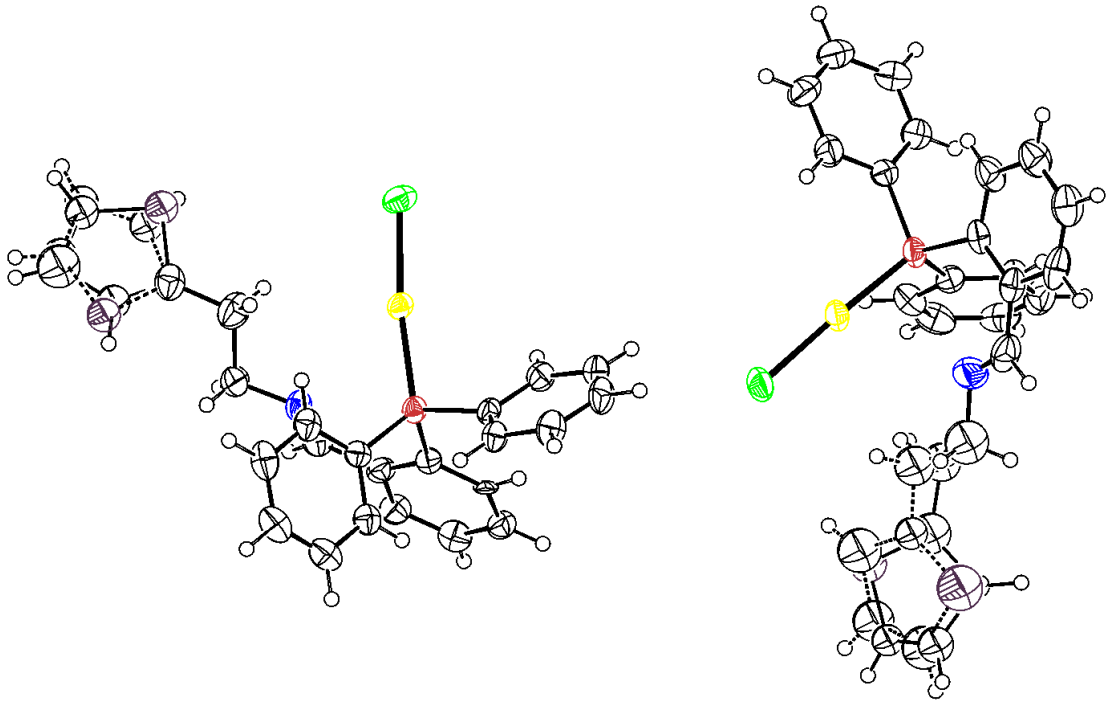

Figure 2.20 Molecular structure of **94** showing the atomic numbering scheme. All non-hydrogen atoms were presented with ellipsoidal model with probability level 40%. There are two **94** molecules in the asymmetric unit. Both have thiophene rings which are disordered over two positions.

The solid state structure of **94** was obtained by X-ray diffraction (Figure 2.20). Pale yellow crystals suitable for single crystal X-ray diffraction were obtained by slow evaporation of a CH_2Cl_2 solution of the complex at room temperature.

Table 2.35 Selected bond distances and angles for the gold complex **94**

	Bond Distances (Å)		**Bond Angles(°)**	
Molecule 1	Au(2A)-Cl(1A)	2.2873(19)	Cl(1A)-Au(2A)-P(3A)	177.39(8)
	Au(2A)-P(3A)	2.2343(19)	C(4A)-P(3A)-C(10A)	102.6(3)
	P(3A)-C(4A)	1.827(8)	C(4A)-P(3A)-C(16A)	104.4(4)
	P(3A)-C(16A)	1.835(7)	Au(2A)-P(3A)-C(10A)	114.2(3)
	P(3A)-C(10A)	1.824(8)	Au(2A)-P(3A)-C(4A)	111.6(2)
	N(23A)-C(22A)	1.257(12)		
Molecule 2	Au(2B)-P(3B)	2.2356(19)	Cl(1B)-Au(2B)-P(3B)	172.64(8)
	Au(2B)-Cl(1B)	2.290(2)	C(4B)-P(3B)-C(16B)	104.9(3)
	P(3B)-Cl(4B)	1.820(7)	Au(2B)-P(3B)-C(4B)	121.6 (3)
	P(3B)-Cl(16B)	1.840(8)	Au(2B)-P(3B)-Cl(6B)	114.9(2)
	P(3B)-C(10B)	1.833(7)	Au(2B)-P(3B)-C(10B)	103.7(2)
	N(23B)-C(22B)	1.255(10)		

Complex **94** also showed a virtually linear Cl – Au – P system (bond angle of 177.39°) for molecule 1 as is anticipated for two-coordinate Au(I) compounds. Suprisingly molecule 2 has an even very lower bite angle of 172.64(8)°. The Au – P bond distances of 2.2343(43) Å for molecule 1 and 2.2356(19) Å for molecule 2 agrees with that reported by Williams *et al*. (2.244(2) Å) and also for our previous complexes **91** and **93.** The length of the carbon-nitrogen bond (1.257(12) Å) for molecule 1 and 1.255(10) Å for molecule 2 are also within the expected range and close to the values determined for complexes **91** and **93.** The torsion angle for molecule 1 Au(2A)-P(3A)-C(16A)-C(21A) = 53.1(7)° indicates that the $=CHC_6H_4$-

unit lies above the AuCl(P,N) plane, but for molecule 2 the torsion angle Au(2B)-P(3B)-C(16B)-C(21B) = -66.0 (6)° indicating that the $=CHC_6H_4$- unit lies below the AuCl(P,N) plane.

2.8 Complexation of tetradentate ligands with platinum and palladium

Despite similar type of ligands having been used to synthesise platinum(II) complexes as reported by Bekhit *et al* [40], our efforts to synthesis the palladium and platinum analogues that are water soluble complexes were futile as the products obtained were insoluble solid products (yellowish in colour) and therefore could not be fully characterized (Scheme).

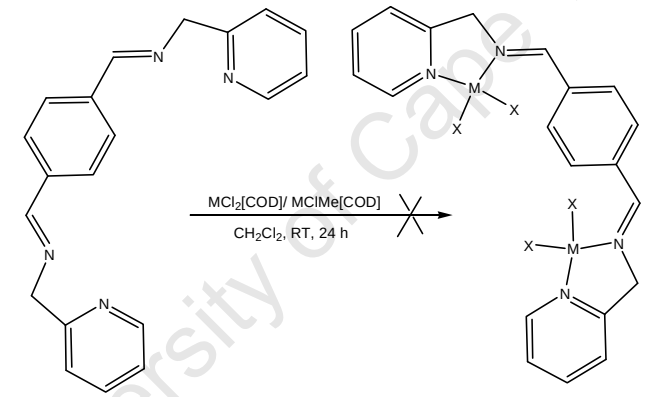

Scheme 2.13 Attempted synthesis of palladium and platinum complexes with tetradentate ligands

We could only postulate that the desired complexes were formed. However, it must be pointed out that the microanalysis data found were in agreement with the calculated values for mass spectra data. Both the dichloropalladium and the dichloroplatinum complexes were insoluble in common chlorinated organic solvents and only slightly soluble in dmso-d_6 and proved to be very difficult to characterise fully and therefore these complexes could not be evaluated for biological activity.

Although the ligands possess several donating sites but for geometry reasons it is plausible that the most active basic site is the azomethine (imine) one. Hence coordination of these ligands would be expected to occur via the lone pair of electrons available on the N atom of the imine group [41].

2.9 Complexation of Schiff base ligands with platinum and palladium

Similar attempts as those for the tetradentate ligands to complex the Schiff base ligands with either palladium or platinum precursors also gave mixtures of products which were difficult to characterise due to their insolubility in organic solvents.

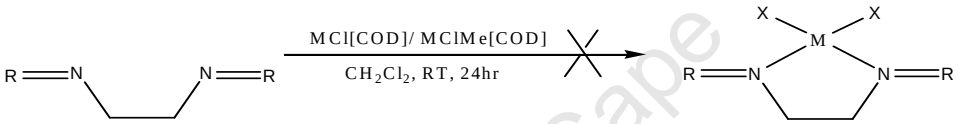

Where M = Pd, Pt

X = Cl, Me

Scheme 2.14 Attempted synthesis of palladium and platinum complexes with Schiff base ligands

These complexes could not be evaluated for biological activity as we were not able to get any conclusive characterisation data.

2.10 REFERENCES

[1] (a) Dilworth J. R, Howe S. D, Hutson A. J, Miller J. R, Silver J, Thomson R. M, Harman M, Hursthouse M. B, *J. Chem. Soc., Dalton Trans*., **1994**, 3553;

(b) Dilworth J. R, Hutson A. J, Lewis J. S, Miller J. R, Zheng Y, Chen Q, Zubieta J, *J. Chem. Soc., Dalton Trans*., **1995**, 1093;

(c) Dilworth J. R, Miller J. R, Wheatley N, Baker M. J, Sunley G, *J. Chem. Soc. Chem. Commun*., **1995**, 1579.

[2] Kapteijn G. M, Spee M. P. R, Grove D. M, Kooijman H, Spek A. L , van Koten G, *Organometallics*, **1996**, 15, 1405.

[3] (a) Barbaro P, Bianchini C, Laschi F, Midollini S, Moneti S, Scapacci G, Zanello P, *Inorg. Chem*., **1994**, 33, 1622;

(b) Stoccoro S, Chelucci G, Zucca A, Cinellu M. A, G. Minghetti G Manassero J, *J. Chem. Soc., Dalton Trans*., **1996**, 1295;

(c) Wehman P, van Donge H. M. A, Hagos A, Kamer P. C. J, van Leeuven P. W. N. M, *J. Organomet. Chem*., **1997**, 535, 183;

(d) Bacchi A, Carcelli, M Costa M, Leporati A, Leporati E, Pelagatti P, Pelizzi C, Pelizzi G, *J. Organomet. Chem*., **1997**, 535, 107.

[4] Gao J-X, Ikariya T, Noyoro R, *Organometallics*, **1996**, 15, 1087.

[5] Brunner H, Fusrt J, *Inorg. Chim. Acta*, **1994**, 220, 63.

[6] Rauchfuss T. B, *J. Organomet. Chem*., **1978**, 162, C19.

[7] Jeffery J. C, Rauchfuss T. B, Tucker P. A, *Inorg. Chem*., **1980**, 19, 3306.

[8] (a) Bhattacharyya P, Parr J, Slawin A. M. Z, *J. Chem. Soc., Dalton Trans.*, **1998**, 3609;

(b) Wehman P, van Donge H. M. A, Hagos A, Kamer P. C. J, van Leeuwen P. W. N. M, *J. Organomet. Chem*., **1997**, 535, 183;

(c) Ankersmit H. A, Loken B. H, Kooijman H, Spek A. L, Vrieze K, van Koten G, *Inorg. Chim. Acta*, **1996**, 252, 141;

(d) Wong W. -K, Chik T. -W, Hui K-N, Williams I, Feng X, Mak T.C.W, Che C.-M, *Polyhedron*, **1996** 15, 4447;

(e) Wong W.-K., Gao J.-X, Wong W.-T, Cheng W.C, Che C.-M, *J. Organomet. Chem*., **1994**, 471, 277.

[9] Rülke R. E, Kaasjager V. E, Wehman P, Elsevier C. J, van Leeuwen P. W. N. M, Vrieze K, Fraanje J, Goubitz K, Spek A. L, *Organometallics*, **1996**, 15, 3022.

[10] Lavery A, Nelson S. M, *J. Chem. Soc. Dalton Trans*., **1984**, 615.

[11] (a) Ghilardi C. A, Midollini S, Moneti S, Orlandini A, Scapacci G, *J. Chem. Soc. Dalton Trans*., **1992**, 3371;

(b) Barbaro P, Bianchini C, Laschi F, Midollini S, Moneti S, Scapacci G, Zanello G. P, *Inorg. Chem*., **1994**, 33, 1622.

[12] Zotto A. D, Barratta W, Ballico M, Hertdweck E, Rigo P, *Organometallics*, **2007**, 26, 5636.

[13] Bayly S. R, Cowley A. R, Dilworth J. R, Ward C. V, *J. Chem. Soc. Dalton Trans*., **2008**, 2190.

[14] Pavia D. L, Lampman G. M, Kriz G. S, *Introduction to Spectroscopy*, 2nd Edition, Saunders College Publishing, **1996**, 116.

[15] Wehman P, Van Donge H. M. A, Hagos A, Kamer P. C. J, Van Leeuwen P. W. N. M, *J. Organomet. Chem*., **1997**, 535, 183.

[16] Shaffer A. R, Schidt A. R, *Organometallics*, **2009**, 28, 2494.

[17] del Campo O, Carbayo A, Cuevas J. V, Garcia-Herbosa G, Munoz A, *Eur. J. Inorg Chem*., **2009**, 2254.

[18] Johnson L. K, Killian C. M, Brookhart M, *J. Am. Chem. Soc*., **1995**, 117, 6417.

[19] Carey D. T, Cope-Eatough E. K, Vilaplana-Mafe E, Mair F. S, Pritchard R. G, Warren J. E, Woods R. J, *J. Chem. Soc. Dalton Trans*., **2003**, 1083.

[20] Mingxing Q, Mei W, He Zhou B. R, *Appl. Catal. A: Gen*., **2001**, 209.

[21] Krautler B, *Chimica*, **1987**, 41, 277.

[22] Derrah E. J, Zhang H, Nikolcheva L. G, Vogels C. M, Decken A, Westcott S. A, *Inorg. Chem. Comm*., **2003**, 6, 1086.

[23] Sacconi L, Nannelli P, Camigli U, *Inorg. Chem*., **1965**, 4, 943.

[24] Hamaker C. G, Halbach D. P, *Inorg. Chim. Acta*, **2006**, 359, 846.

[25] Yan X.-L, Chen L.-G, Zeng T, *Acta Crystallogr.*, **2006**, E62.

[26] Faniran J. A, Patal K. S, Bailar J. C, *J. Inorg. Nucl. Chem*., **1964**, 26, 1577.

[27] Toyssie P, Charette J. J, *Spectrochim. Acta*, **1963**, 19, 1407.

[28] Sanchez G, Serrano J. L, Moral M. A, Perez J, Molins E, Lopez G, *Polyhedron*, **1999**, 18, 3057.

[29] Coleman K. S, Green M. L. H, Pascu S. I, Rees N. H, Cowley A. R, Rees L. H, J. *Chem. Soc. Dalton Trans*., **2001**, 3384.

[30] Petocz G, Rangits G, Shaw M, de Bod H , Williams D. B. G, *J. Organomet., Chem.*, **2009**, 694, 219.

[31] Bhattacharyya P, Loza M. L, Parr J, Slawin A. M. Z, *J. Chem. Soc., Dalton Trans*., **1999**, 2917.

[32] Parr J, Slawin A. M. Z, *Inorg. Chim. Acta*, **2000**, 303, 116.

[33] Clarke M. L, Slawin A. M. Z, Woolins J. D, *Polyhedron*, **2003**, 22, 19.

[34] McIsaac D. I, Geier S. J, Vogels C. M, Decken A, Westcott S. A, *Inorg. Chim. Acta*, **2006**, 359, 2771.

[35] Bandoli G, Dolmella A, Crociani L, Antonetta S, Crociani B, *Transition Met. Chem.*, **2000**, 25, 17.

[36] Dilworth J. R, Howe S. D, Hutson A. J, Miller J. R, Silver J, Thompson R. M, Harman M, Hursthouse M. B, *J. Chem. Soc., Dalton Trans*., **1994**, 3553.

[37] Pascu S. I, Coleman K. S, Cowley A. R, Green M. L. H, Rees N, H, *New J. Chem*., **2005**, 29, 385.

[38] Ankersmit H. A, Loken B. H, Kooijman H, Spek A. L, Vrieze K, van Koten G, *Inorg. Chim. Acta*, **1996**, 252, 141.

[39] Williams D. B. G, Traut T, Kriel F. H, van Zyl W. E, *Inorg. Chem. Comm*., **2007**, 10, 538.

[40] Bekhit A. A , El-Sayed O. A , Al-Allaf T. A. K , Aboul-Enein H. Y , Kunhi M, Pulicat S. M , Al-Hussain K, Al-Khodairy F, Arif J, *Eur. J. Med. Chem.*, **2004**, 39, 499.

[41] Al-Allaf T. A. K, Sheet A. Z. M, *Polyhedron*, **1995**, 14, 239.

CHAPTER 3
EVALUATION OF PALLADIUM, PLATINUM AND GOLD COMPLEXES AS ANTICANCER AGENTS.

CONTENT

3.1 INTRODUCTION

The observation that cisplatin remains a drug of choice in the treatment of diseases like oesophageal cancer, despite the many potential drawbacks associated with its use, makes a strong case for the need to develop better therapies. In Chapter 2 we described the synthesis and characterisation of a group of novel iminophosphines that were complexed to palladium, platinum and gold. The structures of these compounds were established by X-ray crystallography, confirming the novelty of these newly developed compounds.

In this study we examined these palladium, platinum and gold complexes for their activity in WHCO1 and KYSE450 oesophageal cancer cell lines and normal cultured cells. The oesophageal cancer cell lines were selected for the cytotoxic assays because one of the objectives of this project is to identify agents that have activity against this cancer that occurs with a high frequency in many developing countries, including South Africa.

3.2 RESULTS

3.2.2 IC_{50} determination

The palladium, platinum and gold complexes synthesised and characterised in Chapter 2 were evaluated for their cytotoxic activity using the MTT assay to determine IC_{50} values against the oesophageal cancer cell lines WHCO1, KYSE450 and also in normal human fibroblasts (DMB cells) for selected complexes. Dose response curves for each of the complexes were performed against the cell lines as outlined in Experimental Details in Chapter 4 Section 4.8. Each experiment was performed in triplicate and repeated at least three times.

3.2.2.1 Palladium complexes

The structures of the palladium complexes that were investigated are shown in Table 3.1. Complexes **73** and **74** have been reported in the literature [1, 2] but had not been tested for anticancer activity but complexes **80** - **83** are novel and a crystal structure of **80** was determined.

Table 3.1 Palladium complexes evaluated for anticancer activity in WHCO1 and KYSE450 cell lines

Complex	IC_{50} in WHCO1 (µM)	95% CI	IC_{50} in KYSE450 (µM)	95% CI
73 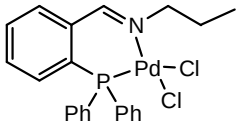	26.59	23.79 –29.76	15.29	13.81 –16.93
74 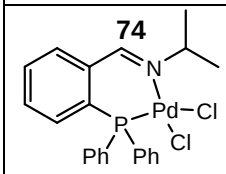	19.02	15.46 –23.42	10.03	8.22 – 12.23
80 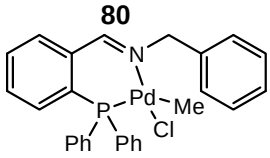	44.14	39.24 –49.65	22.38	14.34 –34.95
81 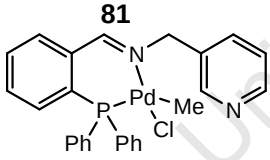	39.07	35.45 –43.08	59.36	52.30 –67.27
82 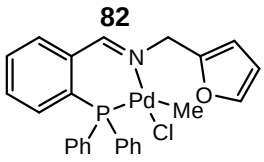	45.27	31.59 –64.88	68.54	54.65 –86.03
83 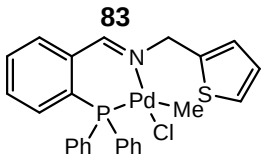	28.50	18.45 –44.02	10.99	8.17 – 14.78

The palladium complexes **73** and **74** were the dichlorides which were very soluble in DMSO as compared to the other dichloride complexes **75 - 79** which were insoluble (see Section 2.5.1). Complexes **80 – 83** were the chloromethyl derivatives and these were very soluble in DMSO. Introduction of a methyl group into the dichloride complexes increased the solubility of the complexes. As described in Section 4.8.1, WHCO1 cells were treated with various concentrations of the indicated compounds (0 – 200 µM) for 48 hr, and then subjected to the MTT assay to determine the effects of these compounds on cell proliferation. Results of treatment in WHCO1 and KYSE450 cells with palladium complexes are shown in Table 3.1.

In WHCO1 cells the palladium complexes displayed low activity with the most active having an IC_{50} of 19.02 µM and the least active 45.27 µM. The values in the adjacent column show the 95% confidence intervals for the IC_{50} values.

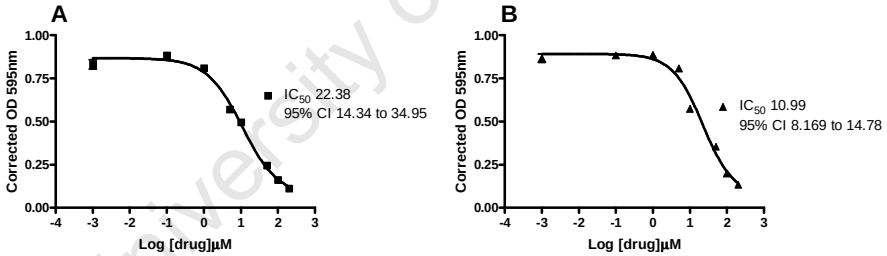

Figure 3.1 Cytotoxicity results for the palladium complexes **80 (A)** and **83 (B)** on KYSE450 cells. Cells in 96 well plates were treated with the indicated concentrations of compounds for 48 hr and then processed for the MTT assay (Section 4.8.1). IC_{50} values were calculated using GraphPad Prism software. The graph shows log drug concentration plotted versus OD at 595 nm. The corrected OD (OD- background) is shown. The experiments were all done in triplicate and were repeated 3 times. A typical experiment is shown and each data point represents the mean ±SD (standard deviation).

Although complexes **74** and **83** displayed significant activity against KYSE450 cells with IC_{50} values of 10.03 and 10.99 µM respectively the activity of the other palladium complexes were not particularly noteworthy in this cancer cell line as well,

as shown in Table 3.1. The highest concentration tested nearly caused 100% cell death as seen in Figure 3.1.

3.2.2.2 Platinum complexes

Several platinum complexes investigated as anticancer agents are shown in Table 3.2. All the platinum complexes reported here are novel and we were able to determine the crystal structures of complexes **84**, **86** and **88** respectively.

Table 3.2 Platinum complexes evaluated for anticancer activity in WHCO1 and KYSE450 cell lines

Complex	IC_{50} in WHCO1 (µM)	95% CI	IC_{50} in KYSE450 (µM)	95% CI
84 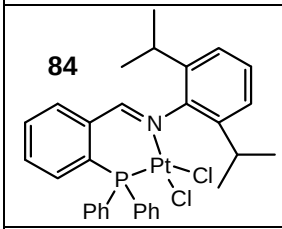	9.47	8.96 – 10.01	2.16	1.96 – 2.38
85 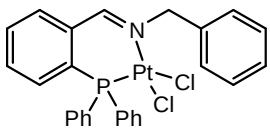	8.45	7.99 – 8.94	6.00	4.91 –7.35
86 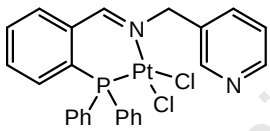	5.49	3.97 – 7.60	3.11	2.83– 3.41
87 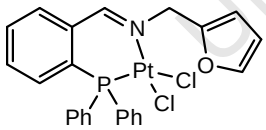	7.24	5.89 – 8.90	7.58	6.29 – 9.12
88 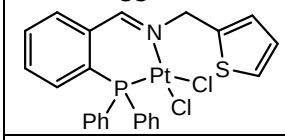	6.66	5.81 – 7.63	7.17	6.24 – 8.25
89 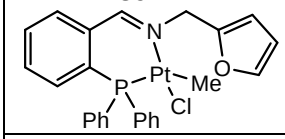	28.85	26.64 –31.24	9.89	8.77 – 11.17
90 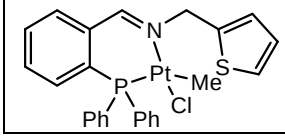	20.52	19.25 –21.87	13.86	11.80 –16.29

Table 3.2 shows the IC_{50} values and 95% confidence intervals for the platinum complexes **84** - **90** in WHCO1 and KYSE450 cell lines, respectively.

Typical cytotoxicity curves obtained for these complexes are shown in Figure 3.4 for complexes **87** and **88,** respectively, in KYSE 450 cells.

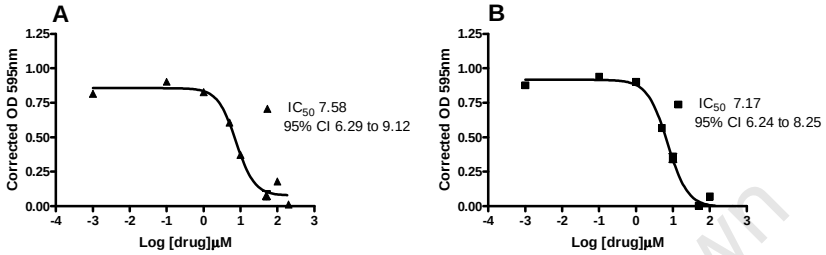

Figure 3.2 Cytotoxicity results for the platinum complexes **87 (A)** and **88 (B)** on KYSE450 cells. 96 well plates were treated with the indicated concentrations of compounds for 48 hr and then processed for the MTT assay (Section 4.8.1). IC_{50} values were calculated using GraphPad Prism software. The graph shows log drug concentration plotted versus OD at 595 nm. The corrected OD (OD- background) is shown. The experiments were all done in triplicate and were repeated 3 times. A typical experiment is shown and each data point represents the mean ±SD (standard deviation).

The results show that platinum complexes show significant cytotoxic activity (< 10 µM) against both WHCO1 and KYSE450 cell lines with the exception of complexes **89** and **90**. These two complexes were less effective against WHCO1 cells (IC_{50} > 20 µM). The curves in Figure 3.2 show that the complexes **87** and **88** induced > 90% cell death at ≥ 50 µM. Complex **86** was the most effective in both WHCO1 and KYSE450 cell lines.

3.2.2.3 Gold complexes

Several gold(I) complexes were evaluated as anticancer agents (Table 3.3). The gold complexes were all novel and crystal structures of three of them (**91**, **93** and **94**) were determined by X-ray crystallography confirming that they existed in a linear coordination mode.

Table 3.3 Gold complexes evaluated for anticancer activity in WHCO1 and KYSE450 cell lines

Complex	IC_{50} in WHCO1 (µM)	95% CI	IC_{50} in KYSE450 (µM)	95% CI
91 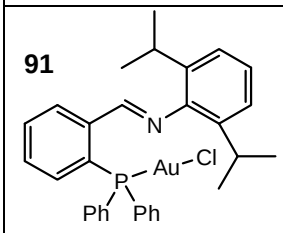	8.42	8.28 –8.58	5.23	4.73 – 5.79
92 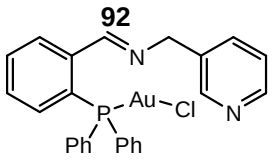	4.15	3.35 – 5.13	6.89	5.87– 8.51
93 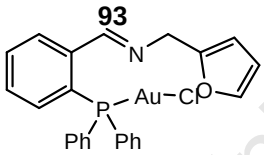	3.41	2.39 – 4.88	5.87	5.29 – 6.51
94 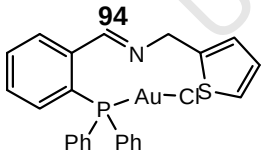	3.61	2.92 – 4.47	5.40	4.88 – 5.98
95 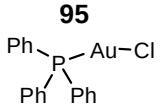	14.44	11.52 –18.09	15.66	13.42 –17.55

Figure 3.3 shows the dose response curves for complexes **93** and **94** against WHCO1 cell lines.

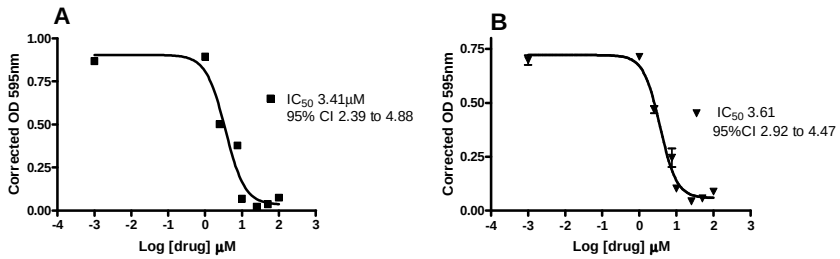

Figure 3.3 Cytotoxicity results for the gold complexes **93 (A)** and **94 (B)** onWHCO1 cells. 96 well plates were treated with the indicated concentrations of compounds for 48 hr and then processed for the MTT assay (Section 4.8.1). IC_{50} values were calculated using GraphPad Prism software. The graph shows log drug concentration plotted versus OD at 595 nm. The corrected OD (OD- background) is shown. The experiments were all done in triplicate and were repeated 3 times. A typical experiment is shown and each data point represents the mean ±SD (standard deviation).

Tables 3.3 shows the IC_{50} values for the gold complexes in WHCO1 and KYSE450 cell lines, respectively. Typical cytotoxicity curves obtained for these complexes are shown in Figure 3.3 for complexes **93** and **94** in WHCO1 cells. The results show that all the gold complexes have significant cytotoxicity against both WHCO1 and KYSE450 cell lines with IC_{50} values < 10 µM, with the exception of complex **95** which has IC_{50} values > 10 µM for both cell lines. Complexes **93** and **94** were the most effective in both cell lines, respectively.

All the gold complexes with the exception of complex **95** showed very good activity against both cancer cell lines. We then selected four complexes to explore further studies in normal fibroblasts. The compounds were selected on the basis that they displayed high cytotoxic activity in the cancer cell lines, they had the same ligands and the only difference was the metal center (platinum or gold). The structures of the compounds selected are shown in Figure 3.4.

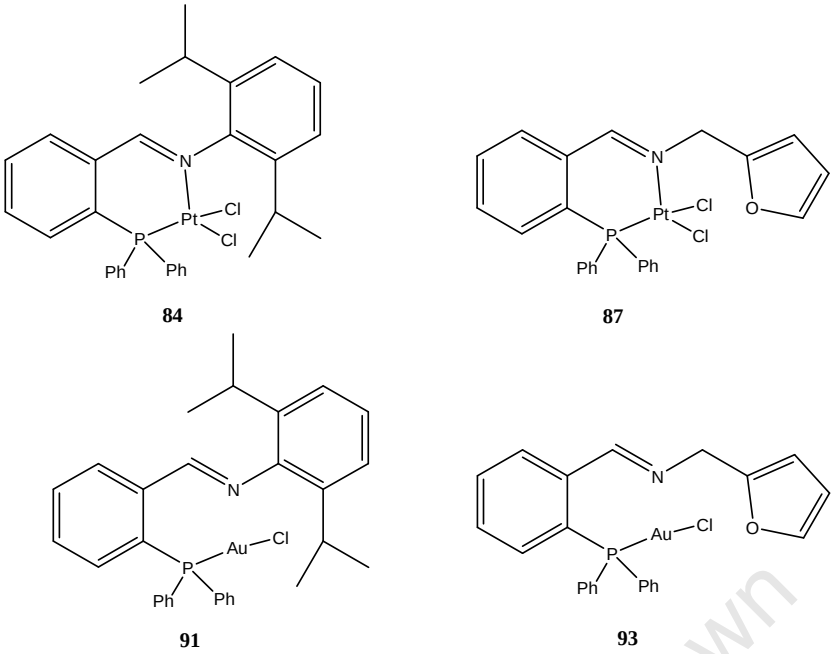

Figure 3.4 Structures of compounds tested in normal cells

In order to investigate whether the complexes were selective towards cancer cells, normal fibroblast cells were treated with the complexes **84**, **87**, **91** and **93** and typical IC_{50} values and 95% CI obtained are as shown in Table 3.4.

Table 3.4 Treatment of DMB cell lines with the most active complexes

COMPOUND	**IC_{50} (µM)**	**95% CI**
84	100.79	95.44 – 112.78
87	134.50	118.70 – 152.40
91	134.10	112.69 – 200.40
93	119.80	102.60 – 139.90

The results show that the complexes do not show significant cytotoxic activity against normal fibroblast cell lines, with IC_{50} values > 100 µM for both platinum (**84**, **87**) and gold complexes (**91**, **93**). The cytotoxicity curves that were used to calculate the IC_{50} data are shown in Figure 3.5.

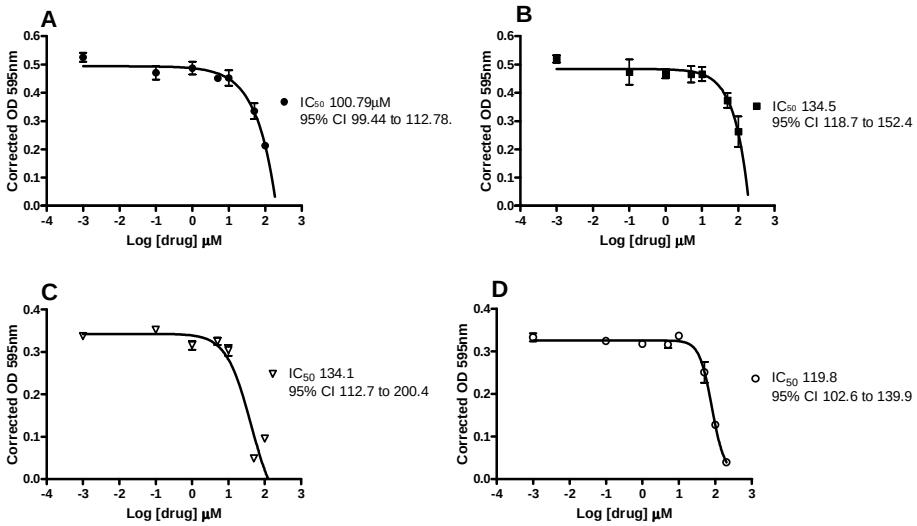

Figure 3.5 Cytotoxicity results for the complexes **84 (A)**, **87 (B)**, **91 (C)** and **93 (D)** on normal fibroblast cells (DMB). 96 well plates were treated with the indicated concentrations of compounds for 48 hr and then processed for the MTT assay (Section 4.8.1). IC_{50} values were calculated using GraphPad Prism software. The graph shows log drug concentration plotted versus OD at 595 nm. The corrected OD (OD- background) is shown. The experiments were all done in triplicate and were repeated 3 times. A typical experiment is shown and each data point represents the mean ±SD (standard deviation).

The results show that the platinum and gold complexes show substantially reduced cytotoxic activity against the normal fibroblast cells (DMB) and that these complexes induced > 90% cell death only at the highest drug concentrations for complexes **91** and **93**. In contrast the highest drug concentration tested for complexes **84** and **87** only reduced cell number by approximately 60% and 50% in **84** and **87**, respectively.

3.2.3 Effects of complexes 87, 84, 91 and 93 on cell morphology

We observed the effect of the selected complexes **84**, **87**, **91** and **93** on the morphology of WHCO1 cells. WHCO1 cells were treated with 2X IC_{50} of the selected complexes (**84**, **87**, **91** and **93**) for 24 hours and 48 hours, and then photographed using phase contrast microscopy, with a Zeiss Telaval 31 with an Axiocam camera and Motic Images Plus 2.0 ML image software.

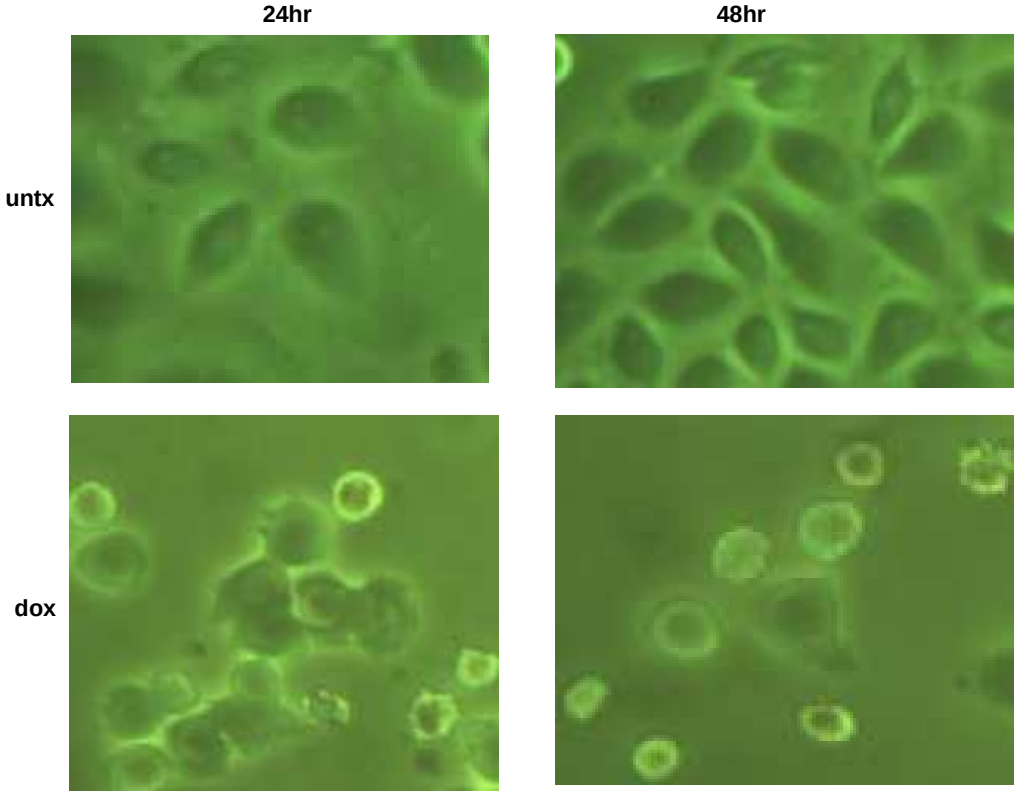

Figure 3.6 Morphology of WHCO1 cells untreated, or treated with 5 µM doxorubicin for 24 and 48 hr. Cells were plated in 60 mm dishes and after an overnight incubation. Photographs of the cells were captured using a Zeiss Telaval 31 with an Axiocam camera and Motic Images Plus 2.0 ML image software.

As a positive control, WHCO1 cells were also treated with doxorubicin, which is an agent that is known to cause cell death. In the cells that have been treated with doxorubicin most cells appear dead after 24 hours, with all cells dead after 48 hours. In contrast, untreated cells show normal morphology at 24 hours and 48 hours (Figure 3.6).

The cells subjected to treatment with complexes **87**, **93**, **84** and **91**, are shown in Figures 3.7 and 3.8.

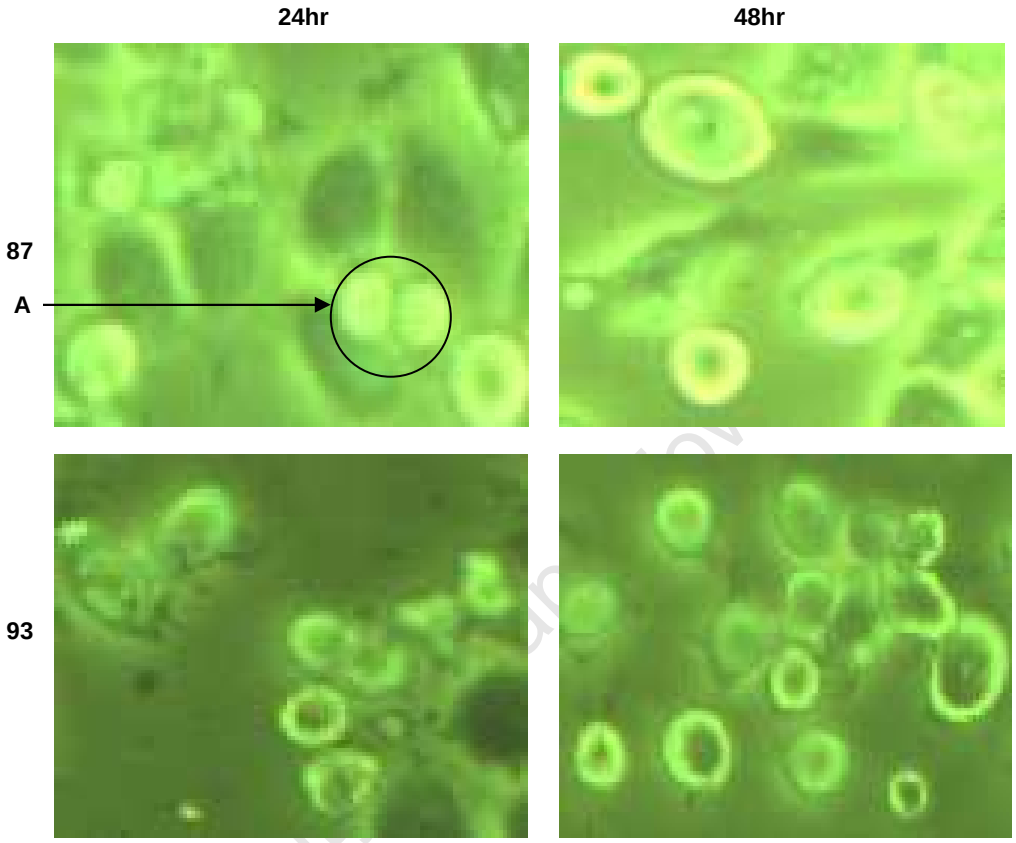

Figure 3.7 Morphology of WHCO1 cells treated with complexes **87** or **93** for 24 and 48 hr. Cells were plated in 60 mm dishes and after an overnight incubation, **87** and **93** were added at 2 X IC_{50} concentration. Photographs of the cells were captured using a Zeiss Telaval 31 with an Axiocam camera and Motic Images Plus 2.0 ML image software after 24 and 48 hr. (**A**) Rounded cells.

In the cells treated with compounds **87** and **93** more than 50% of cells are dead at 24 hours and all the cells are dead after 48 hours for both compounds. A lot of rounded floating cells were observed and there was membrane blebbing in some cells with noticeable debris.

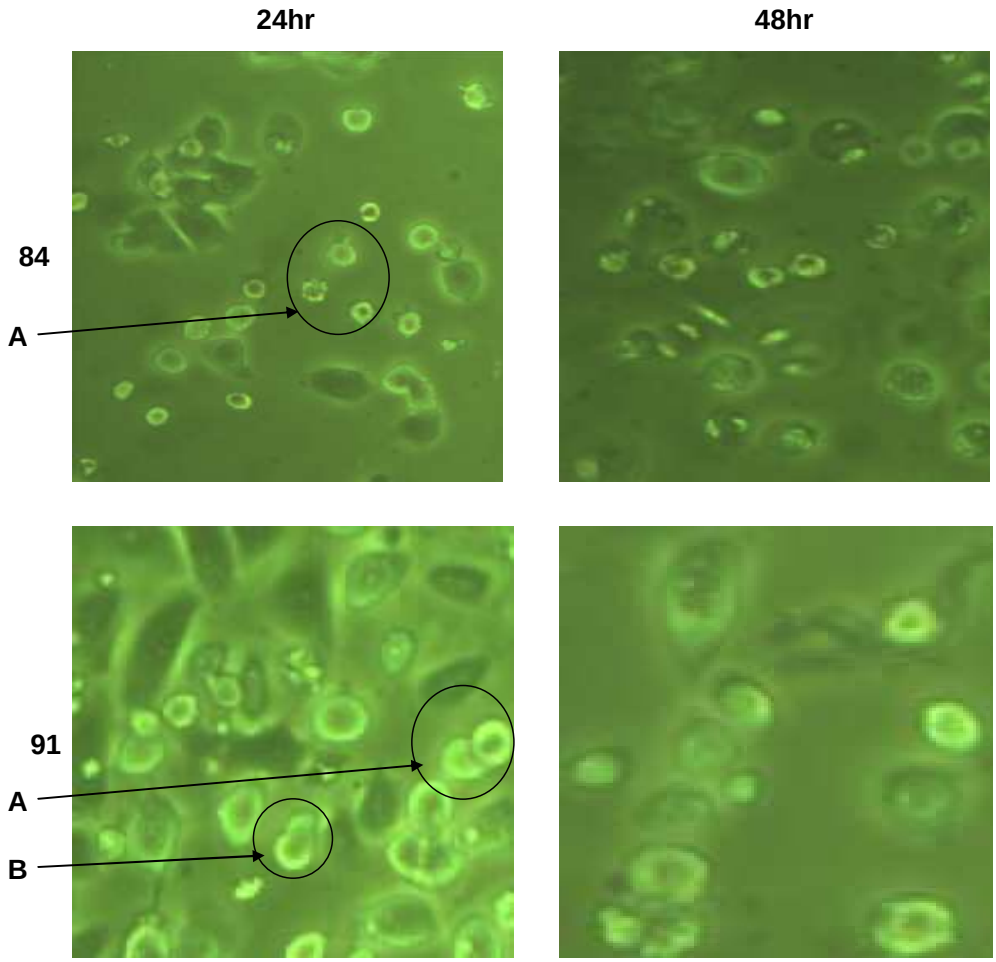

Figure 3.8 Morphology of cells treated with complex **84** or **91** for 24 and 48 hr. Cells were plated in 60 mm dishes and after an overnight incubation, and **84** and **91** were added at 2 X IC_{50}. Photographs of the cells were captured using a Zeiss Telaval 31 with an Axiocam camera and Motic Images Plus 2.0 ML image software. (**A)** shows the rounded cells and (**B)** membrane blebbing**.**

The morphology of the cells treated with the platinum and gold complexes were distinctly different from the untreated cells. The cells are shrunken and rounded, with membrane blebbing also observed in cells treated with complex **91** (Figure 3.8). Cells treated with complex **91** were not as obviously affected as a few live cells can be seen after treatment for 24 hours, but on a closer examination the morphology of cells was altered and there were more floating cells than in the untreated cells with few apoptotic cells observed but a large number of floating cells. After 48 hours all the

cells are dead on treatment with complexes **84** and **91**. From our results, the complexes apparently have a toxic effect on the WHCO1 cells tested as evidenced by the difference in cell morphology of untreated cells compared to the morphology of cells treated with complexes **84**, **87**, **91** and **93**. There also seems to be a reduction in cell density and an increase in the number of floating cells, an indication that cells are dying.

3.2.4 Effect of compounds on DNA damage and induction of apoptosis

Since the morphology of the WHCO1 cells treated with complexes **84**, **87**, **91** and **93** clearly showed that the complexes were killing the oesophageal cancer cells, we investigated the effect of these complexes on DNA damage and the induction of apoptosis in the cancer cells. Phosphorylation of H2AX was used as a marker of Double Strand Breaks (DNA). H2AX by itself cannot repair the damage, but it acts as a recruiter, and collects other repair site of damage to initiate repair. The results show that complexes **84** and **91** very strongly induce the phosphorylation of H2AX, suggesting that these complexes induce DNA damage in the form of DSB's. Our Western blot shows that complexes **87** and **93** also induce DNA damage although to a lesser extent than in complexes **84** and **91**.

Considering that treatment with these complexes resulted in DSB's we determined whether these compounds also induced apoptosis in treated cells. PARP cleavage was investigated by Western blot analysis in order to determine the mode of cell death induced by the complexes **84**, **91**, **87** and **93**. PARP is a known caspase substrate and cleavage of PARP into two distinct fragments serves as a marker of apoptosis. Apoptosis is the process of programmed cell death which involves a series of

biochemical steps resulting in morphological changes to the cell membrane including cell shrinkage, nuclear fragmentation and chromosomal DNA fragmentation.

From the results, there is very little evidence that treatment of the WHCO1 cells with complexes **84**, **87**, **91** and **93** resulted in PARP cleavage and hence apoptosis (Figure 3.9).

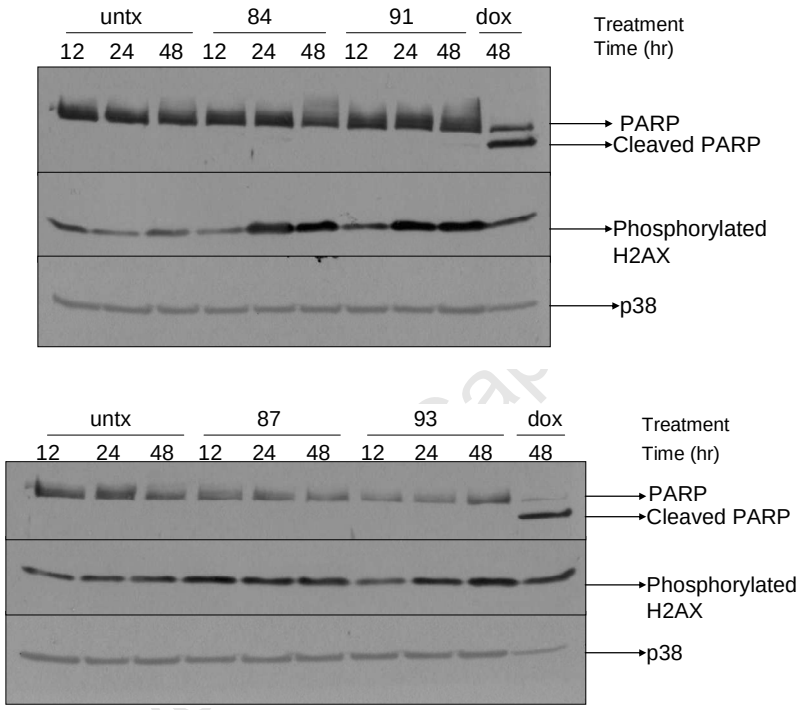

Figure 3.9 Western blots for WHCO1 cells treated with complexes **84**, **91**, **87** and **93**. Cell lysates from cells treated with 2 X IC_{50} for complexes **84** and **91** and 4 X IC_{50} for complexes **87** and **93** were harvested at 12, 24 and 48 hr and analysed by Western blot (as outlined in Experimental Details). p38 was used as a loading control. Treatment of cells with 10 µM doxorubicin served as a positive control. These results are representative of two independent experiments.

The system that we used to detect PARP cleavage was clearly working since we could detect the PARP cleavage in cells treated with Doxorubicin as shown in Figure 3.9.

3.2.5 Effects of complexes 87, 84, 91 and 93 on the cell cycle

Since the complexes **84**, **87**, **91** and **93** exhibited significant DNA damage as evidenced by the phosphorylation of histone H2AX we further explored the effect of the complexes on the cell cycle as it is well documented that DNA damage triggers cell cycle arrest in cells.

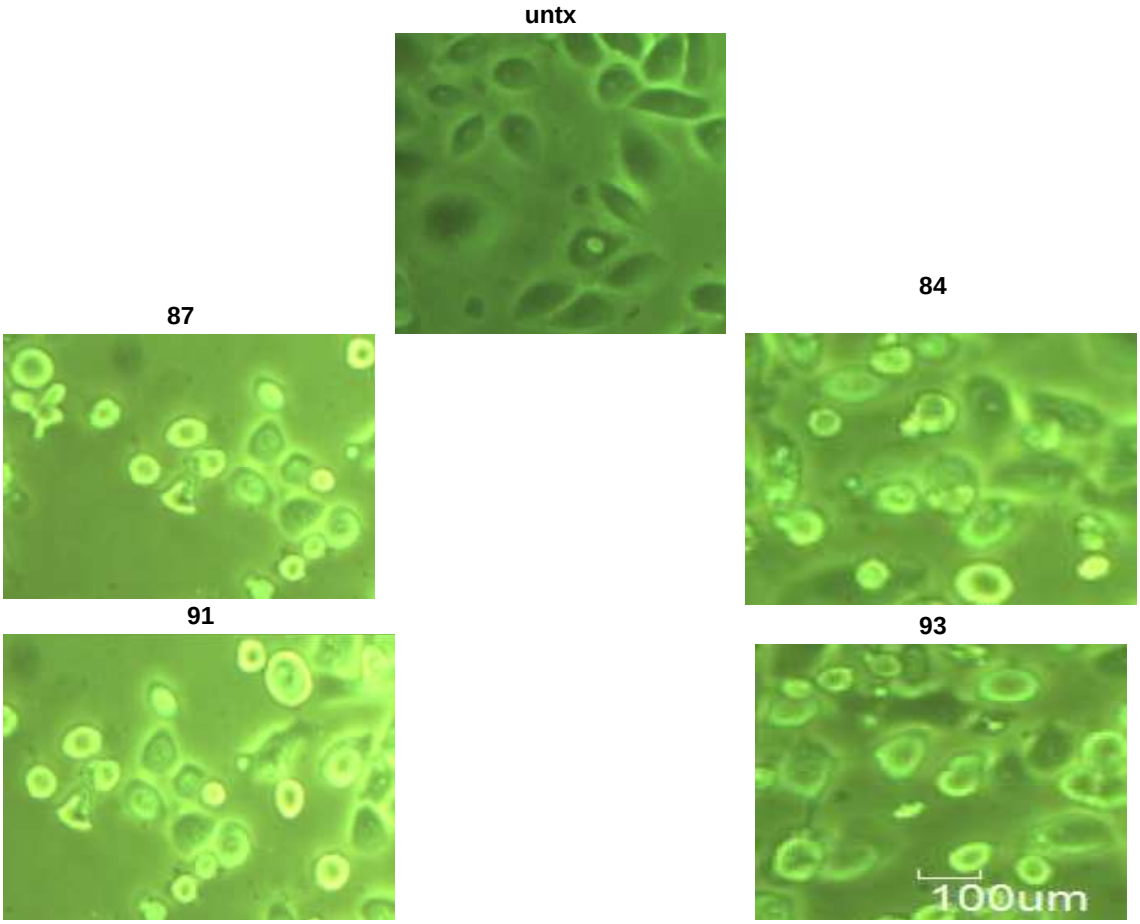

Figure 3.10 Morphology of WHCO1 cells 24 hr after treatment with **87**, **84**, **91** and **93,** prior to harvesting cells for FACS analysis photographs were captured using a Zeiss Telaval 31 with an Axiocam camera and Motic Images Plus 2.0 ML image software.

From the photographs in Figure 3.10 we can clearly see that the compounds have altered the morphology of the cells. The cells appear more rounded, with condensed nuclei and there is membrane blebbing on some cells. There are also a number of floating cells as compared to the untreated cells.

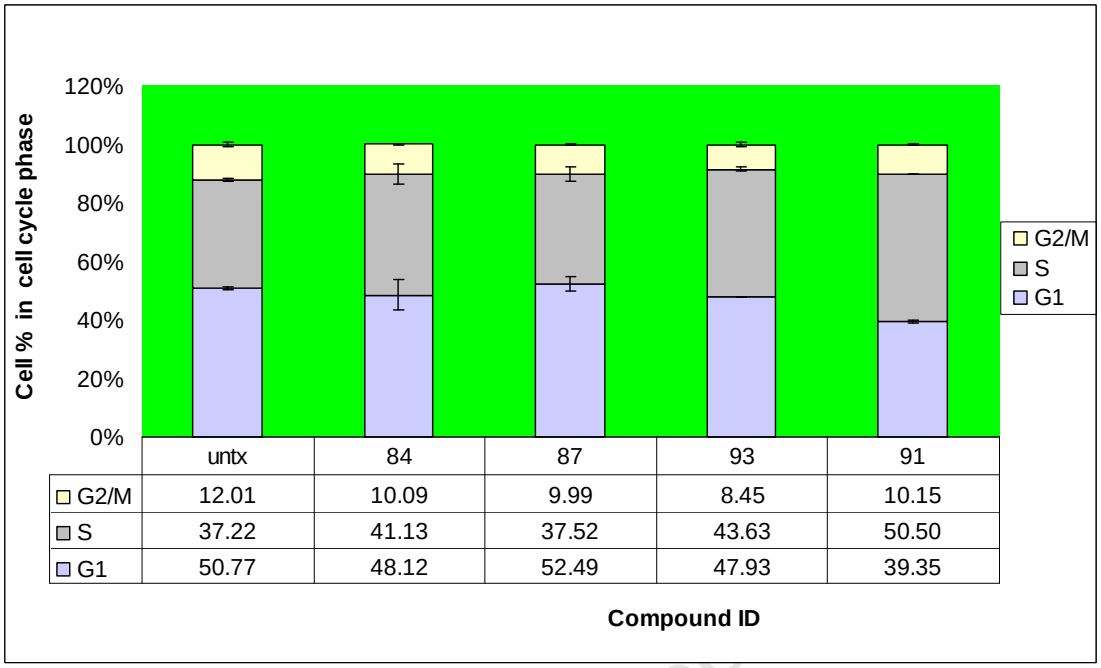

	untx	84	87	93	91
G2/M	12.01	10.09	9.99	8.45	10.15
S	37.22	41.13	37.52	43.63	50.50
G1	50.77	48.12	52.49	47.93	39.35

Figure 3.11 Cell cycle profiles of cells treated with 2X IC_{50} for compounds **84**, **87**, **93** and **91** for 24 hr. They were trypsinised, counted and then processed for cell cycle analysis as described in the Experimental details (Section 4.9). The x-axis indicates identity of the compounds, and the y-axis the percentage of cells in the respective phase of the cell cycle. Results are representative of two independent experiments.

Cell cycle analysis was performed on cells treated with complexes 84, 87, 91 and 93 to determine the effect these complexes might have on the cell cycle. From Figure 3.11 it appears that the compounds do not affect the cell cycle significantly except for complex **91.** Cattaruzza *et al* report that gold(III)-dithiocarbamato derivatives cause cell damage, slightly affecting the cell cycle, thus suggesting a different mechanism of action from established platinum-based compounds [3].

3.3 DISCUSSION

A preliminary investigation into the antitumour activity of several metal-containing complexes prepared during the course of this study was carried out in the form of

cytotoxicity assays on two separate cancer cell lines – human oesophageal cancer cell lines WHCO1 and KYSE450 and normal fibroblasts (DMB cells). The structures of the palladium, platinum and gold complexes that were evaluated for anticancer activity are shown in Tables 3.1, 3.2 and 3.3 respectively.

The complexes that were synthesised initially were not very soluble in a range of solvents and thus proved very difficult to characterise. Consequently biological testing could not be performed on these complexes. These complexes included the palladium and platinum complexes of both the tetradentate and Schiff base ligands as described in Section 2.8 and 2.9 of this thesis. Other workers have reported soluble complexes of Schiff base ligands complexed to metals like zinc, copper, nickel and silver [4]. These complexes have been applied mainly to catalytic reactions [5]. Monobasic bidentate Schiff base complexes of palladium and platinum have also been investigated for their antimicrobial effects on different species of pathogenic fungi and bacteria and have been found to possess significant fungicidal and bacterial properties [6]. The synthesis of tetradentate ligands was relatively simple and could be generalised to a large variety of other aromatic dialdehydes [7, 8] but their major drawback was their insolubility in solvents. The results described in this project confirmed the poor solubility of these complexes, and their unsuitability for further biological testing in the current form.

The new iminophosphine ligands were synthesised as an alternative using a range of amines and their complexes with platinum and gold were very soluble in organic and inorganic solvents. The dichloropalladium complexes were not as soluble but their chloromethyl derivatives were much more soluble as described in Section 2.5.4. In the

literature a whole range of iminophosphine complexes have been synthesised with palladium and platinum but only a few have been reported for gold [17].

3.3.1 Cytotoxic activity of complexes and structure/ function relationships

The antitumour activity of a range of palladium complexes was discussed in Section 1.4 . The palladium complexes are less active than related platinum complexes under the same conditions [9, 10]. These reports show the palladium complexes as having at best marginal success. From a previous study in our laboratory it has been shown that platinum complexes are more active than their palladium analogues with similar pyridyl ring ligands [11]. A series of new multinuclear complexes containing ferrocenyl groups and platinum group metals were successfully prepared and characterized using an array of analytical techniques. Some of the new complexes were tested for cytotoxic activity and a comparison was made to that of cisplatin. Several of the complexes displayed significant cytotoxic activity against the cancer cell line WHCO1 and two of the complexes displayed growth inhibitory activities similar to that of cisplatin. The major drawback with the palladium complexes was their poor solubility in biological media [11].

The dichoropalladium complexes that we synthesised in this project were poorly soluble and proved to be difficult to characterise and were not tested for biological activity except for the complexes with isopropyl and propyl substituents (**73** and **74**). However the chloromethyl palladium complexes (**80**-**83**) were more soluble in DMSO than the dichloropalladium complexes (**75**-**79**) and were evaluated for biological activity. The complexes displayed similar cytotoxic activity in both cell lines and were not very active. The most active in both WHCO1 and KYSE450 cell lines was

complex **74** with IC_{50} values of 19.02 and 10.03 µM, respectively, and the least active was complex **82** in both cell lines with IC_{50} values of 45.27 and 68.54 µM, respectively.

The use of platinum in antitumour drugs has been well established and cisplatin is the most prominent of this class of drugs [7]. Despite the success of cisplatin, some tumours have developed natural as well as acquired resistance to the drug. These effects may only be partially reversed upon termination of treatment. Since the discovery of cisplatin, numerous platinum-containing compounds have been prepared and their efficacy investigated with a view to the reduction of side effects and toxicity and these have been mentioned in Chapter 1 of this thesis including some of the most recent ones. Over 3000 platinum compounds have been synthesised and tested *in vitro* in the past 30 years [12, 13]. However, less than 1% of these have entered clinical trials and very few have as yet emerged as clinically acceptable.

The cytotoxicity of several platinum complexes was examined (see Figure 3.3). These complexes have been fully characterised and here we report three crystal structures of these new complexes **84**, **86** and **88**. In WHCO1 cell lines complex **86** had the highest activity with an IC_{50} value of 5.49µM and the least active was complex **84** with an IC_{50} value of 9.47 µM. In comparison to cisplatin which has an IC_{50} of 13 – 15 µM in WHCO1 cell lines, all the novel platinum complexes described here displayed significant activity against oesophageal cancer cell lines.

The gold(I) complexes exhibited very good activity against both cancer cell lines. Complexes **93** and **94** were the most active with IC_{50} values of 3.41 and 3.61 µM and

complex **95** was the least active with an IC50 of 14.44 µM respectively. A similar trend was also observed in the KYSE450 cell lines.

Considering the close structural relationships between the iminophosphine ligands used here, which were complexed to either palladium, platinum or gold, we may be in a position to comment on the structure/function relationships of the complexes studied here. This may allow us to identify those structural motifs which may be important for biological activity either on their own or in combination with others. Based on information available in the literature, the majority of the vast amount of platinum complexes synthesised fit a set of structure-activity relationships. For a platinum drug to exhibit antiproliferative activity, the Pt(II) complex should have a *cis* geometry and the general formula of cis-$[PtX_2(Am)_2]$, where X is a leaving group and Am is an inert amine with at least one N-H functionality [14, 15]. The leaving group should have intermediate binding strength to platinum and should have a weak *trans* effect to avoid labilising the amine. In recent years, however, a large number of new compounds that do not satisfy the classical SARs have been reported to show antitumour activity. The demonstration of antitumour activity for these complexes indicates that cisplatin-like DNA lesions are not the only cause of cytotoxicity [16].

Not much work has been reported in the literature especially on gold(I) complexes with iminophosphine ligands except for the work reported by Williams *et al* [17]. They report the preparation and characterisation of three new gold(I) complexes with bidentate P-N ligands where, depending on its nature, the ligand binds to Au(I) either in a mono- or bidentate fashion to form the corresponding Au(I) complexes.

The principle question arising from the study of complexes with iminophosphine ligands is to establish the role of the side chain on the phenyl – PPh_2 moiety of the iminophosphine ligand. The complexes have similar iminophosphine ligands, coordinated in a square planar fashion to palladium and platinum but in a linear manner in gold as shown in Figure 3.12. Platinum complexes were more active than palladium complexes, confirming previous observations that platinum complexes perform better than palladium complexes (based on identical ligands). Despite palladium and platinum being elements of the same group and that their ionic radii are nearly the same as a result of lanthanoid contraction, their respective iminophosphine complexes exhibited varied activities with platinum compounds showing higher activity than palladium compounds. This observation is attributed to the associative substitution mechanism of the respective complexes suggesting that their kinetic behaviour is quite different even though they show similar coordinative behaviour [18]. Thus palladium complexes are less kinetically stable and as a result could undergo translabilization and undesired displacement of the non-leaving ligand by other nitrogen donors easily (especially those coordinated in a monodentate fashion) whereas platinum compounds are known to be kinetically inert [19]. This implies that palladium compounds are not stable and therefore in the cellular environment will be caused to dissociate easily by other biomolecules such as GSH and hence reacting to give other intermediates hence hindering it from forming the palladium-DNA adducts.

However, the gold compounds showed higher activity compared to platinum complexes. Gold complexes are mainly known for their use in treating rheumatoid arthritis, but some gold(I) complexes have been reported to show anticancer activity [20]. Recently tetrahedral gold(I) complexes of 1,2 bis(diphenylphosphino) ethane

ligands have shown to display a wide spectrum of anticancer activity [21]. In this project the gold(I) complexes exhibited IC_{50} values in the lower micromolar ranges of 3.41 and 3.61 µM for complexes **93** and **94**. However complex **95** with three phenyl groups was not very active with an IC_{50} of 14.44 µM.

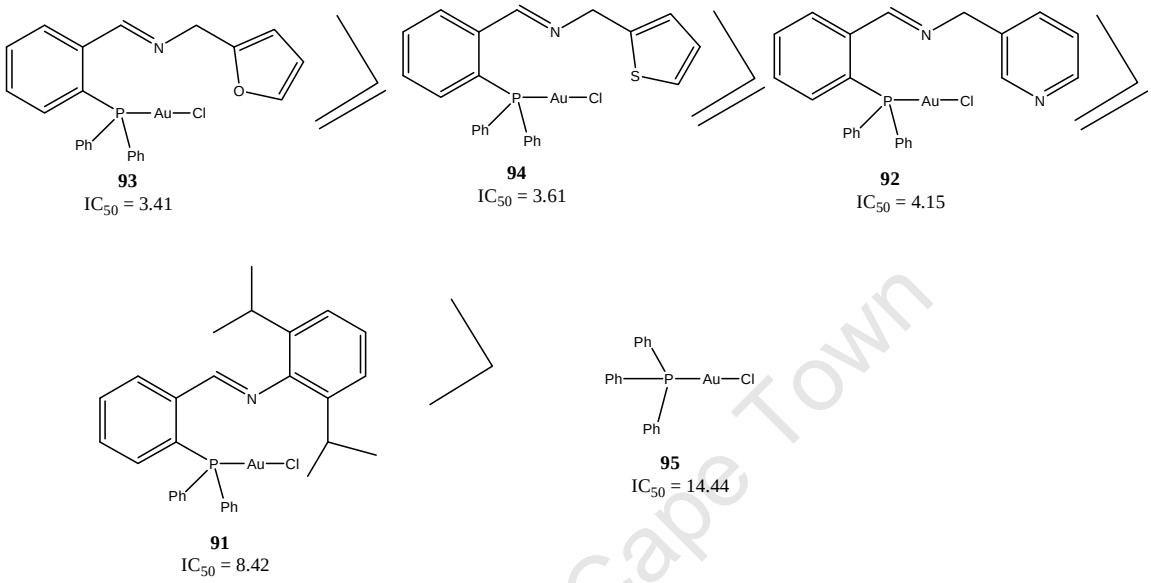

Figure 3.12 Changes in activity based on structure of the side chain for gold complexes

From the above data we can observe that in terms of activity, the complexes can be ranked in the order **93** ≥ **94**≥ **92** ≥ **91**. On performing a two tailed student *t*-test on the IC_{50} values of the complexes we observe that $p > 0.05$ when comparing the IC_{50} values of complex **93** with those of complexes **94** and **92**, suggesting that the difference in IC_{50} values of the complexes are not statistically significant. This suggests that the side chain has no significant effect on the cancer cell killing properties of complexes **92**, **93** and **94**. However for complex **91**, the bulkiness exerted by the diisopropyl group reduces cytotoxicity activity 2-fold. In complex **95** cytotoxicity is further reduced (5 times) with an IC_{50} value of 14.44 µM because of the even more bulkier phenyl groups. Performing the *t*-test on the IC_{50} values for **93**,

94 and **92** were significantly different from the IC_{50} value for **91** ($p < 0.05$) and **95** ($p < 0.05$).

A similar trend was observed for the platinum complexes against WHCO1 cells and is shown in Figure 3.13.

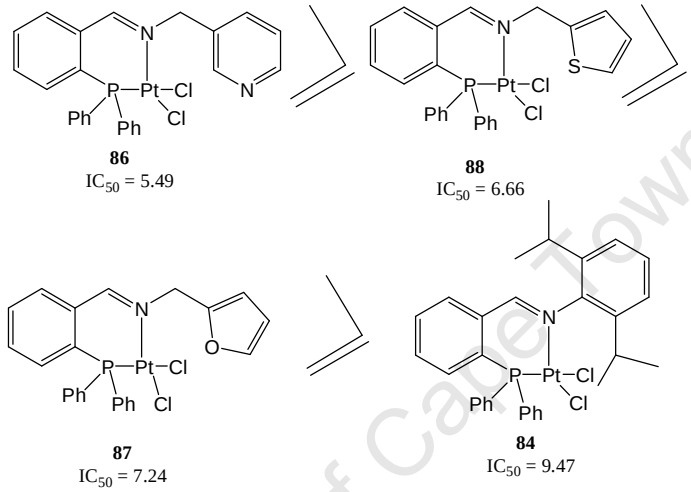

Figure 3.13 Changes in activity based on structure of the side chain for platinum complexes

The IC_{50} values for platinum complexes **86**, **88**, **87** and **84** are almost identical in both the WHCO1 and KYSE450 cell lines. Student *t*-tests performed on the IC_{50} values of the platinum complexes show that $p > 0.05$ indicating that differences in IC_{50} values are not statistically significant and the IC_{50} values can be regarded as equal.

Inorder to fully establish the role played different metals (palladium, platinum and gold) we then compared the IC_{50} values of the different metal complexes which contain the same ligand and the data is shown in Figure 3.14.

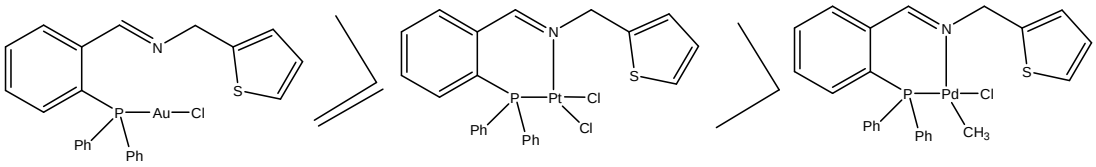

94
IC_{50} = 3.61

88
IC_{50} = 6.66

83
IC_{50} = 45.27

Figure 3.14 Changes in activity based on metal center in WHCO1 cells

The gold complex **94** is the most active in WHCO1 cells with an IC_{50} value of 3.61 µM followed by the platinum complex **88** with an IC_{50} value of 6.66 µM, and the least active is the palladium complex **83** with an IC_{50} of 45.27 µM. From this data we can conclude that in terms of the metal present in the ligand, activity of the complexes follows the order of Au ≥ Pt > Pd. The low activity of palladium complexes may be attributed to very rapid hydrolysis of the leaving groups that dissociate readily in solution leading to reactive species far from their pharmacological targets [22].

The complexes exhibited low cytotoxicity/activity against the normal DMB cells and the IC_{50}'s were very large in the range of 100.79 to 134.50 µM for the most active gold and platinum complexes. This is a very significant result since it suggests that these complexes may display a therapeutic window, causing selective cell death in cancer cells, leaving normal cells unaffected at low concentrations.

These findings are highly significant, since most organometallic complexes display a low selectivity against cancer cells (compared to normal cells). Clearly a number of additional experiments would need to be performed to explore this observation in more detail. These future experiments are described in the concluding comments of this thesis.

3.3.2 Effects of compounds on DNA damage and apoptosis

Cisplatin, that quintescential organometallic chemotherapeutic agent is thought to kill cancer cells by causing the formation of DNA adducts, which is associated with Double strand breaks in the DNA molecule, followed by cell death. In this project we monitored the phosphorylation status of the H2AX histone as a marker of DSB's in DNA, in response to treatment with the novel complexes synthesised here. DSBs arise by an exposure to ionizing radiation or drugs, but they are also generated as part of normal metabolic processes [23]. Our results demonstrate that some of the complexes tested (**84**, **91** and **93**) also induce DSB's in the cancer cells tested. Although these compounds do induce DNA damage as seen by the phosphorylation of H2AX, only minor effects on the cell cycle profile was observed. The biggest effect on the cell cycle was seen with complex **91** but this was not the most active compound tested, since it was the least active in WHCO1 cells.

Coronnello *et al* reported that some organogold(III) compounds produced significant antiproliferative effects to a greater extent than platinum drugs while causing only modest cell cycle modifications [24]. Most recently Ronconi *et al* described the mechanistic studies that have provided insights into the mechanism of action of gold(III)-dithiocarbamato derivates, and these show that these complexes have a slight effect on the cell cycle [25]. Metal containing complexes can react with different macromolecules, producing a wide range of biological effects, including DNA damage. The DNA-damaging potential of the two most commonly studied mercury compounds (mercury chloride and methyl mercury chloride), two nickel compounds (nickel chloride and potassium hexafluoronickelate), two palladium compounds (ammonium tetrachloropalladate and ammonium hexachloropalladate), and two

tellurium compounds has led to the conclusion that, the ability of inducing DNA damage these metal-containing compounds in cancer cells is dependent on the chemical form and, in general, compounds containing the metal in the lower valence state displayed the greater DNA-damaging ability [26]. Kawanishi *et al* reported that various metal compounds, such as cobalt, nickel, and ferric nitrilotriacetate, directly cause site-specific DNA damage in the presence of H_2O_2. They also found that carcinogenic metals could cause DNA damage through indirect mechanisms. Endogenous metals, copper and iron, catalyse ROS generation from various organic carcinogens, resulting in oxidative DNA damage [27].

The compounds **84** and **91** however do show slight PARP cleavage as was also seen in the morphology of the cells with a few apoptotic bodies. From these results we see no obvious apoptosis for the compounds tested and therefore the compounds are killing the cells through some other mechanism. It might therefore be interesting to investigate whether the compounds trigger cell death in WHCO1 cells by necrosis (premature death of cells usually induced by disruption of cell membrane), induce senescence (loss of cell's ability to divide due to DNA double strand breaks or toxins) or autophagy (degradation of a cell by autolysomes).

The lack of a sub-G1 peak in the cell analysis in Figure 3.11 is most likely due to the extended processing of cells for this assay (multiple washes and spins), during which the population may have been lost. The cell-cycle disturbances were associated with inhibition of cell proliferation in agreement with results reported by Martin *et al* [28] in their cell-cycle disturbance studies. This suggests that the reduction in G1-phase cells was as a result of the accumulation of cells a fact that is attributed to induction of

apoptosis by compounds in test. The cells were trapped in G1-phase and therefore paused their progress in the cycle and subsequently entered an indefinite phase. This is attributed to the complex binding to DNA in G1-phase and therefore disrupting its programme of passing the DNA for replication in the S-phase. This then caused the cell receptors to detect the anomaly hence triggering apoptosis. Selenium compounds are the most extensively studied cancer chemopreventive agents, and induce apoptotic death of tumor cells and the selenite-induced apoptosis involves DNA damage. Selenite has also been shown to stimulate phosphorylation of H2AX [29, 30].

The complexes discussed above were studied or their cytotoxicity on oesophageal cancer cells. The morphological changes observed showed that the complexes induced cell death, however apoptosis was not observed and cell death is occurring by some other mechanism. Further analysis of cytotoxicity activities of these complexes by FACS analysis showed that the complexes do not affect the cell cycle. The complexes also displayed selectivity against oesophageal cancer cells and this is a significant finding, which still needs to be pursued further.

3.4 REFERENCES

[1] Antonaroli S, Crociani B, *J. Organomet. Chem*., **1998**, 560, 137.

[2] Sanchez G, Momlona F, Peres J, Lopez G, *Transition Met. Chem.*, **2001**, 26, 100.

[3] Cattaruzza L, Fregona D, Mongat M, Ronconi L, Fassina A, Colombatti A, Aldinucci D, *Int. J. Cancer*, **2010**, 126, 5, 1.

[4] Amirnasr M, Schenk K. J, Salavati M, Dehghanpour S, Taeb A, Tadjarodi A, *J. Coord. Chem*., **2003**, 56, 3, 231.

[5] Chang S, Jones L, Wang C. M, Henling L. M, Grubbs R. H, *Organometallics*, **1998**, 17, 3460.

[6] Biyala M. K, Sharma K, Swami M, Fahmi N, Singh, R. V, *Transition. Met. Chem*., **2008**, 33, 377.

[7] Sondaz E, Jaud J, Launay J. P, Bonvoisin J, *Eur. J. Inorg. Chem*., **2002**, 1924.

[8] Maekawa M, Minematsu T, Konaka H, Sugimoto K, Kuroda S. T, Suenaga Y, Munakata M, *Inorg. Chim. Acta*, **2004**, 357, 3456.

[9] Gale G. R, Howle J. A, Smith A. B, *Proc. Soc. Exp. Biol. Med*., **1970**, 135, 690.

[10] Cleare M. J, Hoeschele J. D, *Platinum Metals Rev*., **1973**, 17, 2.

[11] Rajput J, Moss J.R, Hutton A. T, Hendricks, D.T, Arendse C. E, Imrie C, *J. Organomet. Chem.*, **2004**, 689, 9, 1553.

[12] Wong E, Giandomenico C. M, *Chem. Rev*., **1999**, 99, 2451.

[13] Jamieson E. R, Lippard S. J, *Chem. Rev*., **1999**, 2467.

[14] Cleare M. J, Hoeschele J. D, *Plat. Met. Rev.*, **1973**, 17, 3.

[15] Cleare M. J, Hoeschele J. D, *Bioinorg. Chem.*, **1973**, 2, 187.

[16] Fuertes M. A, Castilla J, Alonso C, Pérez J. M, *Curr. Med. Chem. Anti-Cancer* Agents, **2002**, 2, 539.

[17] Williams D. B. G, Traut T, Kriel F. H, van Zyl W. E, *Inorg. Chem. Comm*., **2007**,

10, 538.

[18] Micheal J. R, Sarah F, Christian M, Ina P, Bernt K, *Inorg. Chim. Acta*, **2003**, 350, 355.

[19] Wang X, Guo Z, *Dalton Trans*., **2008**, 1521.

[20] McKeage M. J, Maharaj L, Berners-Price S. J, *Coord. Chem. Rev*., **2002**, 232, 127.

[21] Urig S, Fritz-Wolf K, Reau R, Herold-Monde C, Toth K, Davioud-Charvet E, Becker K, *Angew. Chem. Int. Ed*., **2006**, 45, 1881.

[22] Gill D. S, in Hacker M. P, Douple E. B, Krakoff I. H, (Eds.), *Platinum Coordination Complexes in Cancer Chemotherapy*, Nijhoff, Boston, **1984**, 267.

[23] Srivastava N, Gochhait S, de Boer P, Bamezai R N. K, *Mutation Research*, **2009**, 681, 180.

[24] Coronnello M, Mini E, Caciagli B, Cinellu M. A, Bindoli A, Gabbiani C, Messori L, *J. Med.Chem.*, **2005,** 48, 6761.

[25] Ronconi L, Donatella A, Dou P. Q, Dolores F, *Anti-Cancer Agents in Medicinal Chemistry*, **2010**, 10, 4, 283.

[26] Guillamet E, Creus A, Farina M, Sabbioni E, Fortaner S, Marcos R, in *Mutation Research/Genetic Toxicology and Environmental Mutagenesis*, **2008**, 654, 1, 22.

[27] Kawanishi S, Hiraku Y, Murata M, Oikawa S. *Free Radic. Biol. Med*., **2002**, 32, 9, 822.

[28] Martin B. Oleksiewicz S. A, *J. Virol.*, **1997**, 71, 1386.

[29] Kim T, Jung U, Cho D. Y, Chung A. S, *Carcinogenesis*, **2001**, 22, 559.

[30] Zhou N, Xiao H, Kunli T, E-Kamal A. N, Liu L. F, *J. Biolog. Chem*., **2003**, 278, 29532.

CHAPTER 4

EXPERIMENTAL DETAILS

CONTENT

4.1 GENERAL EXPERIMENTAL DETAILS

All manipulations were carried out under an atmosphere of nitrogen or argon using standard Schlenk techniques unless otherwise stated. All other glassware was thoroughly dried at 210 º C for at least four hours prior to use.

4.1.1 Solvents and reagents

Hexane and pentane were refluxed and distilled from calcium hydride (CaH_2), tetrahydrofuran (THF), diethyl ether (Et_2O) and toluene were dried over sodium-wire and benzophenone, dichloromethane was dried over P_2O_5 under nitrogen. After the purification procedures the solvents were stored under nitrogen in Teflon sealed storage bottles. All reagents were purchased from Aldrich and used without further purification. Palladium and platinum were obtained as chloride salts from Johnson-Matthey and gold metal obtained from Mintek. Other starting materials such as $[PdCl_2(COD)]$ [1, 2] , [PdClMe(COD)] [3], $[PtCl_2(COD)]$ [4, 5], $[PtCl_2(DMSO)]_2$ [6, 7, 8] [PtClMe(COD)] [3, 9] and [Au(tht)Cl] [10] were prepared according to known literature procedures. Anhydrous magnesium sulphate or sodium sulphate were used for drying reaction solutions.

4.1.2 Instrumentation

Melting points were determined on the Kofler hotstage microscope (Reichart Thermovar) and are uncorrected. Microanalysis data was obtained from the University of Cape Town's Microanalytical Laboratory using a Carlo Erba EA1108 elemental analyser. Infrared Spectra were recorded on a Perkin-Elmer 1000 FT-IR spectrometer,

at the University of Cape Town, as KBr discs for solids. All data are given in wavenumbers (cm^{-1})

^{1}H, ^{13}C and ^{31}P NMR spectra were recorded on either a Varian Unity-400 ^{1}H: 400 MHz; ^{13}C: 100.6 MHz) or Varian Mercury-300 (^{1}H: 300 MHz; ^{13}C: 75.5 MHz) spectrometer at ambient temperatures. ^{1}H NMR spectra were referenced internally using residual protons in the deuterated solvent ($CDCl_3$: δ 7.27; DMSO: δ 2.50 ppm) and values reported relate to tetramethylsilane (δ 0.00). ^{13}C NMR were similarly referenced internally to the solvent resonance $CDCl_3$: δ 77.0; DMSO: δ 39.4 and with values reported relative to tetramethylsilane (δ 0.00). ^{31}P NMR spectra were referenced externally to H_3PO_4. All chemical shifts are quoted in δ (ppm) and coupling constants, *J*, in Hertz (Hz). Mass spectra (EI) were recorded using a JEOL-MATE(II) GC-MS instrument at UCT.

X-ray intensity data were collected on a Nonius Kappa-CCD diffractometer with 1.5 kW graphite monochromated Mo-Kα radiation. The structures were solved by direct methods using SHELXS-97 and refined employing full-matrix least-squares with the program SHELXL-97 [11, 12] refining on F^2.

4.2 SYNTHESIS OF LIGANDS

4.2.1 Iminophosphine ligands

*4.2.1.1 General procedure for the synthesis of iminophosphine ligands **58 - 64***

To 2-(diphenylphosphino)benzaldehyde was added an equimolar amount of desired amine in freshly distilled CH_2Cl_2. Na_2SO_4 or $MgSO_4$ was added to remove water formed as a by-product. The reaction was allowed to stir at room temperature for *ca* 16 hours after which the drying agent was removed by filtration and solvent removed under reduced pressure yielding an oil. The oils were solidified by addition of hot hexane and filtering whilst hot before allowing to cool at -16 ºC overnight. The respective precipitates were then filtered under gravity and washed with dry Et_2O before drying under vacuum for 4 hours.

Preparation of 58 [13]

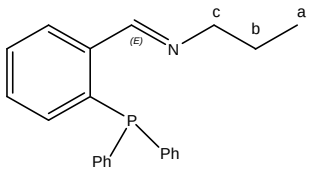

Product was obtained as a yellow crystalline powder in 85% yield

M.p.: 70-71 ºC

^{1}H NMR: (400M Hz, $CDCl_3$): δ_H 8.91 (d, 1H, *J* = 4.8 Hz, HC=N), 8.01 (dd, 1H, *J* = 7.8, 4.2 Hz, ArH), 7.39 – 7.22 (m, 12H, ArH), 6.90 (dd, 1H, *J* = 7.2, 5.4 Hz, ArH), 3.50 (t, 2H, *J* = 6.8 Hz, H_c), 1.54-1.44 (m, 2H, H_b), 0.82 (t, 3H, *J* =7.2 Hz, H_a)

^{31}P NMR: -13.4

EA: Calc. for $C_{22}H_{22}NP$: C, 79.74 %; H, 6.69 %; N 4.23 %;

Found: C, 79.59 %; H, 6.82 %; N 4.12 %;

IR (KBr): 1637 (s) (C=N, imine)

EI-MS: *m/z* 321.22 $[M]^+$

Preparation of 59 [14,15]

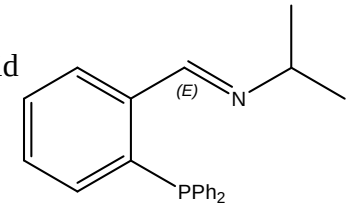

The product was obtained as a pale yellow crystalline solid in 76% yield.

M.p.: 107-108 °C

^{1}H NMR: (400 MHz, $CDCl_3$): δ_H 8.11 (s, 1H, *H*C=N), 7.8 - 6.2 (m, 14H, C_6H_4, Ph), 5.5 (m, 1H, - C*H*Me_2) 1.1 (d, 6H, *J* = 7.6 Hz, - CH*Me*$_2$)

^{31}P NMR: -13.2

EA: Calc. for $C_{22}H_{22}NP$: C, 79.74 %; H, 6.69 %; N 4.23 %;

Found: C, 79.88 %; H, 6.52 %; N 4.52 %;

IR (KBr): 1634s (C=N, imine)

EI-MS: *m/z* 321.24 $[M]^+$

Preparation of 60 [16]

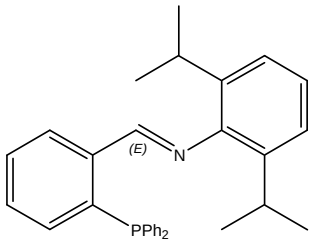

Product was obtained as a yellow crystalline powder in 80% yield

M.p.: 108-110 °C

^{1}H NMR: (400 MHz, $CDCl_3$): δ_H 8.94 (d, 1H, *J* = 5.7 Hz, HC=N), 8.34 (dd, 2H, *J* = 4.0 Hz, *J* = 7.7 Hz, ArH); 7.51 (t, 2H, *J* = 7.5 Hz, ArH), 7.42 (d, 2H, *J* = 1.4 Hz, ArH), 7.40 (d, 2H *J* = 1.5 Hz, ArH), 7.37 (d, 2H, *J* = 1.4 Hz, ArH), 7.31 (ddd, 2H *J* = 2.0 Hz, *J* = 5.0 Hz, *J* = 9.0 Hz, ArH), 7.22 (m, 2H, ArH), 7.07 (m, 2H, C_6H_3), 6.96 (ddd, 1H *J* = 0.8 Hz, *J* = 4.4 Hz, *J* = 7.7 Hz, C_6H_3), 2.75 (m, 2H, C*H*Me_2), 1.01 (d, 12H, *J* = 6.97 Hz, CH*Me*$_2$)

^{31}P NMR; -15.8

EA: Calc. for $C_{31}H_{32}NP$: C, 82.82 %; H, 7.17 %; N 3.12 %;

Found: C, 82.69 %; H, 7.12 %; N 3.32 %;

IR (KBr): 1629 (s) (C=N, imine)

EI-MS: *m/z* 449.56 $[M]^+$

Preparation of 61 [17]

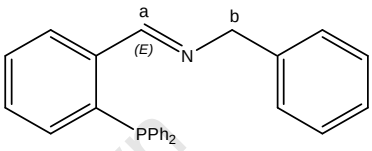

Product was obtained as a pale white powder in 78% yield

M.p.: 80-82 °C

^{1}H NMR: (400 MHz, $CDCl_3$): δ_H 8.91(d, 1H, *J* = 4.8 Hz, H_a), 8.10 (m, 1H, ArH), 7.19 – 7.43 (m, 15H, ArH), 7.09 (m, 2H, ArH) 6.94 (ddd, 1H, *J* = 7.7, 4.7, 1.2 Hz, ArH), 4.67 (s, 2H, H_b)

^{31}P NMR: δ -13.6 (s)

EA: Calc. for $C_{26}H_{22}NP$: C, 82.30 %; H, 5.84 %; N 3.69 %;

Found: C, 82.49 %; H, 5.62 %; N 3.72 %;

IR (KBr): 1636s (C=N, imine)

EI-MS: *m/z* 379.78 $[M]^+$

Preparation of 62

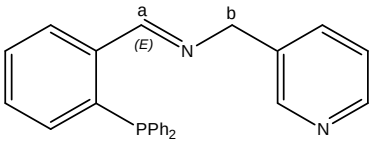

Product was obtained as a pale white solid in 85% yield

M.p.: 79-82 °C

^{1}H NMR: (400 MHz, $CDCl_3$): δ_H 9.02 (d,1H, *J* = 4.9 Hz, H_a), 8.45 (dd,1H, *J* = 1.7 Hz, 4.8 Hz, C_6H_4N), 8.42 (d,1H, *J* = 1.7 Hz, C_6H_4N) 8.01 (ddd,1H, *J* = 1.4, 3.9, 7.6 Hz, C_6H_4N), 7.43 – 7.24 (m, 13H, ArH), 7.12 (ddd, 1H, *J* = 0.8 Hz,

J = 4.8 Hz, *J* = 7.8 Hz, ArH), 6.90 (ddd, 1H, *J* = 7.7, 4.7, 1.7 Hz), 4.67 (s, 2H, H_b),

^{31}P NMR: δ -13.2 (s)

EA: Calc. for $C_{25}H_{21}N_2P$: C, 78.93 %; H, 5.56 %; N 7.36 %;

Found: C, 78.82 %; H, 5.62 %; N 7.52 %;

IR (KBr): 1632 (s) (C=N, imine)

EI-MS: *m/z* 380.80 $[M]^+$

Preparation of 63

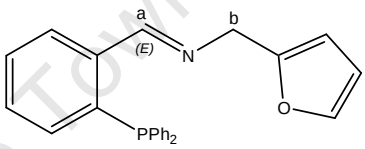

Product was obtained as a pale white powder in 85% yield

M.p.: 77-78 °C

^{1}H NMR: (400 MHz, $CDCl_3$): δ_H 9.01 (d, 1H *J* = 5.1 Hz, H_a), 8.07 (ddd, 1H, *J* = 7.7 Hz, *J* = 4.0 Hz, *J* = 1.4 Hz, ArH), 7.42 – 7.25 (m, 13H, ArH), 6.91 (m, 1H, C_4H_3O), 6.27 (m,1H, C_4H_3O), 6.05 (dd, 1H, *J* = 3.3 Hz, J = 0.7 Hz, C_4H_3O), 4.65 (s, 2H, H_b)

^{31}P NMR: δ -13.9 (s)

EA: Calc. for $C_{24}H_{20}NOP$: C, 78.03 %; H, 5.46 %; N 3.79 %;

Found: C, 78.19 %; H, 5.22 %; N 3.72 %;

IR (KBr): 1635 (s) (C=N, imine)

EI-MS: *m/z* 369.61 $[M]^+$

Preparation of 64

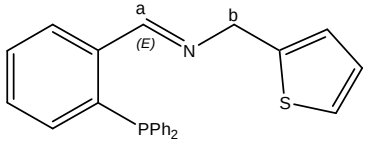

Product was obtained as a pale white powder in 75% yield

M.p.: 70-72 °C .

^{1}H NMR: (400 MHz, $CDCl_3$): δ_H 9.02 (br d, 1H, *J* = 4.9 Hz, H_a), 8.11 (m, 1H, ArH), 7.25 – 7.45 (m, 12H, ArH), 7.59 (d, 1H, *J* = 2.6 Hz), 6.95 (m, 2H, ArH), 6.78 (dd, 1H, *J* = 3.1 Hz, *J* = 1.0 Hz, C_4H_3S), 4.86 (s, 2H, H_b)

^{31}P NMR: δ -13.8 (s)

EA: Calc. for $C_{24}H_{20}NPS$: C, 74.78 %; H, 5.23 %; N 3.63 %; S, 8.32

Found: C, 74.59 %; H, 5.12 %; N 3.72 %; S, 8.11

IR (KBr): 1636 (s) (C=N, imine)

EI-MS: *m/z* 385.32 $[M]^+$

4.2.2 Tetradentate ligands

4.2.2.1 General procedure for the synthesis of tetradentate ligands ***65 - 68***

The tetradentate ligands were prepared by the addition of one equivalent of aromatic dialdehyde (terephthalaldehyde) to two equivalents of the appropriate amine previously dissolved in methanol and the mixture stirred at room temperature for *ca* 36 hours. The formed compound precipitated out alone without adding any solvent, washed with dry Et_2O and dried under vacuum for 4 hours.

Preparation of 65

Product was obtained as a pale white microcrystalline powder in 85% yield

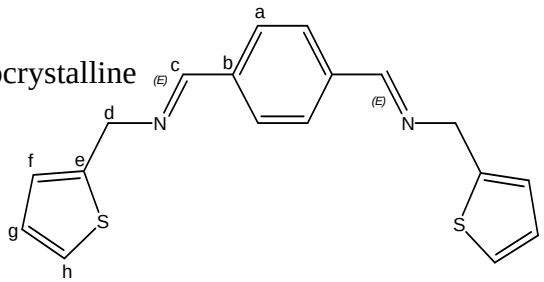

M.p.: 180-182 °C

^{1}H NMR: (400 MHz) δ_H 8.38 (t, 2H, *J* = 1.3 Hz, H_c) 7.82 (s, 2H, H_f) 7.25 (m, 4H, H_a) 7.00 (d, 4H, *J* = 3.4 Hz, H_g) 5.00 (d, 4H, *J* = 1.3 Hz, H_d)

^{13}C NMR: (400 MHz, $CDCl_3$) δ 161.54 (C_c), 141.72 (C_e), 138.10 (C_b), 128.55 (C_g), 126.88 (C_a), 125.11 (C_h), 124.80 (C_f), 59.28 (C_d)

EA: Calc. for $C_{18}H_{16}N_2S_2$: C, 66.63 %; H, 4.97 %; N, 8.63 %; S, 19.77

Found: C, 66.59 %; H, 4.62 %; N, 8.72 %; S, 19.65

IR (KBr): 1612 cm^{-1} (C=N, imine)

EI-MS: *m/z* 103.30 $[M - 2C_5H_5SN]^+$

Recrystallisation by slow diffusion of Et_2O into a concentrated CH_2Cl_2 of the solution gave crystals of **65** suitable for X-ray structure determination.

Preparation of 66

Product was obtained as off white shiny crystals in 75% yield.

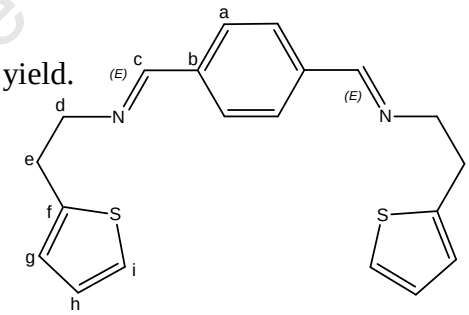

M.p.: 240-242 °C

^{1}H NMR: (400 MHz, $CDCl_3$) δ_H 8.23 (d, 2H, *J* = 1.3Hz, H_c) 7.76 (s, 2H, H_a) 7.13 (dd, 2H, *J* = 3.4 Hz, *J* = 5.1Hz, H_g) 6.92 (dd, 2H, *J* = 1.1 Hz, *J* = 5.1 Hz, H_i) 6.84 (dd, 4H, *J* = 1.3 Hz, *J* = 2.1Hz, H_h) 3.91 (dt, 4H, *J* = 1.1 Hz, *J* = 7.0Hz, H_d) 3.25 (t, 4H, *J* = 7.0 Hz, H_e)

^{13}C NMR: (400 MHz, $CDCl_3$) δ 161.27 (C_c), 142.28 (C_f), 138.15 (C_b), 128.34 (C_h), 126.72 (C_a), 125.18 (C_i), 123.61 (C_g), 62.90 (C_d), 31.42 (C_e)

EA: Calc. for $C_{20}H_{20}N_2S_2$: C, 68.14 %; H, 5.72 %; N, 7.95 %; S, 18.19

Found: C, 68.19 %; H, 5.52 %; N, 7.72 %; S, 18.44

IR (KBr): 1613 cm^{-1} (C=N, imine)

EI-MS: *m/z* 351.76 $[M]^+$

Recrystallisation by slow diffusion of Et_2O into a concentrated CH_2Cl_2 of the solution gave crystals of **66** suitable for X-ray structure determination.

Preparation of 67

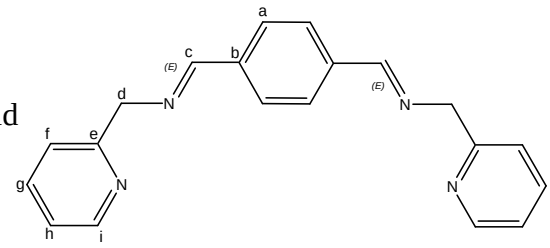

Product was obtained as a white solid in 85% yield

M.p.: does not melt below 260 °C

^{1}H NMR: (400 MHz, $CDCl_3$) δ_H 8.57 (d, 2H, *J* = 4.8 Hz, H_i) 8.50 (s, 2H, H_c) 7.86 (s, 2H, H_a) 7.68 (dt, 2H, *J* = 1.8 Hz, *J* = 7.7 Hz, H_g) 7.44 (d, 2H, *J* = 7.8 Hz, H_f) 7.26 (m, 2H, H_h) 7.18 (dd, 2H, *J* = 4.6 Hz, *J* = 7.2 Hz, H_f) 4.97 (s, 4H, H_d)

^{13}C NMR: (400 MHz, $CDCl_3$) δ 162.67 (C_c), 159.28 (C_e), 149.54 (C_i), 138.43 (Cb), 136.90 (C_g), 128.78 (C_a), 122.56 (C_h), 122.29 C_f), 67.12 (C_d)

EA: Calc. for $C_{20}H_{18}N_4$: C, 76.41 %; H, 5.77%; N, 17.82 %;

Found: C, 76.19 %; H, 5.52 %; N, 17.72 %;

IR (KBr): 1605 cm^{-1} (C=N, imine)

EI-MS: *m/z* 221.84 $[M - C_6H_6N]^+$

Preparation of 68

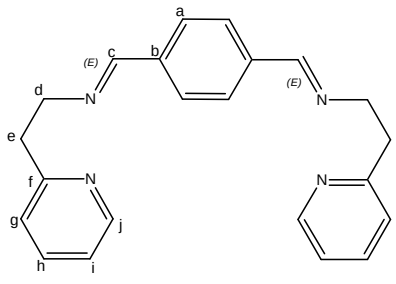

Product was obtained as a white solid in 85% yield

M.p.: does not melt below 260 °C

^{1}H NMR: (400 MHz, $CDCl_3$) δ_H 8.55 (ddd, 2H, *J* =0.8 Hz, *J* = 1.7Hz, J = 4.8 Hz) 8.21 (t, 2H, *J* = 1.3Hz) 7.69 (s, 2H) 7.55 (dt, 2H, *J* = 1.9Hz, *J* = 7.7Hz) 7.11 (m, 2H) 4.03 (dt, 8H, *J* = 1.2 Hz, *J* = 7.2Hz)

3.19 (t, 4H, *J* = 7.2Hz)

^{13}C NMR: (400 MHz, $CDCl_3$) δ 161.05 (C_f), 159.45 (C_c), 149.37 (C_j), 138.88 (C_b), 136.13 (C_b), 128.21 (C_a), 123.67 (C_g), 121.24 (C_i), 61.18 (C_d), 39.61 (C_e)

EA: Calc. for $C_{22}H_{22}N_4$: C, 77.16 %; H, 6.48 %; N, 16.36 %;

Found: C, 77.19 %; H, 6.22 %; N, 16.52 %;

IR (KBr): 1610 cm^{-1} (C=N, imine)

EI-MS: *m/z* 249.90 $[M - C_6H_6N]^+$

Recrystallisation by slow diffusion of Et_2O into a concentrated CH_2Cl_2 of the solution gave crystals of **68** suitable X-ray structure determination.

4.2.3 Schiff base ligands

*4.2.3.1 General procedure for the synthesis of schiff base ligands **69 – 72***

Schiff bases were prepared according to the known method from the condensation of the respective diamine with the corresponding aldehyde in a molar ratio 1:2, respectively, using methanol as a solvent at *ca*. 45 °C. The reaction mixture was stirred for 3 hours. The precipitates were filtered off, washed several times with methanol and finally dried under vacuum for 4 hours.

Preparation of 69

Product was obtained as a white crystalline powder in 83% yield

M.p.: 125-127 °C

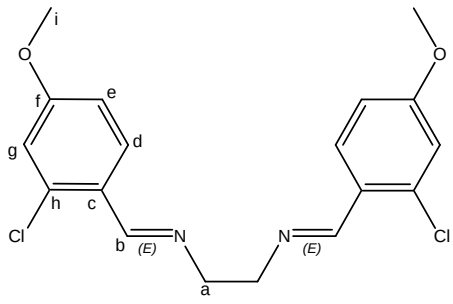

^{1}H NMR: (400 MHz, $CDCl_3$) δ_H 8.64 (s, 2H, H_b), 7.95 (d, 2H, *J* = 8.5 Hz, H_d), 7.24 (dd, 2H, *J* = 0.7 Hz, *J* = 2.0 Hz, H_g), 7.27 (dd, 2H, *J* = 0.6 Hz, *J* = 2.1 Hz, H_e), 4.01 (s, 4H, H_a), 2.17 (s, 6H, H_i)

^{13}C NMR: (400 MHz, $CDCl_3$) δ 158.45 (C_f), 136.96 (C_b), 135.57 (C_c), 131.73 (C_h), 129.52 (C_d), 129.27 (C_g), 127.50 (C_e), 61.34 (C_a)

EA: Calc. for $C_{18}H_{18}Cl_2N_2O_2$: C, 59.19 %; H, 4.97 %; N 7.67 %.

Found: C, 59.39 %; H, 4.72 %; N 7.42 %.

IR (KBr): 1617 cm^{-1} (C=N, imine)

EI-MS: *m/z* 336.74 $[M - CH_3O]^+$

Preparation of 70

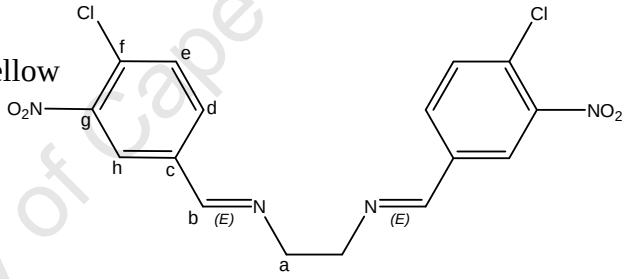

Product was obtained as a yellow crystalline solid in 85% yield

M.p.: 145-147 °C

^{1}H NMR: (400 MHz, $CDCl_3$) δ_H 8.30 (s, 2H, H_b), 8.22 (s, 2H, H_h), 7.83 (d, 2H, *J* = 8.3 Hz, H_d), 7.58 (d, 2H, *J* = 8.3 Hz, H_e), 4.03 (s, 4H, H_a)

^{13}C NMR: (400 MHz, $CDCl_3$) δ 158.81 (C_b) , 149.86 (C_g) 135.93 (C_c), 132.14 (C_e), 131.89 (C_f), 128.80 (C_d), 124.53 (C_h), 61.11 (C_a)

EA: Calc. for $C_{16}H_{12}Cl_2N_4O_4$: C, 48.58 %; H, 3.04 %; N 14.18 %.

Found: C, 48.19 %; H, 3.12 %; N 14.42 %.

IR (KBr): 1614 cm^{-1} (C=N, imine)

EI-MS: *m/z* 363.66 $[M - Cl]^+$

Preparation of 71

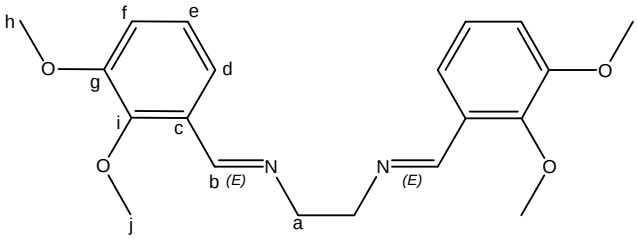

Product was obtained as a yellow crystalline solid in 88% yield

M.p.: 145-147 C°

^{1}H NMR: (400 MHz, $CDCl_3$) δ_H 8.65 (s, 2H, H_b), 7.51 (d, 2H, *J* = 1.6 Hz, H_f), 7.03 (t, 2H, *J* = 7.8 Hz, H_d), 6.92(d, 2H, *J* = 1.6 Hz, *J* = 2.1 Hz, H_e), 4.00 (s, 4H, H_a), 3.85 (s, 6H, H_j), 3.77 (s, 6H, H_h)

^{13}C NMR: (400 MHz, $CDCl_3$) δ 158.54 (C_b), 152.74 (C_g), 149.36 (C_i), 129.96 (C_c), 124.04 (C_e), 118.88 (C_d), 114.24 (C_f), 61.91 (C_j), 61.67 (C_a), 58.85 (C_h)

EA: Calc. for $C_{20}H_{24}N_2O_4$: C, 67.40 %; H, 6.79 %; N, 7.86 %.

Found: C, 67.19 %; H, 6.12 %; N, 7.72 %.

IR (KBr): 1618 cm^{-1} (C=N, imine)

EI-MS: *m/z* 326.69 $[M - CH_3O]^+$

Preparation of 72

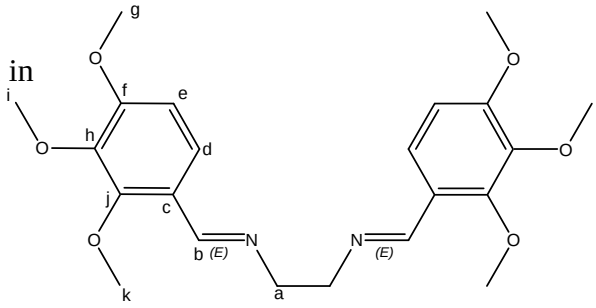

Product was obtained as a yellow crystalline solid in 92% yield

M.p.: 154-155 °C

^{1}H NMR: (400 MHz, $CDCl_3$) δ_H 8.52 (s, 2H, H_b), 7.66 (s, 2H, H_d), 6.66 (s, 1H, H_e), 3.93 (s, 4H, H_a), 3.87 (s, 6H, H_i), 3.85 (s, 6H, H_g), 3.83 (s, 6H, H_k)

^{13}C NMR: (400 MHz, $CDCl_3$) δ 158.10 (C_b), 122.90 (C_d), 122.17 (C_c), 107.70 (C_e), 62.01 (C_i), 61.81 (C_k), 60.87 (C_a), 56.03 (C_g)

EA: Calc. for $C_{22}H_{28}N_2O_6$: C, 63.45 %; H, 6.78 %; N, 6.73 %.

Found: C, 63.19 %; H, 6.52 %; N, 6.72 %.

IR (KBr): 1625 cm^{-1} (C=N, imine)

EI-MS: *m/z* 386.44 $[M - CH_3O]^+$

4.3 PREPARATION OF PALLADIUM COMPLEXES

*4.3.1 General procedure for synthesis of complexes **73** – **79*:** To a dry CH_2Cl_2 (10 ml) solution of the precursor $Pd[COD]Cl_2$ (0.095 g, 0.3 mmol) was added the calculated amount of iminophosphine in CH_2Cl_2 solution, and the reaction was stirred at room temperature for 1 hour. The yellow solution was then concentrated under reduced pressure to half volume and the addition of hexane caused precipitation of complexes, which were filtered off, washed with Et_2O and drying under vacuum for 4 hours. Yellow crystals of the compounds **73** – **79** were obtained in high yield by recrystallization from CH_2Cl_2-hexane.

Preparation of 73 [14]

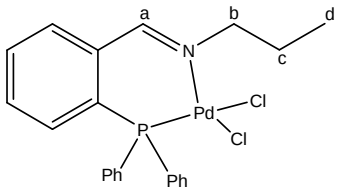

Product was obtained as a yellow crystalline solid in 70% yield

M.p.: 158-160 °C

^{1}H-NMR: (400 MHz, $CDCl_3$) δ_H 8.85 (s, 1H, H_a) 7.89 (m, 3H, ArH) 7.66 (dd, 4H, *J* = 6.3 Hz, *J* = 7.9 Hz, ArH) 7.55 (ddd, 7H, *J* = 2.0 Hz, *J* = 5.2 Hz, *J* = 8.5 Hz, ArH) 2.95 (dddd, 2H, *J* = 5.4Hz, *J* = 8.3Hz, *J* = 13.8 Hz, *J* = 16.7 Hz, H_b) 1.18 (m, 2H, H_c) 0.53 (t, 3H, *J* = 7.3 Hz, H_d)

^{31}P NMR: δ 30.85 (s)

EA: Calc. for $C_{22}H_{22}Cl_2NPd$: C, 51.94 %; H, 4.36 %; N, 2.75 %.

Found: C, 51.69 %; H, 4.12 %; N, 2.72 %.

IR (KBr): 1632 cm^{-1} (C=N, imine)

EI-MS: *m/z* 437.30 $[M - 2Cl]^+$

Preparation of 74 [14]

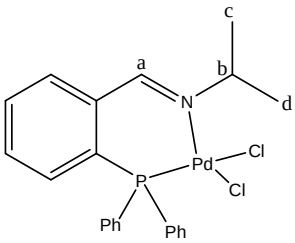

Product was obtained as a yellow crystalline solid in 82% yield

M.p.: 168-170 °

^{1}H-NMR: (400 MHz, $CDCl_3$) δ_H 8.02 (s, 1H, H_a) 7.72 (m, 2H, ArH) 7.51 (m, 11H, ArH) 6.94 (ddd, 1H, *J* = 0.5 Hz, *J* = 7.7 Hz, *J* = 10.6 Hz, Ar) 5.57 (dtd, 1H, *J* = 0.6 Hz, *J* = 6.4 Hz, *J* = 13.0 Hz, H_b) 1.16 (d, 6H, *J* = 6.6 Hz, H_c, H_d)

^{31}P NMR: δ 31.62 (s)

EA: Calc. for $C_{22}H_{22}Cl_2NPPd$: C, 51.94 %; H, 4.36 %; N, 2.75 %.

Found: C, 51.79 %; H, 4.12 %; N, 2.52 %.

IR (KBr): 1634 cm^{-1} (C=N, imine)

EI-MS: *m/z* 474.68 $[M - Cl]^+$

Crystals suitable for single crystal X-ray diffraction were obtained by slow evaporation of a dmso-d_6-CH_2Cl_2 solution of the complex at room temperature.

Preparation of 75

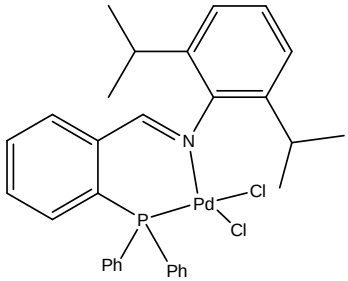

Product was obtained as a yellow crystalline powder in 75% yield

M.p.: 200-202 °C

^{1}H NMR: (400 MHz, dmso-d_6) δ_H 8.74 (s, 1H, HC=N) 7.58 (m, 14H ArH) 7.16 (m, 7.16, 4H, ArH) 1.19 (d, 6H, J = 6.7 Hz, -CH_3) 0.77 (t, 6H, J = 6.3 Hz, -CH_3)

^{13}C NMR: (400 MHz, dmso-d_6) δ 169.31, 135.28, 133.94 (d, J_{CP} = 11.0 Hz), 132.89, 129.74 (d, J_{CP}=11.8Hz), 128.90, 123.80, 28.73, 27.99, 24.31, 23.42

^{31}P NMR: δ 33.34 (s)

EA: Calc. for $C_{31}H_{32}Cl_2NPPd$: C, 59.39 %; H, 5.15 %; N 2.23 %.

Found: C, 59.19 %; H 5.12 %; N 2.42 %.

IR (KBr): 1624 cm^{-1} (C=N, imine)

EI-MS: *m/z* 591.44 $[M - Cl]^+$

Preparation of 76

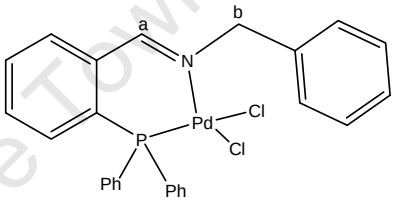

Product was obtained as a yellow powder in 76% yield

M.p.: 200-202 °C .

^{1}H-NMR: (400 MHz, d_6-dmso) δ_H 7.81 (m, 1H) 7.63 (m, 1H) 7.49 (m, 1H) 7.09 (m, 1H) 7.08 (m, 1H) 6.91 (dd, 1H, *J* = 4.6 Hz, *J* = 10.9 Hz) 6.49 (dd, 1H, *J* = 1.1 Hz, *J* = 8.1 Hz) 4.22 (t, 2H, *J* = 12.6 Hz)

^{31}P NMR: δ 34.11 (s)

EA: Calc. for $C_{26}H_{22}Cl_2NPPd$: C, 56.09 %; H, 3.98 %; N, 2.52 %.

Found: C, 56.26 %; H 3.72 %; N, 2.72 %.

IR (KBr): 1627 cm^{-1} (C=N, imine)

Preparation of 77

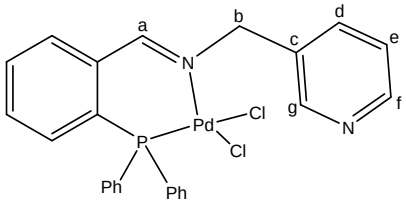

Product was obtained as a yellow powder in 70% yield

M.p.: 210-212 °C .

^{1}H-NMR: (400 MHz, d_6-dmso) δ_H 8.82 (s, 1H, H_a) 8.66 (d, 1H, *J* = 2.3 Hz, H_g) 8.49

(d, 1H, *J* = 3.8 Hz, H_f), 8.34 (s, 1H, H_a) 7.91 (dd, 1H, *J* = 4.1 Hz, *J* = 7.3 Hz, H_e) 7.68 (m, 2H, ArH) 7.55 (dd, 4H, *J* = 6.7 Hz, *J* = 8.3 Hz, ArH) 7.43 (m, 4H, ArH) 7.14 (m, 1H, H_d) 5.45 (s, 2H, H_b)

^{31}P NMR: δ 37.4 (s)

EA: Calc. for $C_{25}H_{21}N_2PPd$: C, 53.84 %; H, 3.80 %; N 5.02 %.

Found: C, 53.69 %; H 3.92 %; N 4.92 %.

IR (KBr): 1626 cm^{-1} (C=N, imine)

EI-MS: *m/z* 557.75 $[M]^+$

Preparation of 78

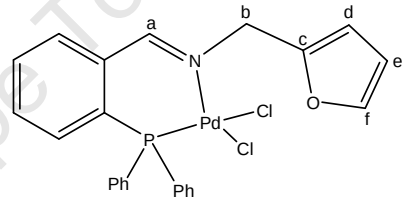

Product was obtained as a yellow powder in 78% yield

M.p.: 200-202 °C

^{1}H-NMR: (400 MHz, d_6-dmso) 8.72 (s, 1H, H_a) 7.98 – 8.08 (m, 1H, ArH) 7.75(t, 1H, *J* = 1.5 Hz, *J* = 7.7 Hz, ArH) 7.58 (m, 2H, ArH) 7.45 (td, 4H, *J* = 2.9 Hz, 4.8 Hz, ArH) 7.05 (dd, 1H, *J* = 8.1 Hz, *J* = 1.8 Hz, H_f) 7.24 (m, 5H, ArH) 6.55 (d, 1H, *J* = 2.9 Hz, H_e) 6.38 (dd, 1H, *J* = 2.9 Hz, H_d) 5.78 (t, 1H, *J* = 1.5 Hz, *J* = 7.7 Hz, ArH) 5.56 (s, 2H, H_b)

^{31}P NMR: δ 32.3(s)

EA: Calc. for $C_{24}H_{20}Cl_2NOPPd$: C, 52.72 %; H, 3.69 %; N, 2.56 %.

Found: C, 52.59 %; H, 3.42 %; N, 2.72 %.

IR (KBr): 1630 cm^{-1} (C=N, imine)

EI-MS: *m/z* 546.71 $[M]^+$

.

Preparation of 79

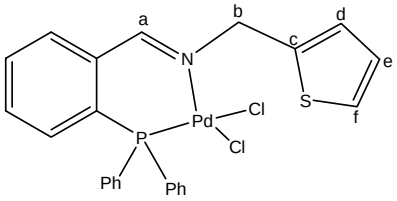

Product was obtained as a yellow powder in 65% yield

M.p.: 234-235 °C

^{1}H-NMR: (400 MHz, d_6-dmso) δ_H 8.80 (s, 1H, H_a) 8.03 – 7.92 (m, 1H, ArH) 7.86 – 7.93 (m, 1H, ArH) 7.74 (m, 1H, ArH) 7.52 – 7.60 (m, 2H, ArH) 7.40 (td, 4H, *J* = 4.9 Hz, *J* = 2.9 Hz, ArH) 7.18 (dd, 4H, *J* = 7.8 Hz, *J* = 4.9 Hz, ArH) 6.99 – 7.07 (m, 2H, H_f) 6.90 (dd, 1H, *J* = 2.9 Hz, *J* = 2.0 Hz, H_d) 5.66 (s, 2H, H_b)

^{31}P NMR: δ 31.8(s)

EA: Calc. for $C_{24}H_{20}Cl_2NPPdS$: C, 51.22 %; H, 3.58 %; N, 2.49 %, S, 5.70

Found: C, 51.48 %; H, 3.32 %; N, 2.72 %, S, 5.86

IR (KBr): 1628 cm^{-1} (C=N, imine)

EI-MS: *m/z* 562.73 $[M]^+$

Crystals suitable for single crystal X-ray diffraction were obtained by slow evaporation of a DMSOd_6-CH_2Cl_2 solution of the complex at room temperature.

4.3.2 General procedure for synthesis of complexes ***80*** *–* ***83*****:** To a dry CH_2Cl_2 (10 ml) solution of the precursor PdClMe[COD] (0.07 g, 0.27 mmol) was added the calculated amount of iminophosphine in CH_2Cl_2 solution, and the reaction was stirred at room temperature for 1 hour. The yellow solution was then concentrated under reduced pressure to *ca* half the volume and the addition of hexane caused precipitation of complexes, which were filtered off, washed with Et_2O and dried under vacuum for

4 hours. Yellow crystals of the compounds **80** – **83** were obtained in high yield by recrystallization from CH_2Cl_2-hexane.

Preparation of 80

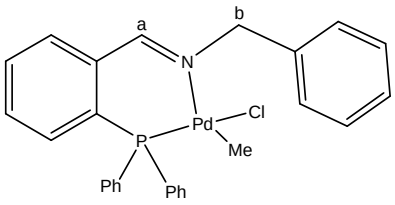

Product was obtained as a pale yellow powder in 85% yield

M.p.: 168-170 °C

^{1}H-NMR: (400 MHz, $CDCl_3$) δ_H 8.81 (s, 1H, H_a) 7.91 (dd, 1H, *J* = 4.3 Hz, *J* = 46.3 Hz, ArH) 7.83 (t, *J* = 7.6 Hz, ArH) 7.69 (t, 1H, *J* = 7.4 Hz, ArH) 7.56 (m, 2H, ArH) 7.45 (dt, 4H, *J* = 2.3Hz, 7.6Hz, ArH) 7.29 (m, 1H, ArH) 7.18 (m, 8H, ArH) 7.09 (dd, 1H, *J* = 7.7Hz, *J* = 10.5 Hz, ArH) 5.10 (s, 2H, H_b) 0.18 (d, 3H, J = 1.2 Hz, C*H*$_3$)

^{31}P NMR: δ 38.5 (s)

EA: Calc. for $C_{27}H_{25}ClNPPd$: C, 60.46 %; H, 4.70 %; N, 2.61 %.

Found: C, 60.72 %; H, 4.51 %; N, 2.81 %.

IR (KBr): 1628 cm^{-1} (C=N, imine)

EI-MS: *m/z* 521.75 $[M - CH_3]^+$

Crystals suitable for single crystal X-ray diffraction were obtained by slow evaporation of a $DMSOd_6$-CH_2Cl_2 solution of the complex at room temperature.

Preparation of 81

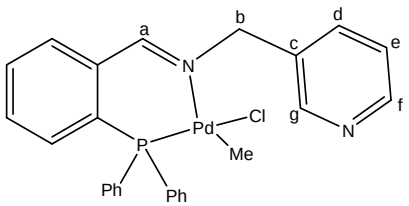

Product was obtained as a pale yellow powder in 85% yield

M.p.: 178-180 °C

^{1}H NMR: (400 MHz, $CDCl_3$) δ_H 8.80 (d, 1H, *J* = 1.6 Hz, H_f) 8.63 (s, 1H, H_a) 8.47 (dd, 1H, *J* = 1.6 Hz, *J* = 4.8 Hz, H_g) 7.88 (ddd, 1H, *J* = 1.3 Hz, *J* = 4.1 Hz, *J* = 7.6 Hz, ArH) 7.66 (m, 2H, ArH) 7.79 (tt, 1H, *J* = 1.4 Hz, *J* = 7.6 Hz, ArH) 7.52 (m, 2H, ArH) 7.39 (ddd, 4H, *J* = 2.0 Hz, *J* = 5.1 Hz, *J* = 7.3 Hz, ArH) 5.41 (s, 2H, H_b) 7.11 (m, 6H) 0.26 (d, 3H, *J* = 3.3Hz, C*H*$_3$)

^{31}P NMR: δ 37.4 (s)

EA: Calc. for $C_{26}H_{24}ClN_2PPd$: C, 58.12 %; H, 4.50 %; N, 5.21 %.

Found: C, 58.19 %; H, 4.12 %; N, 5.54 %.

IR (KBr): 1628 cm^{-1} (C=N, imine)

EI-MS: *m/z* 537.13 $[M]^+$

Preparation of 82

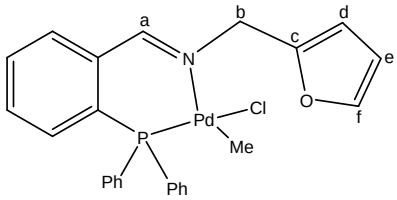

Product was obtained as a pale yellow powder in 75% yield.

M.p.: 195-196 °C

^{1}H-NMR: (400 MHz, $CDCl_3$) δ_H 8.65 (s, 1H, H_a) 7.86 (ddd, 1H, *J* = 1.2 Hz, *J* = 4.1 Hz, *J* = 7.4 Hz, ArH) 7.77 (t, 1H, *J* = 7.5 Hz, ArH) 7.66 (t, 1H, *J* = 7.5 Hz, ArH) 7.51 (m, 6H, ArH) 7.34 (m, 4H, ArH) 7.18 (m, 1H, H_f) 6.43 (m, 1H, H_d) 5.39 (s, 2H, H_b) 0.23 (d, 3H, *J* = 3.2 Hz, C*H*$_3$)

^{31}P NMR: δ 37.6 (s)

EA: Calc. for $C_{25}H_{23}ClNOPPd$: C, 57.07 %; H, 4.40 %; N, 2.66 %.

Found: C, 57.19 %; H, 4.12 %; N, 2.72 %.

IR (KBr): 1631 cm^{-1} (C=N, imine)

EI-MS: *m/z* 526.03 $[M]^+$

Preparation of 83

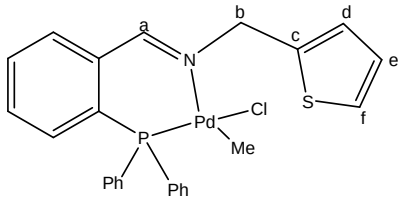

Product was obtained as a pale yellow powder in 80% yield.

M.p.: 186-188 °C

^{1}H-NMR: (400 MHz, $CDCl_3$) δ_H 8.76 (s, 1H, H_a) 7.87 (m, 1H) 7.80 (t, 1H, *J* = 7.5 Hz) 7.69 (t, 1H, *J* = 7.5 Hz, H_f) 7.54 (dd, 2H, *J* = 6.5 Hz, *J* = 8.2 Hz, ArH) 7.44 (m, 5H, ArH) 7.17 (td, 5H, *J* = 6.1 Hz, *J* = 12.2 Hz, ArH) 7.07 (d, 1H, *J* = 2.4 Hz, H_e) 6.96 (dd, 1H, *J* = 3.5Hz, *J* = 5.1Hz, H_d) 5.57 (s, 2H, H_b) 0.25 (d, 3H, *J* = 3.3Hz, C*H*$_3$)

^{31}P NMR: δ 37.6 (s)

EA: Calc. for $C_{25}H_{23}ClNPPdS$: C, 55.36 %; H, 4.27 %; N, 2.58 %; S, 5.91

Found: C, 55.19 %; H, 4.08 %; N, 2.38 %; S, 6.05

IR (KBr): 1629 cm^{-1} (C=N, imine)

EI-MS: *m/z* 531.8 $[M - CH_3]^+$

4.4 PREPARATION OF PLATINUM COMPLEXES

*4.4.1 General procedure for synthesis of complexes **84** – **88*:** To a dry DCM (10 ml) of the appropriate ligand (**60** - **64**) was added an equimolar amount of $Pt[COD]Cl_2$ or $Pt[DMSO]_2Cl_2$ also in dry CH_2Cl_2 (10 ml). The reaction was allowed to stir at room temperature for 4 hours before reducing the solvent to *ca* 5 ml and precipitating out the products with hexane, filtering under gravity and washing the precipitate with Et_2O and drying under vacuum for 4 hours.

Preparation of 84

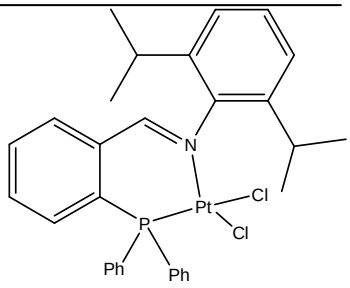

Product was obtained as a yellow powder in 76% yield

M.p.: 201-203 °C .

^{1}H NMR: (400 MHz, $CDCl_3$) δ_H 8.95 (d, 1H, *J* = 111.3 Hz)

8.18 (dd, 1H, *J* = 4.2 Hz, *J* = 9.0 Hz) 7.90 (m, 2H) 7.60 (m, 10H) 7.18 (m, 4H) 3.01 (m, 2H) 1.24 (d, 6H, *J* = 6.8 Hz) 0.83 (d, 6H, *J* = 6.8 Hz)

^{31}P NMR: δ 5.83 *J*(Pt-P) = 3661 Hz

EA: Calc. for $C_{31}H_{32}Cl_2NPPt$: C, 52.03 %; H, 4.51 %; N 1.96 %

Found: C, 52.19 %; H 4.74 %; N 1.99 %

IR (KBr): 1624 cm^{-1} (C=N, imine)

EI-MS: *m/z* 678.34 $[M - Cl]^+$

Crystals suitable for X-ray structure determination were obtained by recrystallisation form a CH_2Cl_2-hexane mixture at room temperature.

Preparation of 85

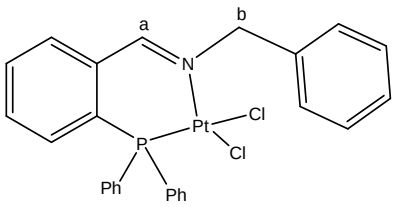

Product was obtained as a light yellow powder in 65% yield

M.p.: 180-183 °C

^{1}H-NMR: (400 MHz, $CDCl_3$) δ_H 7.79 (m, 1H) 7.60 (t, 1H, *J* = 7.4 Hz) 7.47 (t, 1H, *J* = 7.4 Hz) 7.07 (t, 1H, *J* = 8.6 Hz) 6.90 (t, 1H, *J* = 7.7 Hz) 6.49 (d, 1H, *J* = 7.2 Hz) 4.13 (t, 1H, *J* = 12.8 Hz)

^{31}P NMR: δ 8.09 *J*(Pt-P)=3668 Hz

EA: Calc. for $C_{26}H_{22}Cl_2NPPt$: C, 48.38 %; H, 3.44 %; N 2.17%;

Found: C, 48.19 %; H, 3.12 %; N 2.47 %;

IR (KBr): 1632 cm^{-1} (C=N, imine)

EI-MS: *m/z* 609.36 $[M - Cl]^+$

Preparation of 86

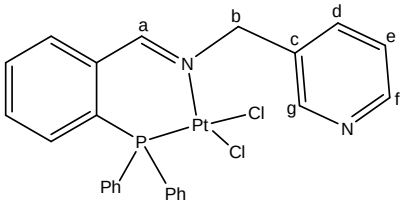

Product was obtained as a yellow powder in 76% yield

M.p.: 168-169 °C

^{1}H-NMR: (400 MHz, $CDCl_3$) δ_H 9.19 (m, 1H) 8.64 (m, 1H) 8.53 (d, 1H, *J* = 4.3Hz) 8.05 (dd, 1H, *J* = 4.1 Hz, *J* = 6.9 Hz) 7.92 (t, 1H, *J* = 7.5 Hz) 7.84 (t, 1H, *J* = 7.4 Hz) 7.60 (m, 2H) 7.41 (m, 3H) 7.09 (m, 5H) 5.80 (d, 2H, *J* = 18.7 Hz)

^{31}P NMR: δ 8.44 *J*(Pt-P) = 3469.9 Hz

EA: Calc. for $C_{25}H_{21}Cl_2N_2PPt$: C, 46.45 %; H, 3.27 %; N 4.33 %;

Found: C, 46.19 %; H 3.12 %; N 4.72 %;

IR (KBr): 1630 cm^{-1} (C=N, imine)

EI-MS: *m/z* 610.92 $[M - Cl]^+$

Crystals suitable for X-ray structure determination were obtained by recrystallisation form a CH_2Cl_2-hexane mixture at room temperature.

Preparation of 87

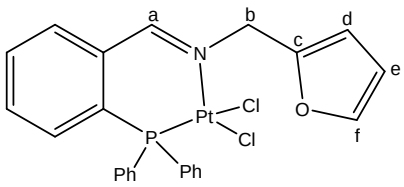

Product was obtained as a dark yellow powder in 72% yield

M.p.: 198-199 °C .

^{1}H NMR: (400 MHz, $CDCl_3$) δ_H 9.06 (m, 1H) 8.02 (m, 1H) 7.88 (td, 2H, *J* = 7.4 Hz, *J* = 19.3 Hz) 7.60 (t, 2H, *J* = 7.2 Hz) 7.49 (t, 4H, *J* = 6.4 Hz) 7.22 (ddd, 6H,

J = 15.4 Hz, *J* = 23.5 Hz, *J* = 30.5 Hz) 6.55 (m, 2H) 5.80 (d, 2H, *J* = 13.0 Hz)

^{31}P NMR: δ 5.66 *J*(Pt-P) = 3777.6 Hz

EA: Calc. for $C_{24}H_{20}Cl_2NOPPt$: C, 48.83 %; H, 3.77 %; N 2.28 %;

Found: C, 48.69 %; H 3.52 %; N 2.52 %;

IR (KBr): 1633 cm^{-1} (C=N, imine)

EI-MS: *m/z* 599.91 $[M - Cl]^+$

Preparation of 88

Product was obtained as a pale yellow powder in 72% yield

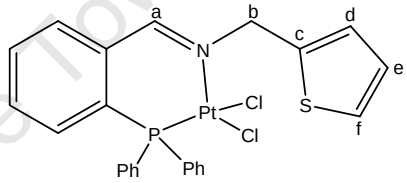

M.p.: 201-203 °C

1H NMR: (400 MHz, $CDCl_3$) δ_H 8.73 (s, 1H) 7.86 (m, 1H) 7.60 (m, 1H) 7.44 (m, 1H) 7.24 (dd, 1H, *J* = 1.2 Hz, *J* = 5.1 Hz) 7.06 (ddd, 1H, *J* = 1.6Hz, *J* = 7.2Hz, *J* = 10.6 Hz) 6.77 (dd, 1H, *J* = 3.4 Hz, *J* = 5.1 Hz) 6.50 (dd, 1H, *J* = 1.0 Hz, *J* = 3.4 Hz) 4.77 (t, 1H, *J* = 7.4 Hz)

^{31}P NMR: δ 8.06 *J* (Pt-P)=3758.5 Hz

EA: Calc. for $C_{24}H_{20}Cl_2NPPtS$: C, 44.25 %; H, 3.09 %; N, 2.15%; S, 4.92

Found: C, 44.19 %; H, 3.12 %; N, 2.42 %; S, 5.03

IR (KBr): 1631 cm^{-1} (C=N, imine)

EI-MS: *m/z* 616.01 $[M - Cl]^+$

Crystals suitable for X-ray structure determination were obtained by recrystallisation form a CH_2Cl_2-hexane mixture at room temperature.

*4.4.2 General procedure for synthesis of complexes **89 – 90***

To a dry CH_2Cl_2 (10 ml) of the appropriate ligand (**63** - **64**) was added an equimolar amount of PtClMe[COD]Cl_2 also in dry CH_2Cl_2 (10 ml). The reaction was allowed to stir at room temperature for 4 hours before reducing the solvent to *ca* 5 ml and precipitating out the products with hexane, filtering under gravity, washing the precipitate with Et_2O and drying under vacuum for 4 hours.

Preparation of 89

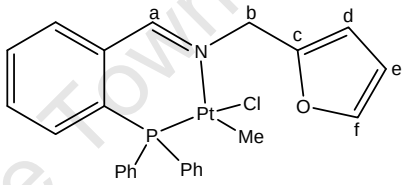

Product was obtained as a pale yellow powder in 73% yield.

M.p.: 220-221 °C

^{1}H-NMR: (400 MHz, dmso-d_6) δ_H 9.005 (s, 1H, H_a) 7.99 (ddd, 2H, *J* = 1.5 Hz, *J* = 4.0 Hz, *J* = 7.1 Hz, ArH) 7.77 (m, 1H, ArH) 7.51 (m, 1H, ArH) 7.33 (dd, 1H, *J* = 0.9 Hz, *J* = 1.8 Hz, ArH) 7.23 (m, 1H, ArH) 7.12 (ddd, 1H, *J* = 3.6 Hz, *J* = 10.1 Hz, *J* = 8.8 Hz, ArH) 6.53 (dd, 1H, *J* = 0.6 Hz, *J* = 3.2 Hz, H_d) 6.41 (m, 1H, H_e) 5.785 (s, 2H, H_b) 0.19 (d, 3H, J = 3.7 Hz, CH_3)

^{31}P NMR: δ 9.28 *J*(Pt-P) = 3782.6 Hz

EA: Calc. for $C_{25}H_{23}ClNOPPt$: C, 47.44 %; H, 3.98 %; N, 2.21 %;

Found: C, 47.29 %; H, 3.69 %; N, 2.08 %;

IR (KBr): 1625 cm^{-1} (C=N, imine)

EI-MS: *m/z* 598.94 $[M - CH_3]^+$

Preparation of 90

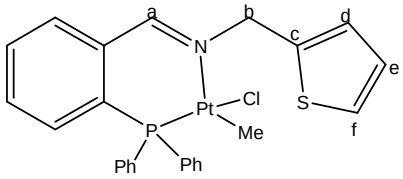

Product was obtained as a pale yellow powder in 75% yield.

M.p.: 230-233 °C

^{1}H-NMR: (400 MHz, dmso-d_6) δ_H 8.73 (s, 1H, H_a) 7.69 (m, 10H, ArH) 7.17 (m, 2H, ArH) 6.90 (dd, 1H, *J* = 3.5 Hz, *J* = 5.1 Hz, ArH) 6.75 (ddd, 1H *J* = 3.4 Hz, *J* = 5.1 Hz, *J* = 12.1 Hz, H_f) 6.51 (dd, 1H *J* = 1.0 Hz, *J* = 3.4 Hz, H_d), 6.46 (dd, 1H *J* = 1.0 Hz, *J* = 3.4 Hz, H_e) 5.824 (s, 2H, H_b) 0.31 (dd, 3H *J* = 3.7 Hz, J = 40 Hz, C*H*$_3$)

^{31}P NMR: δ 8.20 (s) *J* (Pt-P) = 3748 Hz

EA: Calc. for $C_{25}H_{23}ClNOPPt$: C, 48.58 %; H, 3.67 %; N, 2.15 %; S, 4.92 %

Found: C, 48.26 %; H, 3.83 %; N, 2.28 %; S, 4.88 %

IR (KBr): 1627 cm^{-1} (C=N, imine)

EI-MS: *m/z* 595.45 $[M - Cl]^+$

4.5 PREPARATION OF GOLD COMPLEXES

*4.5.1 General procedure for synthesis of complexes **91** – **94:*** To a dry CH_2Cl_2 (10 ml) of the appropriate ligand (**60, 62 - 64**) or PPh_3 for **95** was added Au(tht)Cl also in dry CH_2Cl_2 (10 ml) in a ratio of 1 : 0.9. The reaction was allowed to stir at room temperature for 2 hours before reducing the solvent to *ca* 5 ml and precipitating out the products with hexane, filtering under gravity and washing the precipitate with dry Et_2O and drying under vacuum for 4 hr.

Preparation of 91

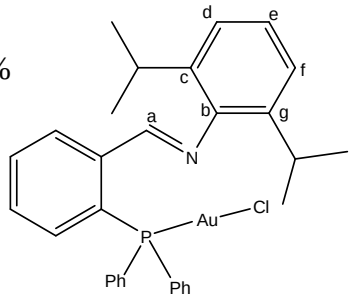

Product was obtained as a pale yellow powder in 73% yield.

M.p.: 200-201 °C

^{1}H-NMR: (400 MHz, $CDCl_3$) δ_H 8.90 (s, 1H, H_a) 8.41 (dd, 1H, *J* = 4.5 Hz, *J* = 7.2 Hz, ArH) 7.60 (t, 1H, *J* = 7.5 Hz, ArH) 7.41 (m, 11H, ArH) 6.94 (m, 3H, ArH) 6.79 (dd, 1H, *J* = 7.8Hz, *J* = 13.2Hz, H_e) 2.47 (td, 2H, *J* = 6.8Hz, *J* = 13.7Hz, -C*H*Me_2) 0.89 (d, 12H, *J* = 6.8Hz, -CH*Me*$_4$)

^{31}P NMR: δ 26.64 (s)

EA: Calc. for $C_{31}H_{32}AuClNP$: C, 54.60 %; H, 4.73 %; N, 2.05 %;

Found: C, 54.88 %; H, 4.57 %; N, 1.97 %;

IR (KBr): 1628 cm^{-1} (C=N, imine)

EI-MS: *m/z* 449.31 $[M - Cl - Au]^+$

Crystals suitable for X-ray structure determination were obtained by recrystallisation form a CH_2Cl_2-hexane mixture at room temperature.

Preparation of 92

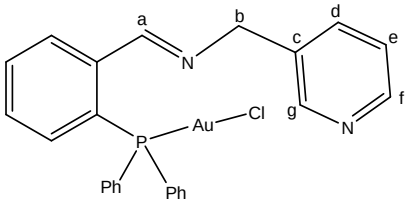

Product was obtained as an off-white powder in 53% yield.

M.p.: 215-217 °C .

^{1}H-NMR: (400 MHz, $CDCl_3$) δ_H 8.64 (s, 1H, H_a) 8.33 (d, 1H, *J* = 4.5 Hz, H_g) 8.28 (d, 1H, *J* = 5.8 Hz, H_f) 8.04 (m, 1H, ArH) 7.78 (m, 1H, H_d) 7.55 (m, 1H, ArH) 7.33 (m, 1H, H_e) 7.17 (m, 1H, ArH) 7.02 (dd, 1H, *J* = 5.0 Hz, *J* = 7.9 Hz,

ArH) 6.79 (dt, 1H, *J* = 8.3 Hz, *J* = 13.6 Hz, ArH) 4.70 (s, 1H, ArH) 4.60 (s, 2H, H_b)

^{31}P NMR: δ 31.38 (s)

EA: Calc. for $C_{25}H_{21}AuClN_2P$: C, 49.00 %; H, 3.45 %; N, 4.57 %;

Found: C, 49.22 %; H, 3.23 %; N, 4.54 %;

IR (KBr): 1630 cm^{-1} (C=N, imine)

Preparation of 93

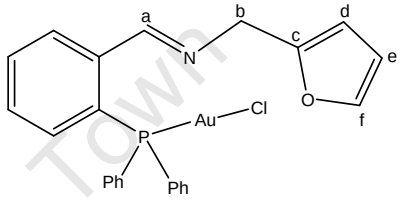

Product was obtained as a pale yellow powder in 59% yield.

M.p.: 220-221 °C .

^{1}H-NMR: (400 MHz, $CDCl_3$) δ_H 8.54 (d, 1H, *J* = 1.4 Hz, H_a) 7.82 (dd, 2H, *J* = 4.8 Hz, *J* = 7.1 Hz, ArH) 7.37 (m, 3H, ArH) 7.17 (m, 2H, ArH) 7.13 (dd, 4H, *J* = 0.8 Hz, *J* = 1.8 Hz, ArH) 6.75 (dd,2H, *J* = 7.8 Hz, *J* = 13.1 Hz, H_f) 6.13 (dd, 1H, *J* = 1.9 Hz, *J* = 3.1 Hz, H_e) 5.91 (d, 1H, *J* = 3.2 Hz, H_d) 4.53 (s, 2H, H_b)

^{31}P NMR: δ 30.51 (s)

EA: Calc. for $C_{24}H_{20}AuClNOP$: C, 46.90 %; H, 3.35 %; N, 2.33 %;

Found: C, 46.77 %; H 3.48 %; N, 2.09 %;

IR (KBr): 1634 cm^{-1} (C=N, imine)

EI-MS: *m/z* 563.87 $[M - Cl]^+$

Preparation of 94

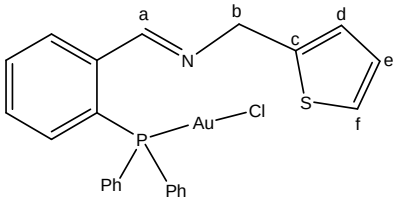

Product was obtained as an off-white powder in 55% yield.

M.p.: 230-232 °C .

^{1}H-NMR: (400 MHz, $CDCl_3$) δ_H 8.59 (d, 1H, *J* = 1.4 Hz, H_a) 8.35 (m, 1H, ArH) 7.84 (m, 2H, ArH) 7.68 (dd, 3H, *J* = 4.6 Hz, *J* = 7.2 Hz, ArH) 7.39 (m, 2H, ArH) 7.17 (m, 4H, ArH) 7.04 (dd, 2H, *J* = 1.1 Hz, *J* = 5.1 Hz, ArH) 6.96 (dd, 1H, *J* = 1.1 Hz, *J* = 5.1 Hz, H_f) 6.77 (m, 1H, H_e) 6.55 (m, 1H, H_d) 4.74 (s, 2H, H_b)

^{31}P NMR: δ 31.93 (s)

EA: Calc. for $C_{24}H_{20}AuClNPS$: C, 46.65 %; H, 3.26 %; N, 2.27 %; S, 5.19

Found: C, 46.80 %; H, 3.42 %; N, 2.45 %; S, 4.97

IR (KBr): 1635 cm^{-1} (C=N, imine)

EI-MS: *m/z* 581.38 $[M - Cl]^+$

Preparation of 95 [18]

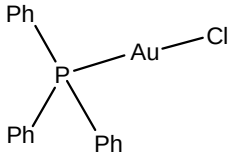

Product was obtained as a white powder in 98% yield.

M.p.: > 240 °C

^{1}H-NMR: (400 MHz, $CDCl_3$) δ_H 7.48 (m, 15H, ArH)

^{13}C NMR: (400 MHz, $CDCl_3$) δ 134.20, 134.02, 131.98, 131.95, 129.29, 129.14

^{31}P NMR: δ 32.95 (s)

EA: Calc. for $C_{18}H_{15}ClPAu$: C, 43.70 %; H, 3.06 %

Found: C, 43.39 %; H, 3.12 %

IR (KBr): 1625 cm^{-1} (C=N, imine)

EI-MS: *m/z* 459.10 $[M - Cl]^+$

4.6 CRYSTALLOGRAPHY

Summaries of crystal data and collection parameters of crystal structures of ligands **65**, **66** and **68** are given in Table 4.1. Those of complexes **74**, **79** and **80** in Table 4.2, **84**, **86** and **88** in Table 4.3, **91**, **93** and **94** in Table 4.4.

X-ray single crystal intensity data for structures were collected on a Nonius Kappa-CCD diffractometer using graphite monochromated MoKα radiation (λ = 0.71073 Å). Temperature was controlled by an Oxford Cryostream cooling system (Oxford Cryostat). The strategy for the data collections was evaluated using the Bruker Nonius "Collect" program. Data were scaled and reduced using DENZO-SMN software (Otwinowski & Minor, 1997). An empirical absorption correction using the program SADABS (Sheldrick, 1996) was applied.

The structures were solved by direct methods and refined employing full-matrix least-squares with the program SHELXL-97 (Sheldrick, 1997) refining on F^2. Packing diagrams were produced using the program PovRay and graphic interface X-seed [19].

Table 4.1: Crystallographic data for ligands **65**, **66** and **68**

	65	**66**	**68**
Empirical formular	$C_{34}H_{30}N_4O_2S_4$	$C_{20}H_{20}N_2S_2$	$C_{22}H_{22}N_4$
Formular weight	654.86	352.52	342.44
T/K	173(2)	173	173(2)
λ/Å	0.7103	0.7103	0.71073
Space group	Triclinic	Monoclinic	Monoclinic
a	8.8517(3)	9.8592(10)	6.0078(6)
b	10.3937(5)	7.1533(3)	26.023(3)
c	10.5763(4)	25.678(2)	6.1319(7)
α(deg)	63.836(2)	90	90
β(deg)	69.023(2)	96.646(5)	106.009(2)
γ(deg)	72.394(2)	90	90
V($Å^3$)	803.22(6)	1798.8(3)	921.47(17)
Z	1	8	2
$Density_{calc}$(mg/ml)	1.354	1.302	1.234
Absorption coefficient (mm^{-1})	0.334	0.299	0.075
F(000)	342	744	364
Crystal size (mm)	0.22x0.20x0.13	0.04x0.20x0.22	0.26x0.24x0.17
Theta range for data collection (deg)	2.50 – 26.44	3.2 – 28.3	3.13 – 28.34
Limiting indices	0<=h<=11, -11<=k<=13, -11<=1<=13	-13<=h<=13, -9<=k<=9, -34<=1<=34	-8<=h<=8, -34<=k<=33, -8<=1<=8
Reflections Collected/ Unique	3283 / 3283 [R(int) = 0.0000]	16248 / 2230 [R(int) = 0.045]	11941 / 2288 [R(int) = 0.0238
Completeness of theta max. and min. transmission	26.44 (99.2%)	28.3 (99.8%)	28.34 (99.9%)
Refinement method	Full-matrix least-squares on F^2	Full-matrix least-squares on F^2	Full-matrix least-squares on F^2
Data / Restraints/ Parameters	3283 /0 / 199	2230/0/109	2288 / 0 / 118
Goodness-of-fit on F^2	1.053	1.06	1.057

Table 4.2: Crystallographic data for palladium complexes **74**, **79** and **80**

	74	**79**	**80**
Empirical formular	$C_{24}H_{28}Cl_2NOPPdS$	$C_{24}H_{20}Cl_2NPPdS$	$C_{27}H_{25}ClNPPd$
Formular weight	586.81	562.74	536.30
T/K	173(2)	173(2)	173(2)
λ/Å	0.71073	0.71073	0.7103
Space group	Triclinic	Monoclinic	Monoclinic
a	8.9935(2)	9.8892(5)	10.0147(8)
b	10.0413(2)	21.6512(12)	21.8935(18)
c	13.9439(3)	10.7050(6)	10.7478
α(deg)	91.189(10)	90	90
β(deg)	97.957(10)	94.7860(10)	94.192(2)
γ(deg)	94.869(10)	90	90
V($Å^3$)	1241.93(5))	2284.1(2)	2350.2(3)
Z	2	4	4
$Density_{calc}$(mg/ml)	1.569	1.637	1.516
Absorption coefficient (mm^{-1})	1.128	1.220	0.986
F(000)	596	1128.0	1088
Crystal size (mm)	0.05x0.1x0.20	0.10x0.26x0.46	0.03x0.12x0.13
Theta range for data collection (deg)	3.0 – 28.7	1.9 – 30.7	2.1 – 28.3
Limiting indices	-12<=h<=12, -13<=k<=13, -18<=1<=18	-14<=h<=14,-31<=k<=31,-15<=1<=15	-13<=h<=13,-29<=k<=29,-14<=1<=13
Reflections Collected/ Unique	45019 / 6342 [R(int) = 0.057]	50973 / 7032 [R(int) = 0.021]	32545 / 5809 [R(int) = 0.043]
Completeness of theta max. and min. transmission	28.66 (99.2%)	30.670 (99.5%)	28.25 (99.6%)
Refinement method	Full-matrix least-squares on F^2	Full-matrix least-squares on F^2	Full-matrix least-squares on F^2
Data / Restraints/ Parameters	6342 /0 / 284	7032 / 0 / 271	6590 / 8/ 270
Goodness-of-fit on F^2	1.059	1.061	1.031

Table 4.3 Crystallographic data for platinum complexes **84**, **86** and **88**

	84	**86**	**88**
Empirical formular	$C_{31}H_{32}Cl_2NPPt$	$C_{25}H_{21}Cl_2N_2PPt$	$C_{25}H_{24}Cl_2NOPtS$
Formular weight	715.54	646.40	683.47
T/K	173(2)	173(2)	173(2)
λ/Å	0.71073	0.71073	0.7103
Space group	Monoclinic	Triclinic	Monoclinic
a	12.0686(7)	9.9684(14)	9.9635
b	13.4007(7)	10.4129(15)	19.0185
c	17.8182	12.526(3)	13.5321
α(deg)	90	97.687(5)	90
β(deg)	105.8190(10)	98.363(5)	95.5100(10)
γ(deg)	90	114.499(3)	90
V($Å^3$)	2772.6(3)	1143.1(4)	2552.4(3)
Z	4	2	4
$Density_{calc}$(mg/ml)	1.714	1.878	1.779
Absorption coefficient (mm^{-1})	5.333	6.457	5.869
F(000)	1408	624	1328
Crystal size (mm)	0.22x0.11x0.09	0.07x0.06x0.04	0.08x0.05x0.03
Theta range for data collection (deg)	1.83 – 29.60	2.20 – 27.09	2.14 – 28.72
Limiting indices	-16<=h<=16, -18<=k<=18, -24<=1<=24	-12<=h<=7,-11<=k<=13,-16<=1<=16	-13<=h<=13, -25<=k<=25, -18<=1<=18
Reflections Collected/ Unique	40326 / 7788 [R(int) = 0.0000]	16090 / 4994 [R(int) = 0.0580]	30138 / 6590 [R(int) = 0.0524]
Completeness of theta max. and min. transmission	29.6 (99.9%)	27.09 (99.3%)	28.72 (99.7%)
Refinement method	Full-matrix least-squares on F^2	Full-matrix least-squares on F^2	Full-matrix least-squares on F^2
Data / Restraints/ Parameters	7788 /0 / 326	4994 / 0 / 280	6590 / 8/ 270
Goodness-of-fit on F^2	1.059	1.005	1.053

Table 4.4 Crystallographic data for gold complexes **91**, **93** and **94**

	91	**93**	**94**
Empirical formular	$C_{32}H_{35}AuClNP$	$C_{24}H_{20}AuClNOP$	$C_{25}H_{22}AuClNPS$
Formular weight	705.00	601.80	631.88
T/K	173(2)	173(2)	173(2)
λ/Å	0.7103	0.71073	0.71073
Space group	Triclinic	Monoclinic	Monoclinic
a	13.0315(3)	13.4559(4)	11.866(2)
b	13.3638(2)	10.3917(2)	10.625(2)
c	19.3489(5)	17.2641(4)	36.452(7)
α(deg)	96.358(2)	90	90
β(deg)	99.2290(10)	111.751(10)	92.63(3)
γ(deg)	116.1910(10)	90	90
V(Å^3)	2921.15(11)	2242.16(10)	4590.9(15)
Z	4	4	4
$Density_{calc}$(mg/ml)	1.603	1.783	1.829
Absorption coefficient (mm^{-1})	5.205	6.766	6.699
F(000)	1396	1160	2448
Crystal size (mm)	0.21x0.18x0.12	0.02x0.011x0.16	0.06x0.13x0.14
Theta range for data collection (deg)	2.31 – 26.38	2.20 – 27.09	1.8 – 29.1
Limiting indices	-16<=h<=16, -16<=k<=16, -24<=1<=24	-17<=h<=17,-13<=k<=13,-23<=1<=23	-16<=h<=16, -14<=k<=14, -49<=1<=49
Reflections Collected/ Unique	119370 / 11941 [R(int) = 0.0534]	74304 / 5534 [R(int) = 0.0680]	115921 / 12327 [R(int) = 0.115]
Completeness of theta max. and min. transmission	26.38 (99.8%)	28.28 (99.7%)	29.13 (99.7%)
Refinement method	Full-matrix least- squares on F^2	Full-matrix least-squares on F^2	Full-matrix least-squares on F^2
Data / Restraints/ Parameters	11941 / 9/ 604	4994 / 0 / 280	6590 / 8/ 270
Goodness-of-fit on F^2	1.050	1.005	1.080

4.7 BIOLOGICAL STUDIES

Biological studies were carried out in the Cancer Laboratory (Prof Hendricks and Dr Leaner) in the Division of Medical Biochemistry in the Faculty of Health Sciences at the University of Cape Town. Unless otherwise stated, all chemicals were AnalR grade, and purchased from Sigma or Merck.

4.7.1 Cell Culture

All cell lines were maintained at 37 °C, in a 5 % CO_2, humidified incubator.

4.7.1.1 Cell lines and media requirements

The human oesophageal cancer cell line WHCO1 derived from a South African patient with squamous cell carcinoma of the oesophagus was obtained from Prof Veale [20]. The human oesophageal cancer cell line KYSE450 was derived from a Japanese patient with squamous cell carcinoma of the oesophagus and was purchased from DSMZ . DMB cells are primary fibroblasts derived from a skin biopsy obtained from a normal subject.

Table 4.5 Cell lines and media requirements

Cell line	Media	% Foetal Calf Serum	Antibiotics 100U/ml penicillin, 100g/ml streptomycin
WHCO1	DMEM – Dulbeccos'Modified Eagle's Media	10%	yes
KYSE450			
DMB			

4.7.1.2 Subculturing protocols

All cell lines were subcultured by removing media, rinsing once with 2 ml PBS (or 0.5 % trypsin), then trypsinising with 3 ml trypsin. Once cells had rounded, 3 ml of media were added to neutralize the trypsin, and cells were centrifuged out of the trypsin:media mix. Cells were then suspended in media and a portion added to a fresh dish in a 1 in 6 split ratio.

4.7.1.3 Freezing and thawing protocols

For all cell lines, a confluent dish was trypsinised, neutralized with complete media, then cells were centrifuged out of the trypsin/media solution. Cells were resuspended in 3-4 ml of cold (4 °C) freezing media (70% DMEM, 20% Fetal Calf Serum, 10% DMSO), and aliquoted into cryotubes (1 ml per tube). Tubes were placed in -70 °C overnight and then transferred to liquid nitrogen. Cells are thawed by placing the tubes in a water bath at 37 °C for *ca* 2 min.

4.7.1.4 Mycoplasma test

All cell lines were tested for mycoplasm contamination every three months. Cells were grown in culture media free of antibiotics for at least one week, then trypsinised and plated onto coverslips in 60 mm dishes. Following an overnight incubation to allow cells to settle onto coverslips, 5 ml fixative was added to the culture media, then discarded and replaced with another 2-5 ml fixative. The cells were then immediately washed gently with water and dried by inversion. Once the coverslip was dry,

mycoplasm staining solution was added for 30 seconds and then thoroughly washed with water. Finally the coverslip was mounted on a slide, using a drop of mounting fluid, and cells were observed using fluorescence microscopy. Cell nuclei stain bright green, and mycoplasm contamination is visualized as minute punctate fluorescence distributed throughout the cytoplasm [21].

4.8 Cytotoxicity screening

4.8.1 MTT assay

1500 cells were seeded per well in 90 µl DMEM in 96 well plates. Cells were incubated for 24 hours, then test samples were plated at a range of concentrations in 10µl media, with a final concentration of 0.2 % DMSO. After 48 hours of incubation, the cells were observed under a phase contrast microscope and the general appearance of the cells together with confluency status and presence of precipitate if any was recorded.

10 µl of MTT reagent was added per well at the end of the experiment, and the plates incubated for 4 hours at 37 °C. 100 µl of solubilisationsolution was then added to each well, and plates were incubated at 37 °C overnight. After 16 hours, the plates were read at 595 nm on an Anthos microplate reader 2001.

4.8.2 IC_{50} data analysis

The resulting dose-response curve was analysed by non-linear regression analysis (Non-linear regression (Sigmoidal dose response with variable slope)) using GraphPad Prism version 4.00 for Windows (GraphPad Software, San Diego Carlifornia USA, www.graphpad.com) to yield an IC_{50} value which is specific for the compound against that particular cell line. The formular used is as follows:

$$Y = \text{bottom} + \frac{(\text{top} - \text{bottom})}{1 + 10^{(\log IC_{50} - X) \times \text{hillslope}}}$$

Where Y is the absorbance reading, X is the concentration of the compound, top is the maximum absorbance, bottom is the minimum absorbance (also the absorbance of the medium blank), and the hillslope is the gradient of the curve.

All experiments were done three times and all experimental points within an experiment were done in triplicate.

4.9 Cell cycle analysis

Cells were seeded in 60 mm dishes at 0.25 x 10^6 cells per dish. Following an overnight settling period, compounds were added to culture media (to avoid the loss of cycling cells that had detached during division). At appropriate time points, cells were harvested by trypsinisation (taking care to collect all washes to avoid discarding floating cells), resuspended in 1 ml PBS, and counted. 9 ml of ice cold 100% EtOH was then added to each sample, and samples were stored at -20 °C for up to 2 weeks. Cells were then centrifuged out of EtOH, rinsed several times in PBS, and 5x10^6

cells/ml were incubated in 50 µg/ml RNAse A in PBS for 30 minutes at room temperature. Cell Cycle Staining solution was added to bring the cell concentration to $1x10^6$ cells/ml, and following a 30 minute incubation in the dark, cells were analysed on a Beckman Coulter FACS-calibur flow cytometer. Analysis of cell cycle results was carried out using ModFit 3.0 (Verity Software House).

4.10 Western blotting

Cells prepared for western blotting were routinely plated at 500 000 cells/ 60 mm dish. Cells were incubated for 24 hours, then treated with the indicated concentrations of compounds for the indicated times

4.10.1 Protein harvest

Media was removed from the cells and the cells rinsed with cold 1xPBS twice. 60 µl RIPA buffer with protease and phosphatase inhibitors, was added to the dish, and cells were lysed manually with a cell scraper. The lysate was transferred to a clean eppendorf tube and placed on ice.

4.10.2 Protein quantitation

The lysates were thawed and sonicated at 4 °C. Protein quantitation was performed in 96 well plates using the BCA kit (Pierce). Various volumes of lysate were pipetted into each well in duplicate, and made up to 10 µl with RIPA buffer. 10 µl of each BSA standard (range 0.1 mg/ml to 2 mg/ml) were pipetted in duplicate for a standard curve, and 10 µl of RIPA was included as a blank. Reagent A and Reagent B from the

kit were mixed at a 1:50 ratio, and 100 µl of this solution was added to each well. Following a 30 minute incubation at 37 °C, the absorbance at 595 nm was measured on an Anthos microplate reader 2001. A standard curve was plotted using Prism, and the protein concentrations of the samples were calculated from this curve.

4.10.3 SDS-PAGE

10% Acrylamide gels with 5% stacking gel were poured using the Protean II minigel casting apparatus (BioRad). Protein samples were prepared by mixing equal amounts of protein with loading dye, and boiled for 10 minutes to denature the proteins. Samples were loaded onto the SDS-PAGE, and the gel was run at 100 volts. Migration of proteins through the gel was monitored by loading a multicolour protein ladder.

4.10.4 Transfer

SDS-PAGE gels were removed from between the glass plates, and the transfer apparatus was assembled. Protein was transferred from the gel onto the nitrocellulose membrane, and these were sandwiched between filter paper and sponges, and inserted into a transfer cassette. The cassette and an ice pack were inserted into the transfer apparatus, which was filled with transfer buffer, and transfer was carried out at 200 volts for 1 hour.

4.10.5 Ponceau S (membrane) and Coomasie (gel) stains

Following transfer, membranes were stained with Ponceau-S for 10 minutes, then destained with dH_2O to assess protein loading and transfer efficiency.

4.10.6 Washes, blocking and primary antibody

Following Ponceau-S staining, membranes were washed with TBS/0.1% Tween, and then blocked in blocking solution. Blocking solution was discarded, and the membrane was then washed with TBS/0.1% Tween, with shaking for three sets of 5 minutes, changing TBS/0.1% Tween each time. Primary antibody was added in the appropriate buffer and incubated with shaking overnight at 4 °C.

4.10.7 Secondary antibody

The primary antibody was removed from the membrane, and the membrane was again washed for three sets of 5 minutes, chaging TBS/0.1% Tween each time. The secondary antibody was removed, and a final set of 5 minute washes with TBS0.1%/ Tween were performed to remove excess antibody. Detection reagent was added, and light emission was detected on X-ray film. The bands were visualized by developing the film in developer for 1 minute, washing for 1 minute with water, then fixed for 5 minutes in fixative.

4.11 Prepared Solutions

4.11.1 Cell culture

Cell-freezing media

70 % DMEM

20 % Fetal Calf Serum

10 % DMSO

MTT (5 mg/ml)

100 mg MTT

20 ml 1 X PBS

Vortex and incubate at 37 °C for 15 min

Filter through a 0.2 µm filter

Wrap in foil and store at 4 °C for up to one month

Solubilisation Reagent for MTT assay

25 g of Sodium Lauryl Sulphate (SLS)

Make up to 250 ml with dH_2O

Add 76.6 µl conc. HCl

Trypsin-EDTA

0.5 g trypsin

8 g NaCl

1.45 g $Na_2HPO4.2H_2O$

0.2 g KCl

0.2 g KH_2PO_4

10 mM EDTA (pH8.0)

Make up to 1 L with PBS

PBS

40 g NaCl

1 g KCl

1.6 g $Na_2HPO_4.2H_2O$ (pH7.4)

1 g KH_2PO_4

Make up to 500 ml with dH_2O

Penicillin/streptomycin solution

Add 5 million units Penicillin G Sodium to 5 ml PBS. Add 5 g 214S Streptomycin to 15 ml PBS. Combine the two and make volume up to 500 ml. Aliqout 5 ml volumes. Add 5 ml to each 500 ml media.

Mycoplasm detection fixative

1 part glacial acetic acid to 3 parts methanol

Mycoplasm detection Stain solution

0.5 µg/ml Hoeschst No. 33258 in Hanks Buffered Saline Solution (without phenol red or sodium bicarbonate. Store in the dark/covered bottle at 4 °C and examine periodically for contamination.

Mycoplasm detection Mounting Fluid

1.05 g citric acid/ 50ml

1.41 g $Na_2HPO_4.2H_2O$/ 50ml

50 ml glycerol

pH 5.5 (Check periodically, pH critical for optimum fluorescence)

Store at 2 - 8 °C

4.11.2 Cell Cycle Analysis

Staining solution

0.1% Triton X-100

2 mM $MgCl_2$

100 mM NaCl

0.01 M PIPES buffer

10 µg/ml propidium iodide

4.11.3 Western blotting

RIPA buffer

1.75 g NaCl

2 ml X-100

500 ml SDS

2 ml Tris (pH 7.5)

2 g deoxycholate

Protease inhibitor

1 cOmplete Mini tablet (Roche, Cat. No. 04 693 124 001) was dissolved in 10ml dH_2O to make a 10x solution. This was aliquated and stored at -20 °C.

30% Acrylamide

30 g acrylamide

0.8 g bis-acrylamide

0.1 g SDS

Add dH_2O and mix

Store at 4 °C

Stacking Buffer

5.9 g Tris

0.4 g SDS

pH to 8.0 and make up to 100 ml with dH_2O

Store at 4 °C

Resolving Buffer

36.2 g Tris

0.8 g SDS

pH to 8.9 and make up to 200 ml with dH_2O

Store at 4 °C

5x Loading Buffer

1.75 g Tris

30 ml glycine

Make up to 40 ml with dH_2O

pH to 6.8 with 1 N HCl

Add H_2O to 50 ml

Loading Dye

100 µl loading buffer

50 µl β-mercaptoethanol

50 µl saturated, filtered bromophenol blue

10x Running Buffer

40 g glycine

63.2 g Tris

10 g SDS or 100 ml 10% stock

Make up to 1000 ml with dH_2O

Dilute 1 in 10 for 1x running buffer

10x Transfer buffer

144 g glycine

38 g Tris

Make up to 1000 ml with dH_2O

1x Transfer Buffer

100 ml 10x transfer buffer

200 ml isopropanol

700 ml dH_2O

Gel stain solution

50% methanol

10% glacial acetic acid

0.25% (w/v) Coomassie Blue

Gel destain solution

10% methanol

7.5% glacial acetic acid

10x Tris buffered saline (TBS)

60.5 g Tris

87.6 g NaCl

pH to 7.5

make up to 1000 ml with dH_2O

TBS/0.1% Tween

100 ml 10x TBS

900 ml dH_2O

1 ml Tween 20

Blocking Solutions

5 g fat free milk powder

Dissolve in 100 ml TBS/0.1% Tween

Fixer (AGFA G333C)

Dilute 100ml stock with 400ml dH_2O

Developer (AGFA G128)

Dilute 100 ml stock with 400 ml dH_2O

4.12 REFERENCES

[1] Chatt J, Vallarino L. M, Venanzi L. M, *J. Chem. Soc.*, **1957**, 3413.

[2] Bailey C. T, Linsesky G. C. J, *J. Chem. Edu*., **1985**, 62, 896.

[3] Rulke R. E, Ernsting J. M, Spek A. L, Elsevier C. J, van Leeuwen P. W. N. M, Vrieze K, *Inorg. Chem*., **1993**, 32, 5769.

[4] McDermott J. X, White J. F, Whitesides G. M, *J. Am. Chem. Soc*., **1976**, 98, 6521.

[5] Drew D, Doyle J. R, *Inorg. Synth*., **1990**, 28, 346.

[6] Al-Allaf T. A. K, Rashan L. J, Abu-Surrah A. S, Fawzi R, Steimann M, *Transition Met. Chem*., **1998**, 23, 403.

[7] Price J. J, Williamson A. N, Schramm R. F, Wayland B. B, *Inorg. Chem*., **1972**, 11, 1280.

[8] Jensen K. A, *Z. Anorg. Allg. Chem*., **1936**, 229, 255.

[9] Lapido F. T, Anderson G. K, *J. Organomet. Chem*., **1994**, 13, 303.

[10] Uson R, Laguna A, *Organometallic Synthesis*, eds. Lang R. B, Eish J. J, Elsevier, Amsterdam, **1986**, 3, 324.

[11] Sheldrick G. M, SHELX97, *Programme for Solving Crystal Structures*, University of Gottingen, Germany, 1997.

[12] Sheldrick G. M, SHELX97, *Programme for the Refinement of Crystal Structures*, University of Gottingen, Germany, 1997.

[13] Ghilardi C. A, S. Midollini S, Moneti S, Orlandini A, Scapacci G, *J. Chem. Soc., Dalton Trans*., **1992**, 3371.

[14] Sanchez G, Momlona F, Peres J, Lopez G, *Transition Met. Chem.*, **2001**, 26, 100.

[15] Crociani B, Antonaroli S, Beghetto V, Matteoli U, Scrivanti A, *Dalton Trans*., **2003**, 2194.

[16] Reddy K. R, Tsai W. -W, Lee S. G. -H, Peng S. M, Chen J. –T, Liu S. T, *J. Chem.*

Soc., Dalton Trans., **2002**, 1776.

[17] Shirakawa E, Yoshida H, Takaya H, *Tetrahedron Lett*., **1997**, 38, 3759.

[18] Preparation of Gold precursor compounds, *AuTEK Biomedical Gold precursors*, **2006**, 3.

[19] Barbour L. J, X-Seed: A Software Tool for Supramolecular Crystallography, *J Supromol. Chem*., **2001**, 1, 189.

[20] Veale R. B, Thornley A, L, *S A J Sci*., **1989**, 85, 6, 375.

[21] Battaglia M, Pozzi D, Grimaldi S, Parasassi T, *Biotechnic and Histochemistry*, **1994**, 69, 3, 152.

CHAPTER 5

CONCLUSIONS AND FUTURE WORK

The aim of this project was to sythesise new organometallic complexes of palladium, platinum and gold and evaluate these against oesophageal cancer cell lines. A series of new iminophosphine and tetradentate ligands have been synthesised in good yields and characterised by spectroscopic and analytical methods. The molecular structures of the new tetradentate ligands **65**, **66** and **68** were also determined and have not been previously reported. A preliminary investigation of their coordination chemistry with palladium(II) and platinum(II) shows interesting reactivity and suggests great promise for future directions in synthesis.

The palladium and platinum and gold complexes were prepared from reaction of the iminophosphine ligands **58**-**64** with $PdCl_2$[COD], PdClMe[COD], $PtCl_2$[COD], $PtCl_2[DMSO]_2$ and Au[tht]Cl to generate the respective neutral iminophosphine complexes. The complexes were fully characterised by spectroscopic methods (^{1}H, ^{13}C-NMR, ^{31}P-NMR, FTIR, and MS) and analytical methods (elemental analysis). The molecular structures of palladium complexes **74**, **79** and **80**; platinum complexes **84**, **86**, **88** and gold complexes **91, 93** and **94** were determined by X-ray crystal structural analysis. To the best of our knowledge these have not been reported before and are therefore novel. On the basis of the analytical data, spectral studies and X-ray crystallography, it has been observed that the ligands coordinate to the metal atoms in a monobasic bidentate manner and thus possess square planar geometry for the palladium and platinum complexes. The gold(I) complexes however exhibit the expected linear coordination geometry.

The metal complexes were screened for their anticancer activities against WHCO1 and KYSE450 oesophageal cancer cell lines. The chloromethyl palladium complexes were not very active and exhibited IC_{50} values in the range 11.0 – 68.5 μM for both cell lines. One of the major problems associated with several of the palladium complexes examined in this project, lies in the insolubility of the complexes in an aqueous medium. Given that solutions of the complexes are administered to biological systems, the choice of solvent is limited. The preparation of palladium salts or cyclodextrin inclusion complexes could potentially stabilise the complexes and render them soluble in an aqueous medium.

The platinum and gold complexes were very active and block the proliferation of WHCO1 cells with an IC_{50} range of 2.5 - 9.4μM, and IC_{50} range of 2.2 - 7.6μM for the KYSE450 cell lines. These complexes kill oesophageal cancer cells, with little effect on normal fibroblast cells (DMB), with IC_{50} values > 100μM which is a very significant finding which shows that these novel complexes are selective towards oesophageal cancer cells. However, a number of experiments still have to be performed to explore this observation in detail. We will test the complexes on other normal epithelial cells (EPC-2), fibroblasts cells (FG0) and other oesophageal cancer cell lines (WHCO5, WHCO6, KYSE70, KYSE180, KYSE410, KYSE520) to validate if selectivity is still maintained. Furthermore, although these results are very promising, they have to be extended in an animal model system.

APPENDICES

Supporting Information: X-ray diffraction data is provided in the form of structure factor tables and tables of data on diskette,

- Appendix 1 – X-ray data for ligand **65**
- Appendix 2 – X-ray data for ligand **66**
- Appendix 3 – X-ray data for ligand **68**
- Appendix 4 – X-ray data for complex **74**
- Appendix 5 – X-ray data for complex **79**
- Appendix 6 – X-ray data for complex **80**
- Appendix 7 – X-ray data for complex **84**
- Appendix 8 – X-ray data for complex **86**
- Appendix 9 – X-ray data for complex **88**
- Appendix 10 – X-ray data for complex **91**
- Appendix 11 – X-ray data for complex **93**
- Appendix 12 – X-ray data for complex **94**